3D cell culture handbook

Culturing and analysis of 3D cell models

ThermoFisher SCIENTIFIC

3D cell models

Cells and tissues that are cultured in a 3D environment show great potential to advance our understanding of complex biological processes. 3D cell models are increasingly being used in many research applications, including drug discovery, toxicology, disease modeling, and regenerative medicine. These models offer an opportunity to better understand complex biology in a physiologically relevant context where 2D models have not proven as successful.

This handbook provides an overview of the cell lines, culture conditions, and analysis techniques that are being used in the transition from 2D to 3D cell models. Whether you are just beginning this transition or are exploring improvements to existing 3D culture methods, we have brought together a variety of resources to help you create better model systems for your experiments.

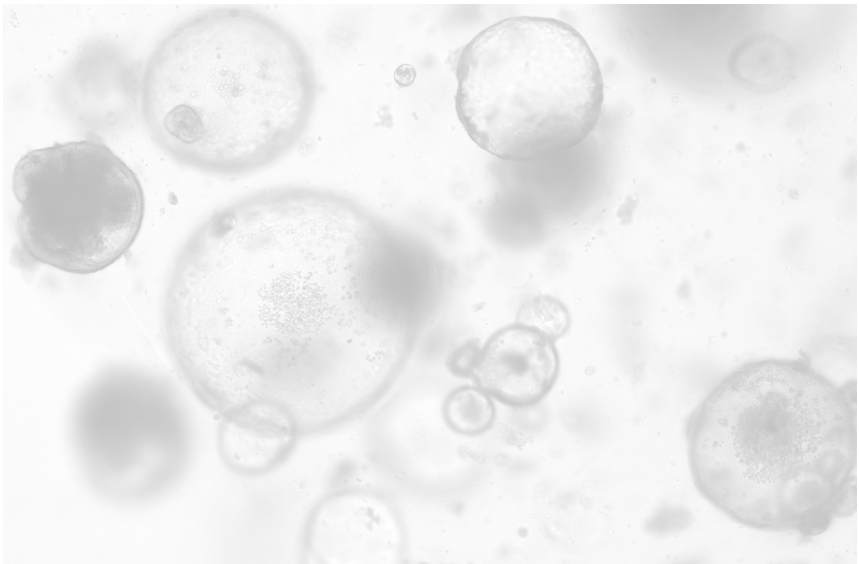

Contents

Section 1

Introduction to 3D cell models

1.1

Introduction to 3D cell culture

Advancing our understanding of biological processes in normal and disease conditions relies on accurate modeling in the laboratory. For decades, researchers used two-dimensional (2D) methods of cell culture, wherein cells were grown in dishes or flasks as monolayers. The 2D method of cell culture has been widely accepted in research, but its limitations for studying more complex systems have become apparent in recent years.

Three-dimensional (3D) cell culture methods recreate more physiologically relevant microenvironments for cells. Critical to each microenvironment is the extracellular matrix (ECM), which provides structural support for cells and regulates diverse processes, including cell migration, cell proliferation, cell differentiation, and cell-to-cell communication. In pivotal work, Bissell and colleagues demonstrated that the ECM and tissue architecture mold how cells—normal and malignant—receive and respond to signals from their surroundings (Bissell 1981; Hall 1982). Later, Petersen and colleagues showed that culturing cells with the appropriate ECM allowed cells to self-assemble, and thus morphogenesis could be observed *in vitro* (Petersen 1992). These cultures were among the first systems to model the 3D structures of organs (Rossi 2018).

Types of 3D cell models include spheroids, organoids, bioprinted cell models, and organs-on-chips. Spheroids are the result of growth and aggregation of one or more cell types in 3D culture. In general, spheroids retain the characteristics of the starting cells but assume a spherical shape. Organoids consist of more highly differentiated structures that are commonly derived from stem cells or other progenitor cells. These cellular structures preserve many of the features of the organ from which they are derived. Tumor spheroids can also be grown from patient tissue, making real the possibility of personalized treatment after testing (Aboulkheyr 2018). Organs-on-chips are microfluidic devices that simulate the cellular structure of organs and enable dynamic flow of media. All of these different models provide an *in vivo* representation of a tissue or organ in an *in vitro* manner. In the table below key differences are shown between 2D and 3D cell culture methods (Table 1.1).

Table 1.1. Key differences between 2D and 3D cell culture systems.

Characteristic or condition	2D	3D
Morphology	Cells grow in a sheet or monolayer	Cells often retain natural shape and proper spatial orientation in aggregates or spheroids
Proliferation	Usually faster than *in vivo* growth	Depending on cell type and system used, may be faster or slower than 2D culture
Gene and protein expression	Often differs from expression *in vivo*	Cells more closely mimic expression *in vivo*
Drug sensitivity	Drugs often appear effective, as exposure is fairly uniform	Cells can have nonuniform toxicity profiles; more closely mimics the true effect *in vivo*
Oxygen tension	High oxygen tension in incubator is not physiological; affects mitochondrial function and development of reactive oxygen species (ROS)	Oxygen tension varies within culture; more closely mimics *in vivo* differences
Genetic drift	Cells in long-term culture undergo genetic drift due to selection following specific growth conditions in individual laboratories; epigenetic and physiological changes may be noted as well	Cells are not in traditional long-term culture, so genetic stability may be improved

Adapted from: Edmondson 2014; Horvath 2016.

Methods to create 3D cell cultures

Several methods are used to generate 3D cell cultures, which are illustrated in Figure 1.1. These methods range from static suspension and hanging-drop culture methods to more complex systems using spinner flasks or bioprinters. All of these methods may be optimized to suit the needs of the laboratory. A static suspension method using a round-bottom (U-bottom) well shape is ideal for growing spheroid cultures, as the rounded surface is more difficult for cells to adhere to and grow on. The reliable cell growth and the ease in controlling spheroid size on **Thermo Scientific™ Nunclon™ Sphera™ U-bottom plates** are important for applications where consistency and reproducibility are valued. Gel-embedding methods use ECM materials, which can be composed of natural (e.g., collagen) or synthetic materials, to support 3D cell cultures. Examples of these materials include gelatin, laminin, hyaluronic acid, polyethylene glycol (PEG), polyactic acid (PA), and polyglycolic acid (PGA). One potential application is to create ECMs specific for the cell type of interest in order to improve *in vitro* modeling of the tumor microenvironment even further (Lv 2017).

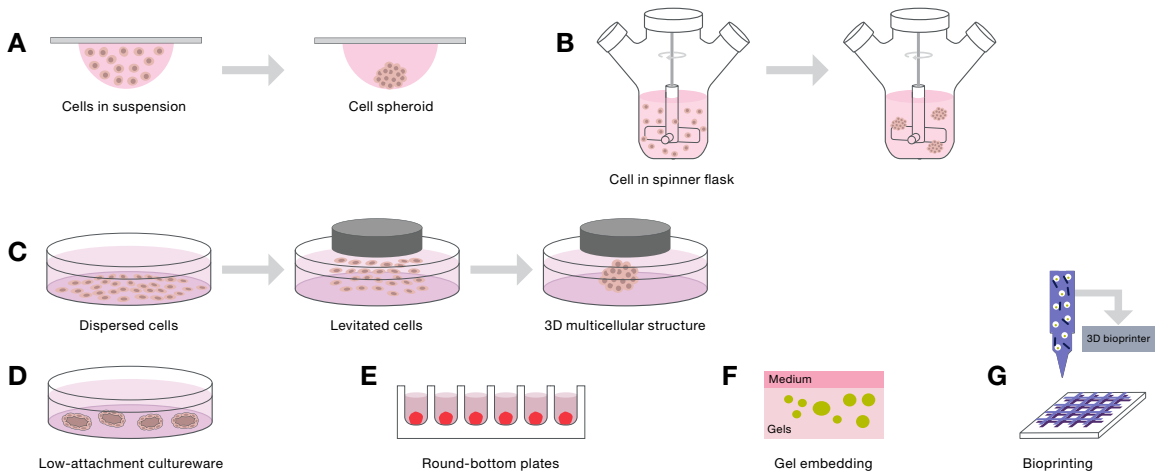

Figure 1.1. Commonly used methods for creating 3D cell cultures. (A) Hanging-drop culture. **(B)** Spinner flask culture. **(C)** Magnetic levitation of cells preloaded with magnetic nanoparticles. **(D)** Static suspension of cells in low-attachment plates. **(E)** Static suspension in round-bottom 3D culture plates. **(F)** ECM embedding. **(G)** 3D bioprinting.

Nunclon Sphera microplates

With their exceptionally low cell attachment surface, Nunclon Sphera microplates consistently promote 3D culture of spheroids and organoids, aiding you in cancer spheroid formation and stem cell differentiation for disease modeling and drug screening.

Optimized performance for 3D cell culture:

- Allows cells to grow in suspension with virtually no cell attachment
- Supports many different cell types to generate spheroids
- Promotes consistent formation of cancer spheroids that simulate the 3D structures of tumor growth

- Demonstrates superior quality for embryoid body formation of pluripotent stem cells with minimal spontaneous differentiation
- Proven efficacy in supporting long-term organoid culture

Find out more at **thermofisher.com/sphera**

1.2

Significant advances

Tumor modeling

3D cell cultures have helped transform research in the area of solid tumor modeling. These systems mimic the biochemical and cellular makeup of tumors in their microenvironments more closely than do 2D cultures. Specifically, 3D cultures can reproduce ongoing processes that occur when a tumor grows within the body. These processes include angiogenesis, hypoxia, necrosis, and cell adhesion (Benien 2014).

In a recent study, researchers used 3D cell culture to mimic a tumor growing in its microenvironment by co-culturing a cancer cell line with a fibroblast line and endothelial cells. In these experiments, the endothelial cells aggregated around clusters of non-small cell lung cancer cells (cell lines A549 or Colo699). The composition of these microtissues were confirmed by sectioning and immunohistochemical staining. Researchers were able to monitor the development of hypoxia in the tumor and also measure the concentration of angiogenic factors secreted into the culture medium. Finally, tumor growth and endothelial cell migration to the tumors were inhibited when anti-angiogenic drugs were added (Amann 2017).

In other studies, researchers studied hypoxia and necrosis at the core of tumors using multicellular 3D techniques. They identified 3 stages of oxygen tension during tumor growth *in vitro*, characterized by normoxia, hypoxia, and hypoxia plus necrosis. Importantly, the hypoxic and hypoxic with necrosis stages were associated with resistance to 5-fluorouracil, a commonly used antitumor agent. These findings were facilitated by the use of multicellular 3D cultures under standardized conditions, which might be used in the future to screen candidate compounds for use as antitumor agents (Däster 2017).

Genetic disease modeling

Organoids are stem cell–derived 3D tissue constructs containing organ-specific cell types; if cancer stem cells are used, the result is sometimes called a primary tumor spheroid, or tumoroid. Organoids can be used to model the organs from which they are derived and to reproduce disease states (Chen 2018). Organoid cultures will be discussed in detail in the next section, and cancer organoid models will be discussed in Section 7.1.

Some diseases are associated with specific DNA sequence variations. With stem cell–derived models, one of two approaches may be taken to generate isogenic lines. First, disease-associated mutations can be introduced into an existing line derived from a healthy donor using gene editing. Alternately, cell lines can be generated from patients carrying the relevant sequence and the mutation corrected to wild type. Wild-type and mutant phenotypes of differentiated cells relevant to disease progression can then be compared in the context of either 2D or 3D models. For example, researchers found that correction of cystic fibrosis transmembrane receptor (CFTR) mutations restored cAMP swelling function in adult stem cell–derived intestinal organoids (Schwank 2013).

The advent of genome editing using the CRISPR-Cas9 system has greatly facilitated the development of engineered cell lines for 3D models. Briefly, the CRISPR-Cas9 system consists of 2 parts, a target-specific guide RNA (gRNA) and a nonspecific endonuclease (Cas9). When introduced into cells, the gRNA and Cas9 form a ribonucleoprotein complex. If sufficient homology exists between the gRNA and the target DNA sequence, the complex will cleave the DNA. The DNA is then repaired by the cells via either of two mechanisms, which can create a gene knockout or allow for insertion of a new DNA sequence of choice (Horvath 2016). Using the CRISPR-Cas9 system, researchers edited the genome of colon organoids to model adenomas, with resulting chromosomal instability and aneuploidy, both of which are seen often in human colorectal cancer (Rios 2018).

Drug discovery

The drug discovery process is complex and multifaceted. 3D cell cultures are emerging as important tools to facilitate this process by allowing greater predictivity of drug efficacy and toxicity (Fang 2017).

From target identification through preclinical testing, 3D cultures of various types play roles in demonstrating activity and safety of lead compounds (Figure 1.2).

Precision medicine

3D cultures, especially organoid cultures, present the opportunity to create personalized therapies for each patient. For example, because cancer cells mutate and therefore differ between and among cancer patients, the capability to grow small tumor explants from individual patients and test these cultures for sensitivity to treatment has been used in multiple studies for identifying new drugs. In the field of respiratory medicine, researchers grew organoids from two patients with cystic fibrosis to identify whether patients would respond to the drug ivacaftor; in both cases the organoid cultures predicted the later positive patient responses (Takahashi 2019). Cancer researchers have observed a similar correlation in drug sensitivity between patient-derived pancreatic cancer tumoroids and the original tumors (Tiriac 2018). Since organoid cultures can be generated from adult tissue (as long as stem cells are present in the tissue), this approach should be a promising one for individualizing treatment paradigms for many diseases.

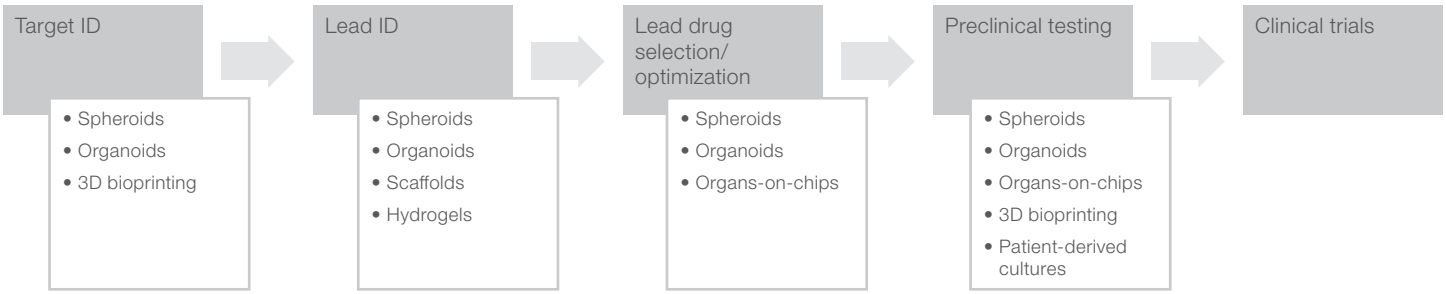

Figure 1.2. 3D cell culture types used in stages of drug discovery.

Organs-on-chips and bioprinting

An organ-on-a-chip is an engineered microfluidic culture device that recapitulates the microarchitecture and functions of a living human organ, including the lung, intestine, kidney, skin, bone marrow, and blood–brain barrier, among others. It is the intersection of microfabrication and cell culture. One type of organ-on-a-chip (Figure 1.3) uses polydimethylsiloxane (PDMS) wafers coated with photoresistant materials to create the microfluid channels and chambers essential for this device. The microfabrication techniques used to create the chips include soft lithography, photolithography, and contact printing. Organs-on-chips are used to study the effects that media flow and perfusion have on single or multicell systems and offer a potential alternative to traditional animal testing. Although organs-on-chips have been adapted to microwell plates, they do not lend themselves yet to high-throughput screens (Fang 2017).

3D bioprinting incorporates printing cells, scaffolding, and supportive materials into a final complex with the architecture, function, and topology resembling the organoid *in vivo*. This is generally done in a layer-by-layer manner to position cells in a specified spatial arrangement necessary for tissue or organ formation (Fang 2017; Figure 1.4). There are 3 approaches used in bioprinting: biomimicry, autonomous self-assembly, and fabrication of building blocks of tissue. Functional tissue such as bone, vascular tissue, heart tissue, and cartilaginous structures for transplant have been generated using bioprinting (Zhang 2017). Moreover, bioprinting has the capability to be adapted for high-throughput screening in the future (Fang 2017).

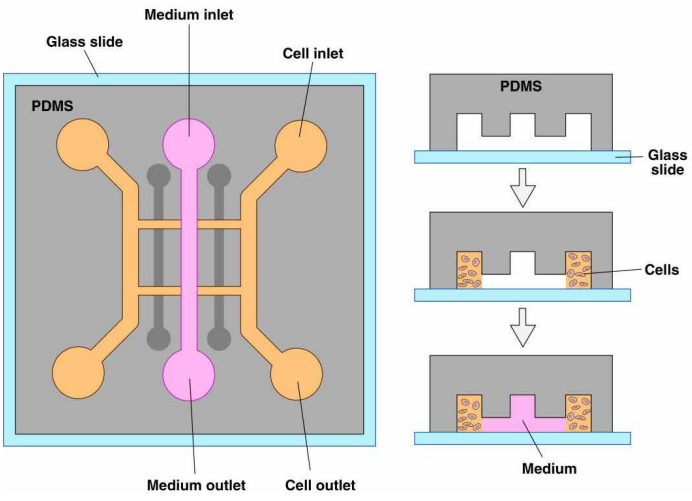

Figure 1.3. Organs-on-chips. Schematic diagram of the organ-on-a-chip device for 3D culture, consisting of microchannels and chambers that are accessible to reagents. Organ-on-a-chip technologies can allow the study of systemic effects when multiple organs are on the same chip.

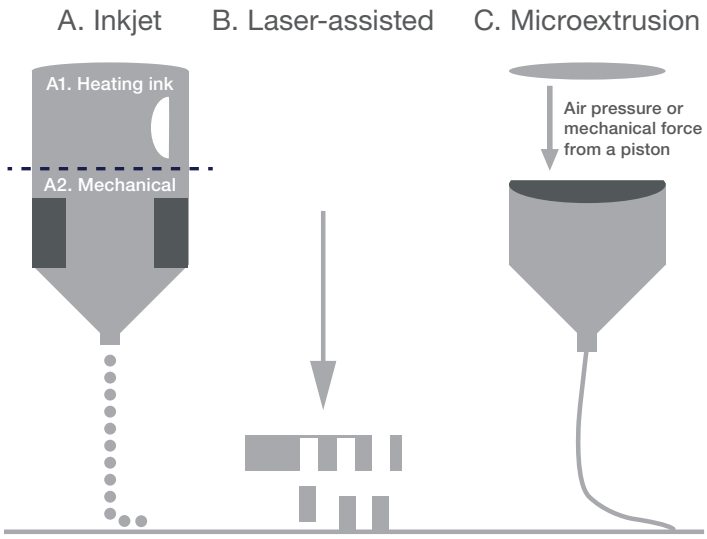

Figure 1.4. Bioprinting to create 3D cell cultures. Some of the techniques used to perform bioprinting are illustrated.

Section 2

Culture overview

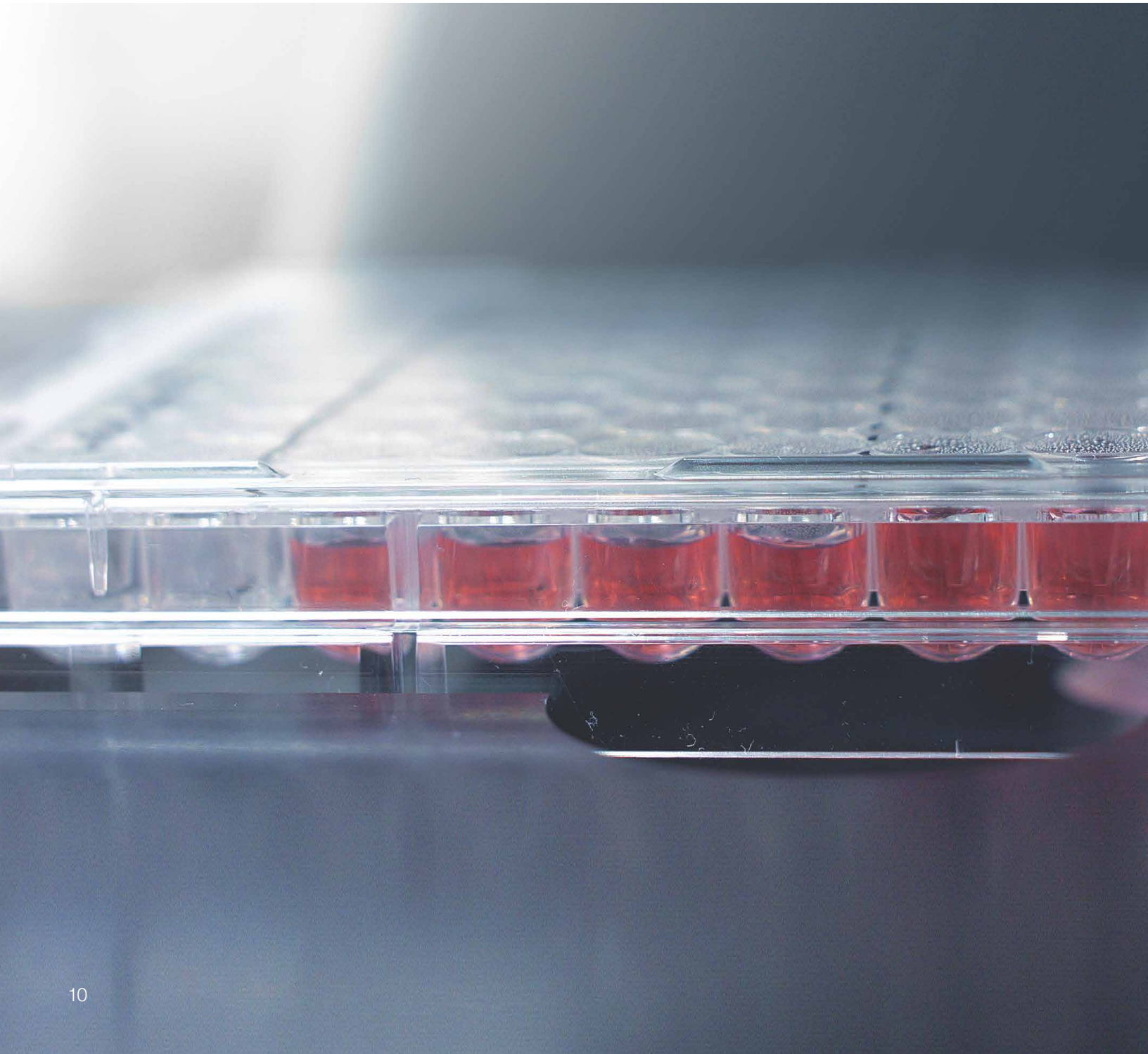

2.1

Spheroid models

A spheroid is a 3D cellular aggregate composed of one or more cell types that grow and proliferate, and may exhibit enhanced physiological responses, but do not undergo differentiation or self-organization. Common cell sources for spheroids are primary tissues or immortalized cell lines (Figure 2.1). Relying on the natural tendency of cells to aggregate in the absence of an adhesive substrate, spheroids more closely represent an *in vivo* environment because of increased cell-to-cell contact, proper spatial orientation, and increased extracellular matrix production within the cellular aggregate.

Spheroids are important in cell biology research because they bridge a gap between monolayers and complex organs. Since more than one cell type can be incorporated into spheroid cultures, research into complex processes such as angiogenesis and hematopoiesis can be carried out with these cultures. By varying the composition of hematopoietic stem cells in the spheroid mix, the differentiation of various lineages may be reproduced and studied. In this way, the important role of osteoblasts and pericytes in hematopoiesis has been elucidated (Fennema 2013; Ding 2012). Moreover, spheroid cultures can be used in high-throughput screening for drug discovery (Fennema 2013).

Applications for spheroid cultures range from assessing drug toxicity profiles to examining nutrient and oxygen gradients within tumor cores to studying hematopoiesis and cardiac development. Hepatic spheroids can be used as a means to screen for drug candidates that can induce liver toxicity by measuring effects on cell viability and cytochrome p450 (CYP) enzyme activity. Compared with traditional 2D screening, tumor spheroids allow for testing anticancer agents in a more relevant *in vitro* system that better recapitulates native tumor architecture. In early studies, Sutherland and colleagues found that the growth rate of CHO cells in a spheroid decreased as the diameter of the spheroid increased, due to a lack of nutrients reaching the cells at the center of the spheroid. In general, these spheroids resembled nodules seen in some cancer patients (Sutherland 1971). In a recent set of studies, researchers used cardiomyocytes plus vascular cells in spheroid culture to study cardiac development *in vitro* (Yan 2019).

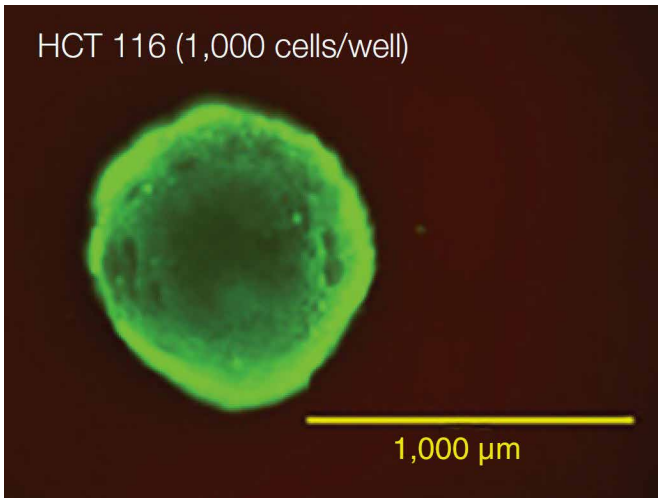

Figure 2.1. Photomicrograph of a spheroid composed of HCT-116 colorectal cancer cells in culture.

Spheroids composed of tumor cells represent model systems for studying the *in vitro* growth of tumors in their microenvironments. Using spheroid cultures, it is possible to remove cells from different regions of the spheroid and study how they differ with respect to clonogenicity, cell cycle state, and drug response (Sutherland 1981). When dissociated, tumor spheroids can be analyzed by flow cytometry; the effects of oxygen and nutrient gradients, as mentioned above, can be measured as well (Figure 2.2).

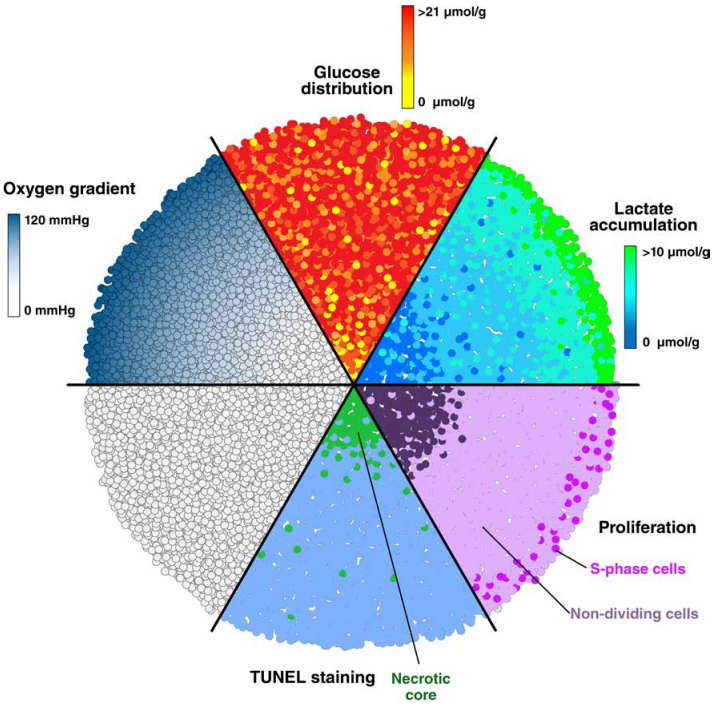

Figure 2.2. Zones in a spheroid tumor culture. Oxygen and nutrients fail to permeate to the necrotic core of the spheroid, and proliferating cells are more likely to be seen in the outer perimeter of the spheroid than within.

Besides drug resistance, drug toxicity can be studied, especially with regard to permeation to the center of the spheroid (Sutherland 1981). For example, studies have shown that tumor spheroids are more likely to show anticancer drug resistance than 2D cultures. In one study, the difference in sensitivity between 2D and 3D HCT-116 colorectal cancer cell cultures was 4-fold (Edmondson 2014). From the brief discussion above, one can conclude that spheroid cultures have an important role in advancing studies of cell physiology, cancer, and drug discovery.

2.2
Organoid models

An organoid is a 3D structure derived from either pluripotent stem cells (PSCs), neonatal tissue stem cells, or adult stem cells, in which cells spontaneously self-organize into properly differentiated functional cell types and progenitors that resemble their *in vivo* counterparts and recapitulate at least some function of the organ (Huch 2015). Organoids have a higher order of structure than do spheroids and reproduce organs of interest more closely than do spheroid cultures (Fang 2017). Organoids assemble and organize themselves, capture the complexities of their derived organs, display representatve cellular polarity, and recapitlulate proper cellular spatial architecture. Organoids can be used to study differentiation, physiology, and complex multicellular interactions *in vitro*. Their potential to advance drug discovery in cancer, neurobiology, and other fields is becoming increasingly evident (Editorial, *Nat Cell Biol* 2018).

The stem cells used to create organoid cultures may be embryonic stem cells (ESCs) or induced pluripotent stem cells (iPSCs), or derived from adult tissue (de Souza 2018). ESCs are derived from blastocysts (Huch 2015), while iPSCs are adult somatic cells reprogrammed to an embryonic-like state; the cells can then redifferentiate along another path of choice (Takahashi 2006; Figure 2.3). The use of iPSCs obviates the need to use embryos and the ethical concerns that might be raised. It has been shown that tissue-specific stem cells may reside in the epithelial compartment of several organs, including esophagus, stomach, and large intestine (Huch 2015; Figure 2.3).

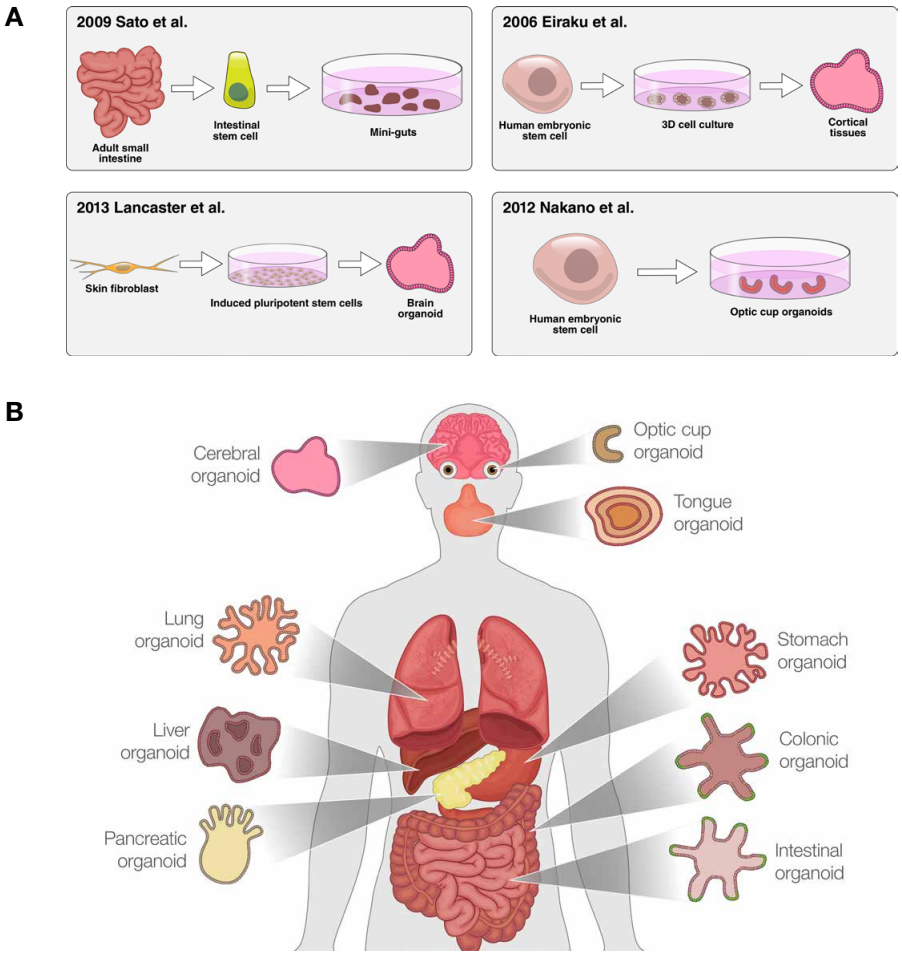

Figure 2.3. ESCs and iPSCs vs. adult stem cells. (A) PSCs derived from embryonic cells or somatic cells can differentiate into germ layers. **(B)** Adult stem cells are precommitted to their lineages by the organ from which they came.

Organoid cultures possess tremendous potential for disease modeling and studies on organ development (Kaushik 2018). For example, Dekkers and colleagues created intestinal crypt organoids from mice and human biopsy specimens. Using this approach, they studied the architecture of crypts from patients with cystic fibrosis, a disease caused by mutations in the *CFTR* (cystic fibrosis transmembrane conductance regulator) gene, and assessed the effect of inhibitors specific to the gene product (Dekkers 2013). In studying human cardiac development, Yan and colleagues used iPSCs to show that cell density and Yes-associated protein signaling were important for cardiac development (Yan 2019). In another example, Song and colleagues used iPSC-derived organoids to study angiogenesis and neural development and patterning *in vitro*. Using iPSCs plus adult-derived mesenchymal stromal cells, this group found elevated expression of blood–brain barrier genes, and expression of hallmarks of cortical neural differentiation, including synaptic activity (Song 2019). Researchers have noted early senescence among iPSC progeny, epigenetic differences compared with embryo-derived PSCs, and laboratory-specific gene signatures of iPSCs (Narsinh 2011). One conclusion to draw from these studies is to use the PSCs or adult stem cells best suited for the problem to be studied.

2.3
Barrier models

Organoid cultures have broad applications in cancer modeling and drug discovery studies. Sachs and colleagues created a biobank of >100 primary and metastatic mammary tumor lines derived from patients. In doing so, they established the culture conditions necessary to grow the mammary organoids and showed that the organoids retained the histology and genetics of the tumors of origin. These organoids may represent a third preclinical breast cancer model in between 2D cell lines *in vitro* and patient-derived xenograft (PDX) models *in vivo* (Sachs 2018). In addition, they developed an approach to use organoid cultures for high-throughput drug screening and for personalizing treatment for breast cancer (Sachs 2018). A similar approach for gastrointestinal cancer was reported by Vlachogiannis and colleagues, who created a biobank of gastrointestinal organoids. The goal was molecular profiling of the patient-derived organoids in order to assess responses to anticancer drugs. The patient-derived organoids in these studies showed similar responses to anticancer drugs as the patients from whom they were derived; the researchers observed 93% specificity and an 88% positive predictive value for the patient-derived organoids in forecasting response to targeted agents in the clinic (Vlachogiannis 2018).

Finally, organoids can be cultured from hepatocarcinoma cells grown in gel scaffolds, as shown by Takai and colleagues. The organoids grown retained epithelial–mesenchymal transition capability, part of the initiation to metastatic progression of cells (Takai 2016). In prostate biology, it is possible to create organoids that capture both luminal and basal epithelial lineages, and to study these in healthy and cancerous conditions (Drost 2016). The applications for these organoids include drug discovery, tumorigenesis, and prostate homeostasis (Drost 2016).

Another method employed for generating 3D cell culture involves using cell culture inserts that fit inside a multiwell plate with a small space below the insert for cell culture medium (Figure 2.4). The inserts (e.g., **Thermo Scientific™ Nunc™ Cell Culture Inserts**) are lined with a semipermeable membrane that allows for medium under the 3D construct in the well bottom and above the construct in the insert basket. 3D models that have used this method include skin, kidney, and gut models (Carlson 2008; Hoppensack 2014; Ootani 2009; Ude 2019). The cell culture insert method permits the study of barrier function of the tissue, if the model can maintain full-well coverage throughout its culture time. Barrier function can be assessed by measuring transepithelial electrical resistance (TEER), which is indicative of the integrity of the cellular barriers before they are evaluated for transport of drugs or chemicals (Srivinasan 2015). This is a popular system for 3D tissues that are fabricated through bioprinting methods, but certain models can be achieved in the absence of a printer.

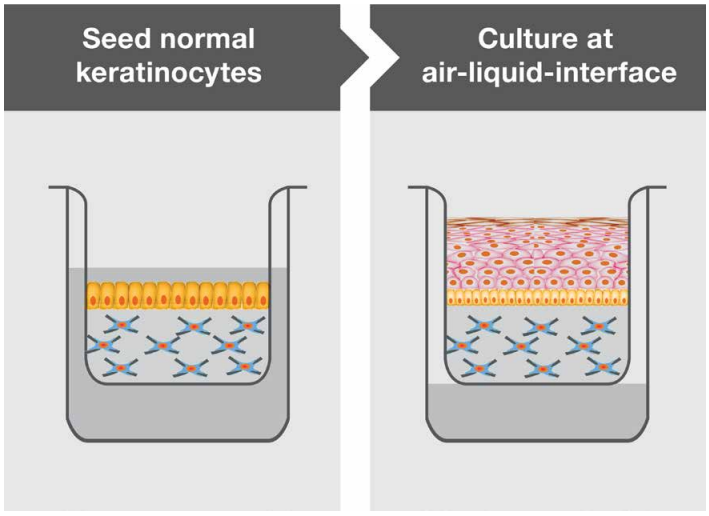

Figure 2.4. Representation of 3D skin culture using inserts in a multiwell plate. Dermal fibroblasts are embedded in an extracellular matrix, then layered on top with keratinocytes. The initial cultures are seeded submerged in media and then cultured at the air–liquid interface to promote keratinocyte differentiation and stratification.

Section 3

Sources for cell lines used in 3D cell models

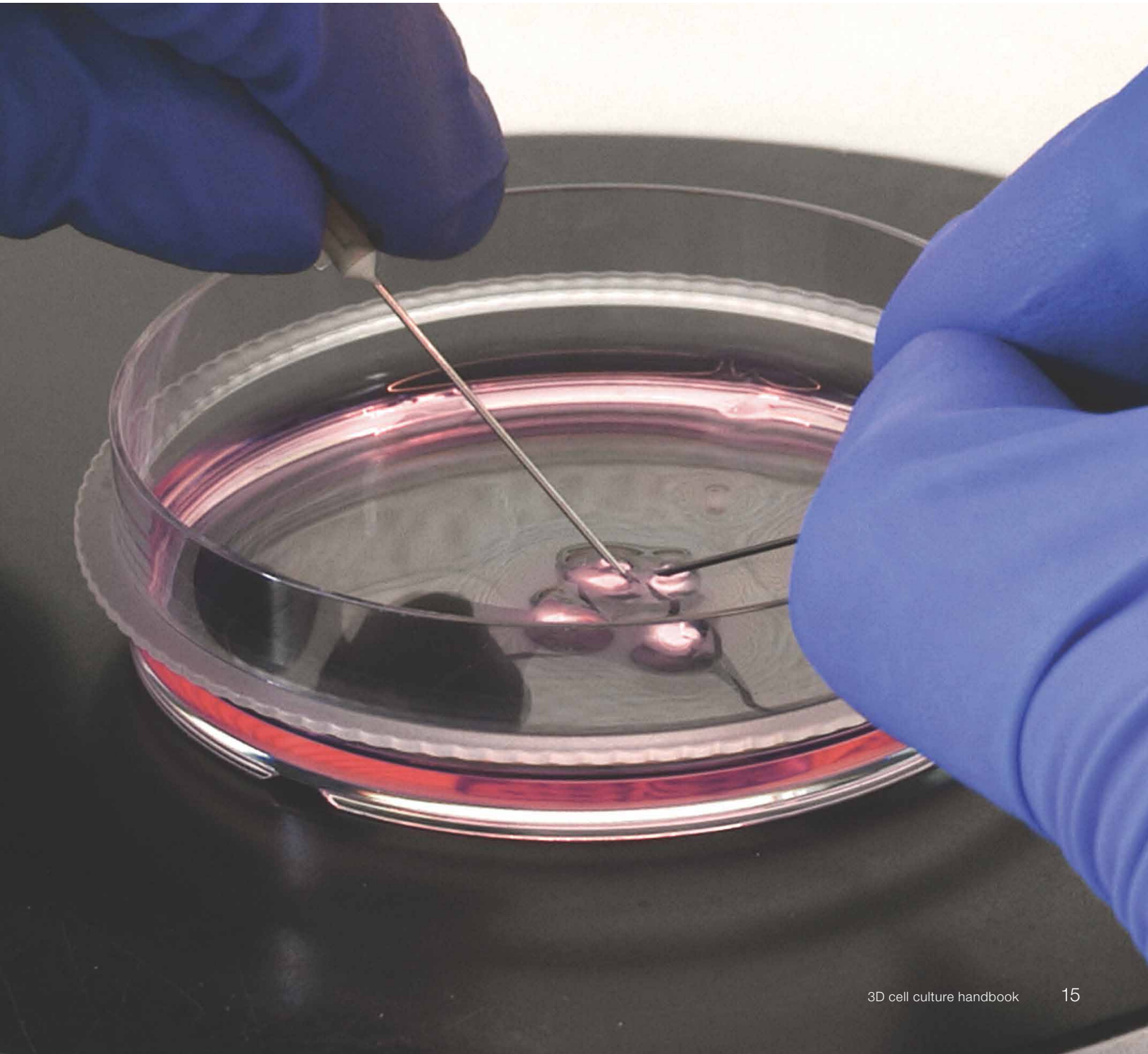

3.1

Introduction to cell lines

Cells for use in 3D cultures may be derived from several sources: cell lines, primary cells, and donor-derived cells. Typically, cell lines are obtained from cell bank repositories. Cell lines can proliferate indefinitely as long as appropriate culture conditions (medium, gas tensions) are met (Ulrich 2001). Commonly used tumor lines are easily available (Goodspeed 2016; Table 3.1) from commercial or public sources.

Cancer cell lines are fairly homogenous. However, this can be disadvantageous, as the cell lines may no longer display the heterogeneity of the primary tumor. Using sufficient numbers of cell lines may help recreate this diversity more accurately. Moreover, long-term culture may affect the genotype and therefore the phenotype and function of cell lines. It is recommended to begin with low–passage number cultures, expand and freeze cultures, and limit the number of passages during experiments. Finally, journals may require that laboratories prove the organ source of cell lines prior to publication of research. This stems from widespread contamination of many laboratories by the HeLa cell line (Gillet 2013).

Cell lines have been used to generate 3D cultures for drug screening. The lines from the NCI-60 cell bank—which include cell lines from liver, skin, and endothelium (Table 3.1)—were used to create spheroid cultures in order to test various compounds for anticancer activity (Selby 2017; Goodspeed 2016; Gholami 2013). The cultures were created in multiwell plates treated to prevent cell adhesion. Cells could be imaged *in situ* by microscopy and cell viability quantified *in situ* by luminometry (Selby 2017). Recently, the National Institutes of Health (NIH) entered into an international collaboration with Cancer Research UK, the Wellcome Trust Sanger Institute, and the Hubrecht Organoid Technology foundation to create a Human Cancers Model Initiative. Organoids for cancer research will be part of this cell bank to help evaluate and develop new treatments (Staudt 2016).

Table 3.1. Representative cancer cell lines in pharmacogenomic databases.

Tumor origin	Number of cell lines*			
	CCLE	GDSC	CTRP	NCI-60
Bladder	28	18	5	0
Breast	60	43	1	5
Colon	63	35	37	7
Hematopoietic and lymphoid	181	113	24	6
Liver	36	14	4	0
Lung	187	141	91	9
Ovary	52	20	26	7
Prostate	8	5	1	2
Skin	62	45	9	10

* CCLE: Cancer Cell Line Encyclopedia; GDSC: Genomics of Drug Sensitivity in Cancer; CTRP: Cancer Therapeutics Response Portal; NCI-60: a set of 60 cell lines collected by the National Cancer Institute.

3.2

Primary cells

Many types of primary cells have been used in 3D cultures. They include hepatocytes (Gomez-Lechon 1998), prostatic luminal and basal cells (Drost 2016), fibroblasts (Sanchez 2019), endothelial cells (Sanchez 2019), osteoblasts and osteoclasts (Skottke 2019), breast cancer cells (Wang 2018), and epithelial cells (Zhang 2019). Cells may be obtained from volunteer or patient tissue or from research animals. The number and breadth of cell type of primary cells is limited by donor availability and how large a sample might be obtained from a single specimen. Also, fewer primary cells from different donors may be available from rarer tumor types. Despite their limited availability and lifespan, primary cells are widely used in research because they may offer greater biological relevance than immortalized cell lines (Hussain 2017; Figure 3.1).

Although cancer cell lines have yielded valuable insight into the malignant process, their limitations discussed above can now be partially overcome by the use of primary cells in culture. Primary cell culture had formerly been limited by the short time span the cultures survived. For example, primary hepatocytes survived only 4–6 days when grown in traditional 2D cultures. Growing hepatocytes in a gel matrix extended survival of the cultures to 3 weeks (Hussain 2017; Gomez-Lechon 1998). However, not all investigators achieve these results with human hepatocytes grown in gel matrix.

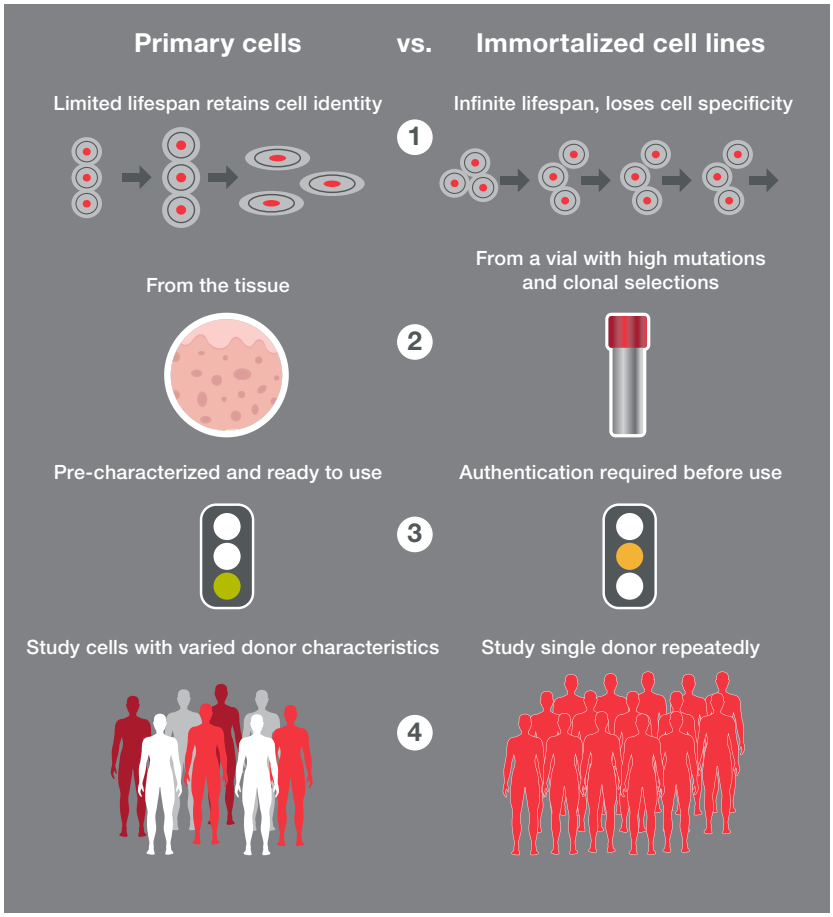

Figure 3.1. Differences between primary cells and immortalized cell lines. Primary cells retain biological relevance compared with immortalized cell lines. Their short culture spans can be overcome by growing them under 3D culture conditions.

Here are some common Thermo Scientific™ and Gibco™ products we offer:

Part of the body	Cell type	Medium	Supplement	Plastic	Matrices (or attachment factor)	Dissociation
Skin (neonatal and adult)	• Epidermal keratinocytes • Epidermal keratinocytes, pooled (neonatal)	• EpiLife Medium • M154 • Keratinocyte SFM • Defined Keratinocyte SFM	• HKGS • EDGS • S7 (Defined and animal origin–free)	• Nunclon Delta Dishes and Plates • Nunc Collagen I-Coated Plates • Nunc Cell Scrapers	• Coating matrix—used in conjunction with Supplement S7 or EDGS when growing human keratinocytes to enhance attachment, growth, and population doublings	• TrypLE Select enzymes • Trypsin-EDTA solutions
	• Melanocytes	• M254	• HMGS (for neonatal HEM) • HMGS-2 (for adult HEM)		• Not needed	
	• Dermal fibroblasts	• M106	• LSGS			
Heart	• Aortic smooth muscle • Coronary smooth muscle	• M231	• SMGS (for growth) • SMDS (to enhance differentiation)	• Nunclon Delta Dishes and Plates • Nunc Collagen I-Coated Plates • Nunc cell scrapers		
Skeletal muscle	• Skeletal myoblast	• DMEM	• 2% Horse Serum		• Vitronectin protein • rhLaminin • Attachment factors • Coating Matrix Kit	
Umbilical cord	• Umbilical vein endothelial • Umbilical vein endothelial pooled	• M200 • M200PRF	• LVES			
Breast	• Mammary epithelial	• M171 • HuMEC Ready Medium	• MEGS • HuMEC Supplement Kit	• Nunclon Delta Dishes and Plates • Nunc cell scrapers		
Liver*	• Cryo hepatocytes, pooled	• Hepatocyte Thaw Medium • CHRM • CHPM • Williams' E Medium	• HepExtend Supplement • Hepatocyte plating supplements • Hepatocyte maintenance supplements	• Gibco collagen I coated plates • Nunc cell scrapers	• Geltrex matrices • Collagen I protein	
	• Suspension hepatocytes	• Hepatocyte Thaw Medium • CHRM • Williams' E Medium	• Hepatocyte maintenance supplements			
	• Plateable hepatocytes	• Hepatocyte Thaw Medium • CHRM • Williams' E Medium	• HepExtend Supplement • Hepatocyte plating supplements • Hepatocyte maintenance supplements		• Geltrex matrices • Collagen I protein	
	• Kupffer cells	• Advanced DMEM • RPMI 1640 Medium	• Hepatocyte maintenance supplements (excluding dexamethasone) • Fetal bovine serum (FBS)		• Collagen I (no overlay)	

* If you'd like to inquire about any liver products not listed here, or to find out about custom projects, email **hepaticproducts@thermofisher.com**

Learn more at **thermofisher.com/primarycells**

3.3

Embryonic and induced pluripotent stem cells

As discussed in the previous section, primary cells are isolated directly from living tissue and, consequently, may be more representative of the *in vivo* environment than are immortalized cell lines (Hussain 2017). However, primary cells have limited availability, have a finite lifespan, and are terminally differentiated. In contrast, pluripotent stem cells (PSCs) can differentiate into any cell type in the body and have an unlimited capacity for self-renewal (Centeno 2018). Stem cells may therefore provide better models than primary cells for investigating long-term processes, such as those involving progression, degeneration, or development.

PSCs have been broadly utilized as *in vitro* models in 2D cell cultures. With 2D culturing, cells are grown in a monolayer and therefore do not interact with other cells or the environment as they would in complex, three-dimensional tissues or organs. To address these limitations, methods were developed to culture cells in 3D (Centeno 2018). Since PSC-derived 3D structures, such as organoids, more closely resemble the *in vivo* environment, they offer advantages for studying development, as well as for disease modeling and other applications (McCauley 2017; Rossi 2018). Organoids can be derived from PSCs that are cultured in suspension and self-aggregate into embryoid bodies. Cells in these aggregates can subsequently differentiate into different cell types and undergo self-organization and morphogenesis to create more physiologically relevant models as compared to 2D systems. To date, organoids have been generated for multiple organs, including but not limited to kidney, liver, lung, brain, and intestine (Dutta 2017, Lancaster 2013, McCracken 2014).

Organoids can be created with the two types of PSCs, embryonic stem cells (ESCs) and induced pluripotent stem cells (iPSCs), and studies with both ESCs and iPSCs have contributed to the understanding of disease and basic cell biology. ESCs are derived from embryos, and iPSCs are derived from somatic cells that are reprogrammed to an ESC-like state. Among the advantages of iPSCs is that iPSCs are not subject to local legislation or ethical concerns that surround the use of ESCs (Centeno 2018). Moreover, the ability to generate iPSCs has given researchers greater access to embryonic-like stem cells. Additionally, iPSCs can be obtained directly from individuals and therefore retain the genetic information of the individual. This genetic background can be critical for studying monogenic diseases and could potentially improve treatment and diagnosis in personalized medicine (Centeno 2018, Dutta 2017).

To generate iPSCs, somatic cells can be reprogrammed through several methods, including single-cassette vectors (Cre-Lox), mRNA or miRNA transfection, episomal plasmids, or non-integrating viral vectors (Malik 2013). Mature immune cells and hematopoietic stem cells, for example, have been reprogrammed to iPSCs. These iPSCs can then re-differentiate and subsequently be utilized for modeling disease and for possible future clinical applications (Jiang 2014; Figure 3.2). Systems using episomal vectors and a non-integrating virus are the **Invitrogen™ Epi5™ Episomal iPSC Reprogramming Kit** and the Invitrogen™ CytoTune™-iPS 2.0 Sendai Reprogramming Kit, respectively. The Epi5 reprogramming vectors work well for parental cells that are easy to reprogram, particularly when viral particles cannot be used. The **CytoTune-iPS 2.0 Sendai Reprogramming Kit** has the highest success rate among non-integrating technologies and can be used for both fibroblast and blood cell reprogramming. The workflow of this kit can also be simplified with the use of feeder-free media, such as **Gibco™ StemFlex™ Medium**.

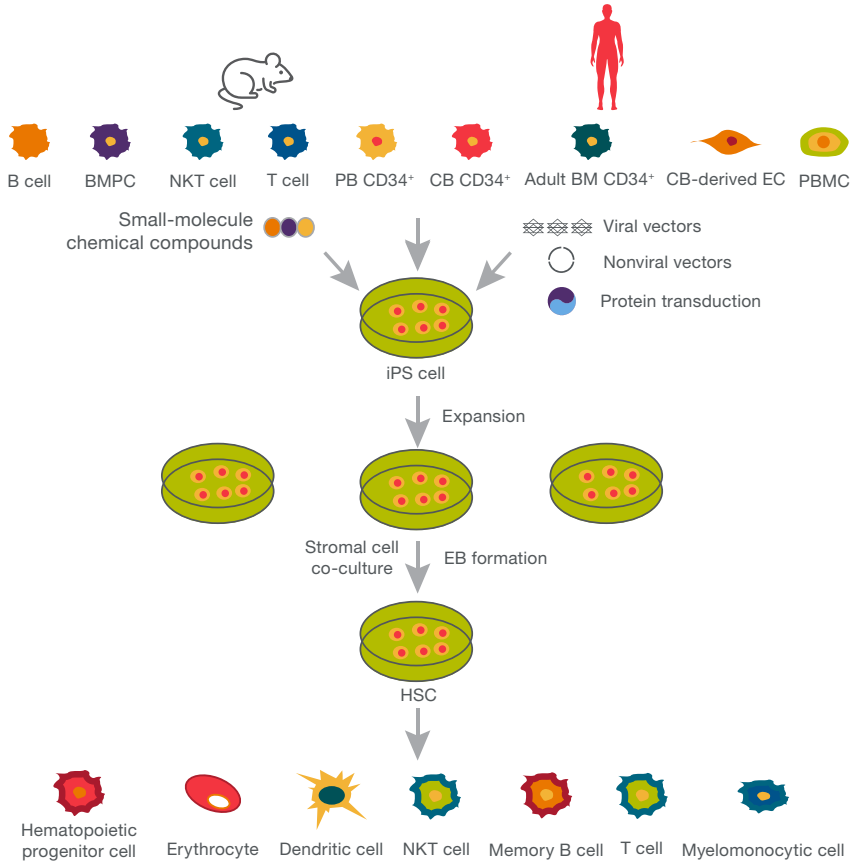

Figure 3.2. Reprogramming hematopoietic cells. Reprogramming hematopoietic and mature immune cells to iPSCs can be done using more than one technique. iPSCs then redifferentiate as needed. BM: bone marrow; BMPC: bone-marrow progenitor cell; CB: cord blood; EC: endothelial cell; iPSC: induced pluripotent stem cell; NKT: natural killer T; PB: peripheral blood; PBMC: peripheral blood mononuclear cell.

Both 2D and 3D models using iPSCs can be applied to various areas of research. With novel tools for gene editing, iPSCs can be used to generate (1) knockouts to study the impact of genes on cellular processes, (2) knock-ins to assess the impact of reversing point mutations on diseased states, and (3) reporter cell lines. CRISPR-Cas9 systems provide simple and efficient locus-specific editing and have enabled researchers to create disease model systems using iPSCs (Ben Jehuda 2018). This technology was used to create iPSC clones bearing the autosomal defect responsible for the rare autosomal disorder known as immunodeficiency, centromeric instability, and facial anomalies syndrome (ICF) (Horii 2013). In another example, frameshift mutations were corrected using CRISPR-Cas9 in cells from patients with Duchenne muscular dystrophy, restoring partial dystrophin function, and thereby changing the disease to the milder form, Becker muscular dystrophy (Young 2016). For efficient genome editing, optimal delivery of the CRISPR-Cas9 tools, such as the **Invitrogen™ TrueCut™ Cas9 v2** nuclease and TrueCut™ gRNA, is a key factor and can be accomplished under feeder-free conditions using StemFlex Medium. This medium has been designed to deliver superior performance not only in reprogramming but also in additional applications such as gene editing. In gene editing, StemFlex Medium provides faster recovery, maintenance of pluripotency, and more robust clonal expansion after single-cell sorting than other media (Chen 2018).

Not only has gene editing enabled significant advances in disease modeling in 2D systems using PSCs, but this technology has also been successfully applied to PSC-derived organoids. Using brain organoids, CRISPR-mediated gene editing can contribute to studies of neural development and neurological diseases (Kelava 2016). In another example, an investigation into the disease dyskeratotis congenita (DC) included intestinal organoids derived from isogenic pairs of iPSCs. The disease-causing DKC1 mutation was introduced if the iPSCs were derived from a healthy individual, or restored to wild type if derived from an affected individual. No genomic changes were introduced to the other line in each pair. Observations comparing maturation between the defective and wild-type organoids were consistent with clinical data for DC (Driehuis 2016). Similarly, organoids with mutations in genes that result in polycystic kidney disease (PKD) showed phenotypes that differed from the wild-type organoids and were similar to those described in patients (Driehuis 2016).

Throughout the processes utilizing PSCs, characterization of the cells is required to ensure pluripotency, to register cell lines, or to compare results when multiple cell lines are obtained. PSCs can be characterized by several methods. Alkaline phosphatase activity can be assayed using reagents such as the **Invitrogen™ Alkaline Phosphatase Live Stain**. Expression of this enzyme correlates with pluripotency (Marti 2013). Expression of key markers of PSCs, such as Oct4, SSEA4, Tra-1-60, and Sox2 (Marti 2013), can be assessed by immunocytochemistry using the **Invitrogen™ Pluripotent Stem Cell 4-Marker Immunocytochemistry Kit**. The **PluriTest™ Analysis Tool** with global gene expression data can also verify pluripotency. Karyotypic analysis to detect chromosomal abnormalities is commonly conducted, and the **Applied Biosystems™ KaryoStat™ Assay** provides a simple procedure that is accurate and reproducible. Finally, gene expression analysis by microarray or whole-genome sequencing can be performed to characterize PSCs even further.

As both 2D and 3D technologies continue to advance and translate to clinical research, large-scale sources of PSCs, especially iPSCs, will be required for drug screening, disease modeling, and potential therapeutic applications (Kropp 2017). As an example, the number of engineered cells required for an adult organ exceeds 10^9, so large-scale production of PSCs is necessary for research into regenerated organs (Mesquita 2019). Expansion of PSCs might be accomplished by adapting 3D culture methods combined with bioreactors (Kropp 2017) or growth on laminin substrates (Mesquita 2019).

StemFlex Medium

Gibco™ StemFlex™ Medium supports the robust expansion of feeder-free pluripotent stem cells (PSCs) and is formulated to deliver superior outcomes in today's more challenging applications, such as reprogramming, single cell passaging, and gene editing. StemFlex Medium allows for superior flexibility to select an optimal feeding schedule and a choice of matrices and passaging reagents.

Find out more at **thermofisher.com/stemflex**

3.4

Adult stem cells

Adult stem cells are not PSCs; rather, they are multipotent and committed to the lineage from which they derive. It is thought that tissue with high proliferation rates (e.g., intestinal epithelium) may harbor higher numbers of adult stem cells than more quiescent tissue (Mummery 2011). Many types of organoids can be derived from adult stem cells (Rossi 2018; Table 3.2 and Figure 2.3B).

Table 3.2. Organoids arising from adult stem cells.

Tissue or organ	Species source
Gastric corpus and pyloric antrum	Mouse
Small intestine	Mouse
Colon	Human, mouse
Liver	Human, mouse
Trachea and/or bronchi	Human, mouse
Pulmonary alveolus	Human, mouse
Prostate	Human, mouse
Fallopian tube	Human
Mammary gland	Human, mouse
Salivary gland	Human, mouse
Bone	Human

Adapted from: Rossi 2018; Baptista 2018.

It should be noted that adult stem cells tend to generate only the epithelial compartment of organs, whereas PSC-derived organoids have the ability to differentiate into potentially all organ-specific cell types. However, PSCs tend to retain fetal genotypes or phenotypes, whereas adult stem cell–derived models form differentiated cells (Huch 2015).

Mesenchymal stromal cells (MSCs) are adult stem cells that are present in many tissues and are widely known for their capacity to differentiate into osteoblasts, adipocytes, and chondrocytes. MSCs have been grown in spheroid cultures, where they differentiated into several types of cells with delayed senescence (Cesarz 2016). As well, the spheroid aggregates enhanced paracrine secretion of angiogenic, inflammatory, and other factors (Malik 2013).

Recreating the proper environment for differentiation of adult stem cells into the desired end organoid has been the focus of recent studies. Parameters such as composition of the extracellular matrix (ECM), growth factors and supplements included in medium, and presence of feeder layers of cells affect the final outcome. For example, in cardiac research the use of ECM derived from decellularized cardiac tissue has proven to be superior to single-component ECMs. Another advancement has been the development of serum-free techniques, as the field moves to clinical applications. Serum-free culture is intended to reduce spread of potentially harmful agents such as latent viruses (Bardelli 2017).

An interesting use of 3D culture techniques with adult stem cells was described recently by Baptista and colleagues. Using 3D-printed scaffolding (made of a ceramic-like material), they seeded adult stem cells as spheroid cultures, and grew bone. This is noteworthy because of the crystalline and organic nature of bone, which must be strong enough to bear weight. Here, the use of bioceramic composites in the culture as an additional material showed promise for developing substitutes for bone grafts (Baptista 2018).

3.5

Patient-derived cells

Patient-derived cells obtained from primary tissues, normal and diseased, can be used to create organoids and have obvious applications in cancer research, such as investigating resistance to treatment (Chonghalle 2018). Organoids have been derived from diverse tumor types, including breast cancer, liver cancer, bladder cancer, glioblastoma, and pancreatic cancer (Nagle 2018). Using a basement membrane–derived matrix to create organoids from patient specimens, researchers created a library of nearly 100 pancreatic cancer organoids. Since this cancer type is very difficult to treat, the creation of an organoid library spanning cancer subtypes and stages is expected to be useful in drug discovery (Tiriac 2018). In prostate cancer research, organoids derived from 3D cultures of tumor specimens can be used with high-throughput screening techniques and for xenografts in mouse tumor models (Namekawa 2019). Patient-derived cells in spheroid culture were created from glioblastoma obtained by resection or biopsy. These spheroids were then screened for response or resistance to various anticancer agents. In this way, several nonstandard drugs were identified for potential use in the treatment of glioblastoma (Yu 2018).

Section 4

Matrices

4.1

Introduction

Selecting the right culture matrix is an important first step in developing a successful culture system for organoids and spheroids. Organoid and spheroid cell culture models can use either matrix-independent or matrix-dependent systems that are naturally derived or synthetic (Rossi 2018). Matrix-dependent systems are used to transition more easily from a 2D monolayer environment to 3D models. Matrix-independent systems can be used for scale-up and full organ development. For organoid development, the matrix should enhance self-assembly (Xie 2017).

Matrix materials include hydrogels and peptide hydrogels (Jongpaiboonkit 2009; Tibbit 2009; Worthington 2015), polysaccharides (Diekjurgen 2017), collagen, laminin, alginate, and more commercially available products. These will be discussed in more detail in the following subsections.

4.2

Extracellular matrices

Extracellular matrices (ECMs) are used increasingly in research because they form a microenvironment that resembles the *in vivo* environment sufficiently to allow for proper cell behavior, such as growth and signaling (Godugu 2018). There are two main types of matrix-dependent systems, natural/organic (derived from animals or plants) and synthetic ECMs.

Among the ECMs derived from natural sources are **Gibco™ Geltrex™ matrix**, a basement membrane extract (BME) purified from murine Engelbreth-Holm-Swarm (EHS) tumors; the **Gibco™ AlgiMatrix™ 3D Culture System**, derived from algae; collagen, derived from animal tissue and other by products; and laminin, derived from mouse tumor cells or human cells. Synthetic ECMs include peptide-acrylate surfaces, poly[2-(methacryloyloxy)ethyl dimethyl-(3-sulfopropyl) ammonium hydroxide] (PMEDSAH), hydrogel interfaces of aminopropylmethacrylamide, and polyvinylalcohol-based hydrogels (Hayashi 2016). Another synthetic hydrogel is polyethylene glycol (PEG). PEG is often used because it adsorbs little protein, making it suitable for the scientist to define ligand presentation to cells. Furthermore, PEG can be modified by adding various functional groups (Caliari 2016). Peptide hydrogels may be natural or synthetic in origin (Worthington 2015). References for using many of these reagents are given in Table 4.1.

Table 4.1. Protocols for ECM reagents.

Matrix	Advantages or uses	Protocol	Reference
AlgiMatrix (alginate sponge)	Cells closely match normal morphology and behavior in natural matrix	*In situ* harvesting of spheroids from AlgiMatrix plates	These protocols can be found at **thermofisher.com/algimatrix**
		Isolation of viable spheroids from AlgiMatrix reagent	
		Anticancer drug screening	
Laminin	Mimics properties of the natural basement membrane more closely	Differentiation of corneal epithelium	**Matrices sourcebook from Thermo Fisher Scientific**
Collagen	For cell migration studies	General protocol	Doyle 2016
Fibronectin	For studying cell-to-matrix interactions	General protocol	Franco-Barraza 2016
Geltrex	For cell invasion and differentiation studies	Degradation of 3D cultures	Goertzen 2018
		Beta-cell differentiation	Sui 2018
		In vitro angiogenesis	Endothelial tube formation assay (**thermofisher.com/manuals**)*
Hydrogel	Identify conditions that promote cell viability	General protocol	Jongpaiboonkit 2009

* Protocol is used with Gibco™ Human Umbilical Vein Endothelial Cells (Cat. No. C0035C). Search our manuals page using the Cat. No. to view this protocol.

Naturally derived basement membrane extracts are the most widely used ECMs today for the growth and propagation of 3D models. While these ECMs have a number of advantages, including preservation of biological architecture, promotion of normal biological function, and maintenance of integrin binding sites (Dhaliwal 2012; Diekjurgen 2017), they also have their own unique challenges. As these materials are purified from murine EHS tumors, there is an inherent lot-to-lot variability in these ECMs that may require lot testing or pre-validation prior to use. Implementing additional purification steps during the production of BMEs, as in the Geltrex matrix product, can help limit the lot-to-lot variability, but it never completely eliminates the issue. On top of the lot-to-lot variability issue, the exact composition of BMEs is unknown—they and contain multiple undefined ECM proteins and growth factors. While these ECM proteins and growth factors likely play a key role in helping to promote the growth of the 3D models, the use of an undefined or variable BME can make moving into clinical applications a challenge.

As a result of the inherent variability of naturally derived ECMs, some scientists have started to explore more chemically defined or synthetic versions. Synthetic ECMs include the certainty that the matrix is free of exogenous or extraneous growth factors, can be customized for desired porosity and stiffness, and have greater reproducibility among experiments (Hayashi 2016; Dhaliwal 2012). However, some synthetic ECMs have poor biocompatibility, and the potential for release of toxic by-products during cell culture.

4.3

Matrix-independent systems

Matrix-independent systems lack a user-provided ECM. Instead, these systems provide conditions in which cells may create their own ECM (Diekjurgen 2017). Thus, matrix-independent systems have the advantage over matrix-dependent systems in eliminating the unwanted biological impact from ECMs of animal origin and in being less tedious to synthesize and fabricate (Turker 2018; Knight 2015). Additionally, matrix-independent systems may benefit from a lower cost of reagents.

The types of matrix-independent systems include low cell attachment plates (e.g., **Gibco™ Nunclon™ Sphera™ plates**), hanging-drop culture, spinner flasks, rotary culture systems, and engineered tissue constructs. References for using many of these systems are given in Table 4.2.

Table 4.2. References for matrix-independent systems.

System	Use	Reference
Nunclon Sphera plates	Spheroid cultures	• Guzman 2017 • Stadler 2017 • Takagi 2016 • Sin 2017 • Chittajallu 2015
Hanging-drop culture	Tumor spheroid generation	Raghavan 2016
Spinner flasks	Expansion of iPSCs on microcarriers	Gupta 2016
Engineered tissue	Multilayered 3D cardiac tissue	Shimizu 2002; Shimomura 2018

Advantages of the simpler systems like hanging-drop culture are lower cost and ease of use, whereas their disadvantages include variability in resulting spheroid size (if flat-bottomed, low-attachment plates are used) (Breslin 2013). Among agitation-based approaches like rotator and spinner cultures, large-scale cultures are easily created but specialized equipment is required, which may be costly (Breslin 2013).

Combining matrices with matrix-independent systems creates a synergy for enhanced cell growth and differentation (Ovsianikov 2018). Enhanced self-assembly has been observed using the combined systems, wherein the matrix protects the spheroids from mechanical damage (Ovsianikov 2018). Moreover, matrices increase cell density within a cell culture well and may also provide support for morphogenesis, as well as physical cues for polarization, differentiation, and organization. The synergy of combining matrices and matrix-independent systems is illustrated by using specific ECM to facilitate desired differentiation. For example, encapsulation of embryoid bodies with Geltrex matrix before transfer to Nunclon Sphera plates enhances neural differentiation from pluripotent stem cells.

We offer a range of products for use in matrix-dependent and matrix-independent systems. To help guide your selection, products compatible with specific cell types are shown in Table 4.3.

Nunclon Sphera 3D culture system

The Nunclon Sphera system is designed for spheroid culture (e.g., 3D tumor spheroids) and organoid culture (e.g., brain organoids) with a wide selection of formats from plates to dishes and flasks. The 3D cell culture surface allows virtually no cell attachment to the cultureware, supporting the establishment of 3D spheroids and organoids via cell-to-cell aggregation through naturally secreted ECMs.

The proprietary surface coating of Nunclon Sphera cultureware prohibits any protein adsorption to the surface, thereby minimizing monolayer cell adhesion to the culture vessel.

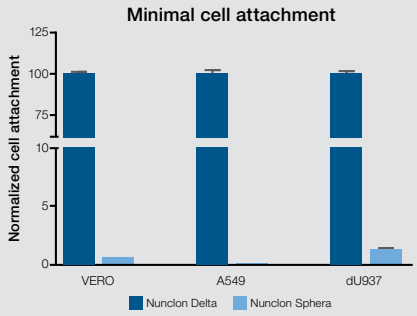

Find out more at **thermofisher.com/sphera**

Another option for creating 3D cell models is using **Thermo Scientific™ Nunc™ dishes with UpCell™ surface** treatment for culturing your cells. The UpCell surface is specially coated to allow for non-enzymatic methods for cell dissociation, relying instead on reduction in temperature. With the UpCell surface, you can create confluent cell sheets that utilize naturally produced ECM from the cells to create layers of different cell types that can add complexity to your model.

The UpCell surface enables harvested cell sheets to be stacked in order to form 3D tissue models. Stacking of cell sheets, also known as cell sheet engineering, was pioneered by Okano and colleagues (Yamada 1990; Yang 2005 and 2007). The preserved subcellular matrix of a harvested cell sheet provides the adhesive necessary for stacking. It functions as a natural glue to bond the cell sheet to an underlying recipient cell sheet or to a recipient site in a transplantation model, without the use of fibrin glue or sutures.

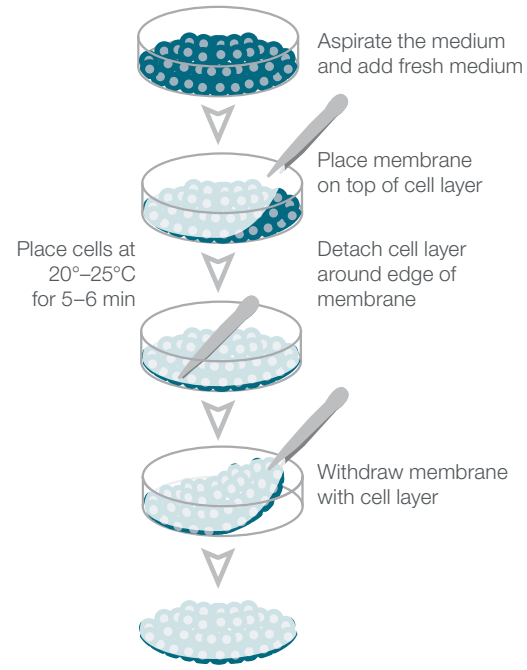

Table 4.3. Selection guide for Thermo Scientific™ cell culture plastic surfaces.

Select your Thermo Scientific surface								
		Thermo Scientific surface treatments						
Cell types		Nunclon Delta	Nunclon Vita	Collagen I	Poly-D-lysine	Nunclon Sphera	Nunc UpCell	Untreated surface
Hepatocytes		•	•	•		•	•	
Endothelial cells		•		•		•	•	
Neuronal cells	Neurons	•			•		•	
	Neurospheres					•		
Epithelial cells		•	•	•		•	•	
Tumor cells		•	•	•	•	•	•	
Blood cells	Macrophages, dendritic cells, neutrophils	•				•	•	
	Lymphocytes	•						•
	Platelets	•		•			•	
Stem cells	MSC	•	•	•		•	•	
	HSC	•			•	•		
	ESC and EB	•†	•§			•		

† Requires extracellular matrix (ECM) coating. § Requires conditioned media from feeder cells and ROCK inhibitor.

Section 5

Media and supplements

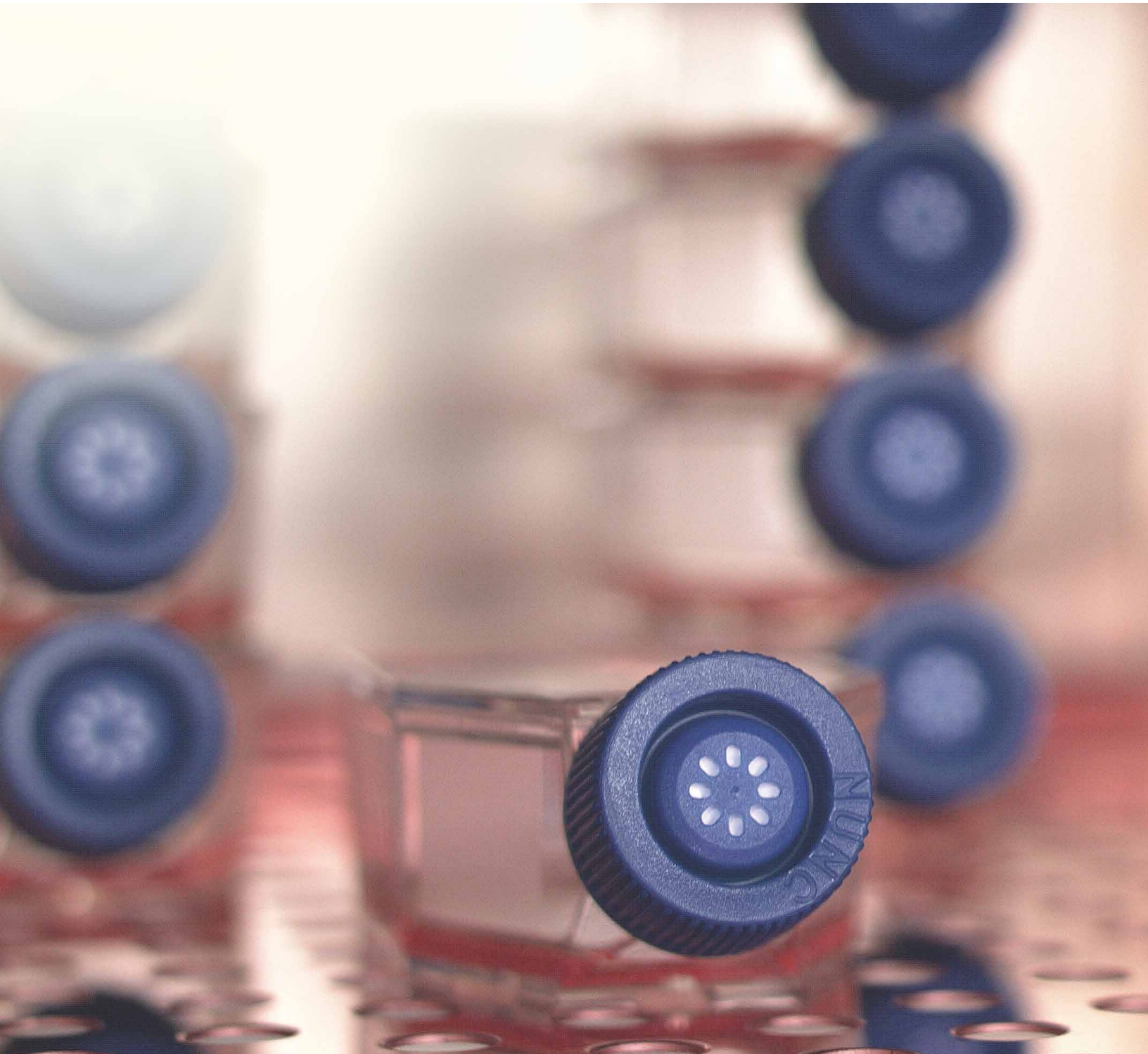

5.1

Introduction

Cell culture began with a balanced salt solution, devised by Sidney Ringer in 1882 to keep frog hearts beating after dissection (Yao 2017). Several other balanced salt solutions followed shortly, including Earle's and Hank's balanced salt solutions (Yao 2017). In 1907, Harrison observed nerve cell outgrowth in a culture medium that was mainly lymph fluid (Yao 2017; Simian 2017). Harrison used a technique that would come to be known as hanging-drop culture, a 3D culture method (Rodriguez-Hernandez 2014; Simian 2017). Further work in Harrison's laboratory showed in 1909 that mammalian cells required plasma in place of lymph fluid for growth (Yao 2017), again using the hanging-drop method (Rodriguez-Hernandez 2014). By 1911, Margaret and Warren Lewis showed that a solution composed of balanced salt, amino acids, bouillon, and glucose was better for chick embryo culturing than balanced salt solution alone (Yao 2017). This observation represented an advance towards creating a basal medium for cell culture.

In the 1940s and 1950s, Earle and later Gey established immortalized cell lines (Lucey 2009). Earle established fibroblast lines after treating primary fibroblasts with carcinogens. Gey experimented with the media and culture conditions to determine what supported the growth of cervical cancer cells best (spinner bottles and nearly any medium, as it turned out) (Yao 2017; Lucey 2009).

With the establishment of immortalized cell lines and some basal media, other investigators soon showed that cells require pyruvate and 13 of the 20 amino acids in the medium, as well as vitamins (Yao 2017). Investigators also showed that basal medium could be tailored to cell type, such as lymphocytes, fibroblasts, and liver epithelial cells (Yao 2017).

Basal media and supplements provide nutrition, growth factors, vitamins, trace elements, and pH buffering to cells in culture, whether the culture is 2D or 3D (Rodriguez-Hernandez 2014). The best practice is to choose the medium most suited for the cells to be grown. For example, many people use RPMI 1640 to grow lymphocytes in short- and long-term cultures, whereas many tumor cells are often grown in DMEM or DMEM/F-12.

5.2

Media

The same basal media used in 2D cell culture are used in 3D cell culture. As discussed in the previous subsection, cell culture media were developed in part using 3D culture techniques, so it is not unexpected that the same media would be used for both culture types. Table 5.1 lists several types of 3D culture and suggested media for each.

Media can be divided into natural or synthetic, the former being mainly biological fluids and the latter being the basal media in common use (Yao 2017). Synthetic media can be augmented with serum or plasma or can be completely serum-free. Synthetic media can also be completely free of nonhuman-derived components (xeno-free) or can be completely chemically defined (Yao 2017). Specialized or custom-made media are available from commercial sources. Customer service from vendors of cell culture media can help users determine which medium might be best suited for the application.

Table 5.1. Examples of media used for 3D cell culture.

Cell type	Medium	Reference
Brain, PSCs	DMEM/F-12, Neurobasal Medium	Lancaster 2013
	DMEM/F-12, Neurobasal Medium	Pasca 2015
	DMEM/F-12, Neurobasal Medium	Iefremova 2017
	DMEM/F-12, Neurobasal Medium, Essential 6 Medium	Zhou 2017
	Neurobasal Medium	Muotri 2018
	Neurobasal Medium	Smits 2019
	Neurobasal Medium	Kim 2019
Intestine, PSCs	Knockout DMEM	Uchida 2017
	RPMI 1640, Advanced DMEM	Watson 2014
	DMEM/F-12, RPMI 1640, Advanced DMEM/F-12	Spence 2011
Kidney, PSCs	Advanced RPMI 1640	Morizane 2015; Freedman 2015
Fetal-derived cells	DMEM/F-12	Li 2016
Liver, PSCs	RPMI 1640, DMEM/F-12, StemPro-34 SFM	Takebe 2017
Adult stem cells	Advanced DMEM/F-12	Huch 2013
Primary cells	HepaRG Medium	Proctor 2017
Lung, PSCs	RPMI 1640, Advanced DMEM/F-12	Dye 2015
	Advanced DMEM/F-12	Wilkinson 2016
Intestinal cells	Advanced DMEM/F-12	Sato 2009
	F-12	Ootani 2009
Tumor organoids		
Esophageal	Advanced DMEM/F-12	Sato 2011; Li 2018
Colon	Advanced DMEM/F-12	Sato 2011
Pancreatic	Advanced DMEM/F-12	Boj 2015
Mammary	Advanced DMEM/F-12	Lee 2007; Sachs 2018

PSCs: pluripotent stem cells; SFM: serum-free medium.

5.3

Supplements

In general, basal media such as those listed in Table 5.1 are supplemented, often with serum and additionally with specific growth factors, cytokines, and hormones. The supplements added help make a medium specific for growing the cell line of interest, whether in 2D or 3D culture. **Gibco™ B-27™ Supplement** is best known as the most cited neural cell culture supplement. Scientists are discovering that the supplement benefits more than just neural cell types in adherent culture. In the realm of 3D culture, it has been used in a plethora of applications, spanning a wide range of cell types. Example references for B-27 supplements added to 3D cultures are given in Table 5.2. The application note "The use of B-27 Supplement in establishing and characterizing functional 3D neural spheroid models from monolayer-expanded NSCs" is provided in Appendix A.2 to demonstrate the effects of different supplements on neural spheroids.

Table 5.2. References for B-27 supplements used in 3D cell culture.

Cell type	Reference
Brain, PSCs	Smits 2019
Brain, PSCs	Kim 2019
Colon	Devall 2020
Lung	Strikoudis 2019
Esophagus	Guha 2019
Intestine	Szvicsek 2019
Kidney	Koning 2019
Kidney	Grassi 2019
Fallopian tube	Kessler 2019
Retina	Kaya 2019
Prostate	Pappas 2019
Sweat glands	Diao 2019
Breast	Ísberg 2019

One type of supplementation is conditioned medium, which is the cell-free supernatant fluid removed from cells grown under specific conditions (i.e., spent medium). In the early 1970s, Iscove and colleagues used the spent medium from human leukocyte cultures to promote the growth of human bone marrow cells (Iscove 1971). Now it is known that under the correct growth conditions, the spent medium may contain growth factors, cytokines, angiogenesis factors, and other factors that enhance cell growth. Indeed, sophisticated studies of the composition of conditioned media have been performed to identify the exact factors secreted under different conditions in disease and health (Dowling 2011).

3D cultures can be sources of conditioned media. For example, stem cell–conditioned medium may prove useful in regenerative medicine. Conditioned medium from spheroid cultures of adult human stem cells has been found to contain vascular endothelial growth factor, platelet-derived growth factor, fibroblast growth factor 2, hepatocyte growth factor, and CXCL12 (Pawitan 2014). It is important to understand that because conditioned medium is undefined, it can add a source of variability to cultures.

Section 6

Imaging and analysis

6.1

Importance of visualization in 3D cell cultures

As in 2D cell culture, examining cells as they are cultured is an important part of the process to ensure growth conditions have been proper or to track efficacy of a novel therapeutic compound. 2D cultures are easily viewed *in situ* by phase-contrast microscopy, but the thickness of 3D cultures presents more challenges for *in situ* microscopy. Beyond this, cells function over time, so an ideal system would collect images over time (Freimark 2010).

There are several types of microscopy and other imaging methods that can be used with 3D cell culture. Among the microscopy and imaging techniques are confocal and multiphoton microscopy, live-imaging fluorescence microscopy, and optical coherence tomography (Graf 2010; Waters 2013; Huang 2017; Lakner 2017; Kim 2016). Types of microscopy used for 3D cell culture are summarized in Table 6.1.

Table 6.1. Microscopy techniques used with 3D culture.

Imaging technique	Advantages and disadvantages	Accessibility
Brightfield (light) microscopy, histology, phase-contrast microscopy	• Brightfield microscopy requires stained samples • Histology requires fixed, sectioned, and stained samples • Phase-contrast microscopy visualizes live cells but at relatively low density	• Commonly available • Low cost • Ease of use
Widefield fluorescence microscopy	• Flexible for both fixed- and live-cell imaging	• Standard fluorescence microscopes are generally available • May be expensive • Training required
Confocal microscopy	• Stained samples only • Fixed and sectioned samples yield higher-resolution images • Live cells can be visible using reporters • Reconstruction of 3D architecture of thicker samples is feasible	• Limited availability • Expensive • Training required
Transmission electron microscopy	• Samples must be fixed and sectioned	• Limited availability • Expensive • Extensive training required
Scanning electron microscopy	• Samples must be fixed and sectioned	• Limited availability • Expensive • Extensive training required
Multiphoton microscopy	• Allows imaging of structures deep within a tissue block	• Limited availability • Expensive • Extensive training required

6.2

Tools to monitor 3D cell model characteristics

As with 2D cell culture, one should monitor 3D cultures to ensure cultures are healthy. When using fluorescent dyes and ultraviolet microscopy, culturing cells in phenol red–free media may be preferred. A simple fluorescent method to determine viability is the use of fluorescein diacetate, which can be used with a fluorescence microscope or flow cytometer (Proffitt 1996). A simple light microscopy method is the use of trypan blue (Piccinini 2017). For both fluorescent and light microscopy techniques, traditionally a hemocytometer was used to count the number of cells per unit volume. For greater speed and reproducibility, an automated cell counter with reusable slides, such as the **Invitrogen™ Countess™ II FL Automated Cell Counter**, can be used to quantify cell viability using fluorescent or nonfluorescent dyes.

Note that for these techniques, 3D cultures are not assessed *in situ* but rather cells are removed from culture for analysis, as they would be from a 2D culture. A detailed discussion on choosing fluorophores and other considerations for fluorescence microscopy can be found on the Molecular Probes School of Fluorescence web page (**thermofisher.com/mpsf**), and a discussion on confocal imaging protocols can be found in an online article (Sargent 2019).

Spheroids may be harvested simply by rinsing them out of wells, but cells grown on some scaffolds may need to be removed from the scaffold for further downstream analysis. There are special reagents created to dissolve some scaffolds, such as Gibco™ AlgiMatrix™ Dissolving Buffer for the Gibco™ AlgiMatrix™ 3D Culture System. Once cells are free of the scaffold, they may be quantified and assessed for viability using a variety of methods, such as measuring the metabolic activity with redox dyes (e.g., Invitrogen™ PrestoBlue™ HS Cell Viability Reagent, alamarBlue™ HS Cell Viability Reagent, CyQUANT™ XTT Cell Viability Assay) or measuring the DNA content (e.g., Invitrogen™ CyQUANT™ Direct Cell Proliferation Assay).

Automated imaging helps users analyze cellular events taking place over time, such as angiogenesis or wound healing. In tumor research, an automated light microscopy system was used to monitor cell survival and proliferation (Eka 2015). The system was measured against the same parameters for the cells grown in 2D culture conditions to assure its robustness (Eka 2015). Automated systems such as Invitrogen™ EVOS™ imaging systems can be used to assess viability by acquiring live-cell fluorescence images with the help of the Invitrogen™ EVOS™ Onstage Incubator (**thermofisher.com/evososi**), which offers stagetop incubation in an easy-to-operate format.

Automated imaging is commonly used for analysis of individual cells, whereas microplate readers are used for homogenous assays to quantify cellular behavior as an average of the population. Microplate readers can be used to detect chemical, biological, or physical reactions by measuring emitted light produced from commonly used assays, such as PrestoBlue HS or CyQUANT XTT assays. Through this readout, cell viability for both 2D and 3D models can be assessed (Montoya 2019).

Countess II FL Automated Cell Counter

With options for a reusable slide and fluorescence capabilities—brightfield and two user-changeable fluorescence channels—the Countess II FL Automated Cell Counter can count cells and measure cell viability in as little as 10 seconds.

Find out more at **thermofisher.com/countess**

EVOS M5000 and M7000 Imaging Systems with Celleste Software

These systems are designed for long-term live-cell imaging, image tiling and stitching, and a wide range of automated imaging applications. A wide selection of reagents and kits are available for labeling and detection, including Invitrogen™ Alexa Fluor™ dyes.

Find out more at **thermofisher.com/evos**

6.3

Challenges of analyzing 3D cultures

Imaging of 3D cell models can be challenging due to the reflection or absorption of excitable light by the thick sample. Antifade mountants and clearing reagents are commonly used to aid sample preparation for microscopy (Waters 2013). The use of these reagents is essential for viewing 3D cultures, in part to reduce light scattering by the sample (Richardson 2015; Zhu 2017).

Invitrogen™ ProLong™ antifade mountants and **Invitrogen™ CytoVista™ clearing reagents** are designed to enhance imaging of 3D cell cultures. Table 6.2 summarizes the specific uses for these products. With the proper techniques and reagents, challenges associated with imaging of 3D cultures can be overcome (Figure 6.1).

Table 6.2. Mountants and clearing reagents used with 3D cell culture.

	ProLong Glass Antifade Mountant	CytoVista 3D Cell Culture Clearing Reagent
Form	Hard-setting, ready-to-use	Soft-setting, ready-to-use
Medium type	Aqueous	Solvent
Refractive index	–1.52 post-curing	1.48
Sample archiving	Months to years	Weeks to months
Imaging depth	<150 µm	<1 mm
Signal-to-noise ratio	Best	Good
Protection from photobleaching	Best	None
Mounted microscope slides	Yes	Yes
Microplate imaging	No	Yes
Sample prep time	Overnight to 4 days	30 min to a few hours
Tissue recovery	Yes	Yes

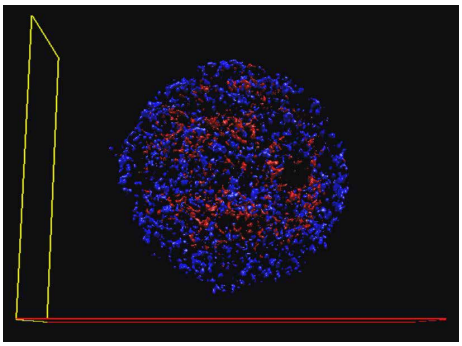

Figure 6.1 Spheroid staining and imaging. HepG2 spheroids were grown in a bioreactor and plated on a Thermo Scientific™ Nunc™ glass-bottom 96-well plate. Following fixation and permeabilization, spheroids were stained with Invitrogen™ Hoechst™ 33342 and Alexa Fluor™ 555 Phalloidin. An Invitrogen™ EVOS™ M7000 Imaging System with 10x S-Apo objective and DAPI and RFP light cubes were used to capture 110 Z-stacks with 2 µm step size. Invitrogen™ Celleste™ 5.0 Image Analysis Software was used for 3D deconvolution, 3D rendering, iso-surface generation, and animation.

For flow cytometry or any imaging technique that uses antibody staining, care must be taken not to destroy surface antigens by use of harsh proteolytic enzymes for removing cells from scaffolds, carriers, or culture vessels. Caution should still be employed when using non-enzymatic methods to harvest cells. Heng and colleagues determined that use of a non-enzymatic dissociation buffer reduced viability of mesenchymal stromal cells, compared with trypsin (Heng 2009). Tsuji and colleagues used a highly purified trypsin reagent, **Gibco™ TrypLE™ Select Enzyme**, to harvest mesenchymal stromal cells for further analysis by flow cytometry. They found that cell dissociation with TrypLE Select Enzyme resulted in superior viability and retention of surface antigen markers compared with cell dissociation with trypsin, divalent cation chelation, or collagenase (Tsuji 2017). If a certain surface marker is particularly labile to enzymatic action, it is recommended to try **Gibco™ Versene Solution** and check for viability as well as marker expression.

Acquiring and analyzing large amounts of imaging data for high-throughput studies can be challenging. These studies can be facilitated with high-content analysis (HCA) platforms, which combine large-scale cell imaging with multiparameter analysis capabilities. In 3D culture models, the Thermo Scientific™ CellInsight™ CX7 LZR HCA Platform was used to evaluate the formation of bile canaliculi in hepatic spheroids. For details on this procedure, see the application note "*In vitro* evaluation of hepatic function using a primary human hepatocyte 3D spheroid culture system", provided in Appendix A.6 of this handbook.

CellInsight CX7 or CX7 LZR HCA Platform

Designed for quantitative microscopy and flexibility in imaging, the CellInsight CX7 HCA Platform offers an integrated way to develop and automate high-content assays using a combination of 5-color brightfield and 7-color fluorescence imaging in confocal or widefield modes. The platform enables broad assay development that transitions to screening, at an excellent value. The CellInsight CX7 HCA Platform is available with either a fluorescence LED- or laser-based light engine to accommodate both 2D and 3D screening projects.

Find out more at **thermofisher.com/hca**

6.4

Functional analysis

Functional analysis of 3D cell cultures can be performed using many of the same techniques used to analyze cells grown in 2D culture. This subsection is intended not to be an exhaustive list of functional methods one might use, but rather to give examples of methods in current use.

RNA analytical methods include use of quantitative PCR (qPCR). In 3D culture, this is done similarly to 2D culture in that RNA must be obtained from the cell lysate. Gieseck and colleagues used 3D cultures to grow human iPSCs and analyze gene expression from cells with cell junctions, compared with gene expression from single cells. RNA preparation was the same for both cell culture conditions (Gieseck 2014). More recently, Burgess and colleagues devised a method for extracting RNA from peptide hydrogels, a scaffold not conducive to using the common approaches for preparing RNA, due to interactions between RNA and the scaffold material (Burgess 2018). Once RNA has been isolated, further analysis can be done using reagents and instruments such as **Applied Biosystems™ TaqMan® Assays** and **Applied Biosystems™ QuantStudio™ Real-Time PCR Systems**.

Flow cytometry is a method used to quickly analyze a large number of cells obtained from culture and also to perform multiparameter analysis on single cell types. Cells from 3D cell culture can be stained with antibodies or other reagents. Which antibodies are used depends upon what is being interrogated; the process of using antibodies to describe a cell population is known as immunophenotyping. Since cells need to be removed from culture vessels in order to be analyzed by flow cytometry, the same methods for washing and staining cells grown in 2D or 3D cultures are used. Buffers should be free of phenol red, which increases background fluorescence. RNA analysis can be done by flow cytometry using **Invitrogen™ PrimeFlow™ RNA assays**. A major advantage of PrimeFlow assays is the capability to analyze RNA and protein simultaneously. Multiparameter analysis of thousands to millions of cells can be facilitated with the Invitrogen™ Attune™ NxT Flow Cytometer. This efficient, flexible system uses acoustic-assisted hydrodynamic focusing for rapid processing of samples and is available with up to 4 lasers and 16 detection channels for multicolor analysis.

Attune NxT Flow Cytometer

Run samples faster and achieve greater resolution while minimizing sample loss due to clogging. The Attune NxT Flow Cytometer combines precision with performance in a true benchtop flow cytometer, with up to 4 lasers and 16 parameters of detection. The Attune NxT Flow Cytometer was developed with the goal of removing barriers associated with flow cytometry and enabling new research. This includes bringing the power of flow cytometry to the analysis of more sample types, including cancer cells. The addition of the Invitrogen™ CytKick™ Autosampler enables significantly faster high-throughput screening on a multiparametric platform.

Find out more at **thermofisher.com/attune**

- **Time savings**—up to 10x faster data acquisition speeds
- **Reduced clogging**—engineered for even large or sticky cell types
- **Efficient protocols**—rapid no-wash, no-lyse sample prep helps reduce protocol time and minimize cell loss
- **Robust software**—developed to offer user-focused functionality with many automated, user-definable, and administrative features
- **Reduced need for compensation**—spatially separated lasers
- **Elegant fluidics design**—readily accessible, easy to fill, and requires minimal maintenance
- **Rare-event detection**—technology for identifying very rare subpopulations of cells with high efficiency and certainty
- **Flexibility**—choice of lasers and parameters
- **Multiple configurations**—for a broad array of applications

A recent example of immunophenotyping from peripheral blood mononuclear cells (PBMCs) and mesenchymal stromal cells (MSCs) grown in hydrogels was published by Hanson and colleagues. PBMCs and MSCs were harvested from the hydrogel and stained with antibodies to determine the expression of CD14, CD16, CD206, and HLA-DR (a human histocompatibility antigen; Hanson 2011). The washed, stained cells were then analyzed by flow cytometry to determine how much of each marker of interest was expressed as a result of the co-culture (Hanson 2011). A more sophisticated flow cytometer was used to examine 3D rat liver spheroid cultures grown on chips compared with the same cells grown as 2D cultures. In these experiments, viability was the main parameter evaluated by flow cytometry (Sart 2017). In another series of experiments, PSCs grown in matrix were assessed by Takeuchi and colleagues for differentiation into pancreatic cells. The technique used here was to stain intracellular proteins of interest (e.g., transcription factors) to determine the extent to which the PSCs differentiated (Takeuchi 2014). To meet the challenge of removing cells from scaffolds in order to prepare them for flow cytometry, Wu and colleagues have developed a microcarrier that will allow cells to be grown, analyzed, and sorted in a single format (Wu 2018).

PrimeFlow RNA Assay

The PrimeFlow RNA Assay can be used for the direct detection of multiple viral transcripts within a single cell by flow cytometry, thus facilitating the detailed study of coinfected populations of cells. Hepatocytes were infected with two strains of hepatitis C virus, JFH1-wild type (JFH1-WT, top left) or JFH1-codon altered (JFH1-CA, top right). Hepatocytes from these two single infections were mixed post-infection (bottom left), or hepatocytes were coinfected with JFH1-WT and JFH1-CA (bottom right). Hepatocytes were analyzed for strain-specific viral RNA using the PrimeFlow RNA Assay. Data courtesy of Nicholas J. van Buuren and Karla Kirkegaard (PI), Stanford University School of Medicine.

Find out more at **thermofisher.com/primeflow**

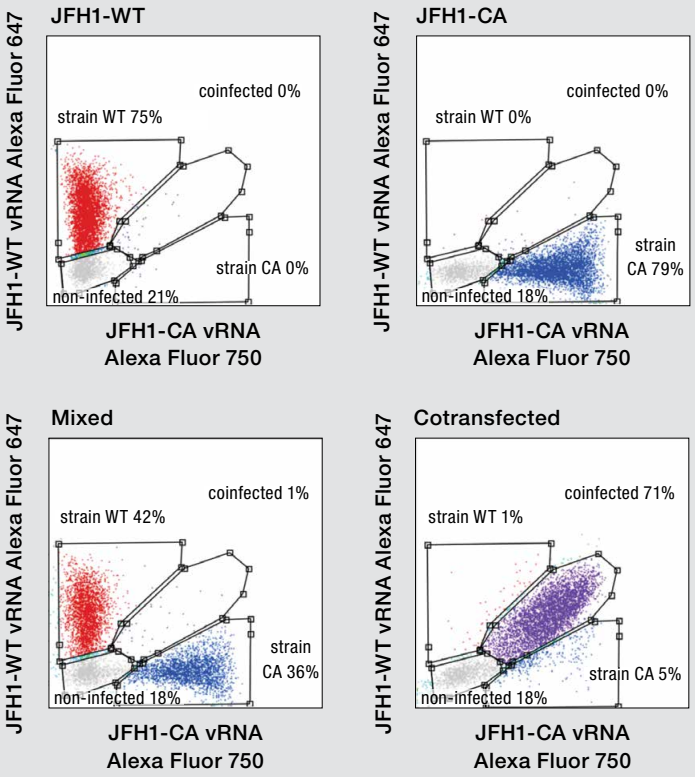

Assays of cell physiological function include calcium flux, caspase activity (during apoptosis), oxidative stress, metabolism, endocytosis, and colocalization. Many of these assays are performed using a flow cytometer, fluorescence or laser-scanning microscope, imaging cytometer, or other instruments, and relevant dyes or antibodies. Table 6.3 summarizes some of the assays, reagents, and references primarily used with flow cytometers.

Table 6.3. Assays and reagents for cell physiology.

Process	Reagents	Reference	URL
Cell proliferation	Click-iT and Click-iT Plus EdU Kits	BioProbes 65 (2011), 66 (2011) 70 (2014), and 75 (2017)	**thermofisher.com/cell-proliferation**
Cell viability	LIVE/DEAD Cell Viability and Imaging Kits	BioProbes 75 (2017)	**thermofisher.com/cell-viability**
Spheroid morphology	Nuclear dyes, CellMask stains, phalloidin conjugates	BioProbes 70 (2014)	**thermofisher.com/organelle-stains**
Calcium flux	Fluo-4, Fura Red dye, Indo-1	Assinger 2018	**thermofisher.com/calcium-flux**
Apoptosis	Annexin V, caspase 3/7	Holville 2016	**thermofisher.com/apoptosis**
Oxidative stress	2′,7′-dichlorofluorescein diacetate	Almasi 2019	**thermofisher.com/oxidative-stress**
Metabolism (glucose)	GLUT-1, 2-NBDG	Palmer 2016	**thermofisher.com/2-nbdg**
Mitochondrial membrane potential	JC-1	Nunez 2004; LeGrand 2001	**thermofisher.com/mito-function**
Endocytosis	Fluorescent nanoparticles	Goldshtein 2019	**thermofisher.com/phrodo**

6.5

High-throughput screening

Viability assays using microplate readers are often the primary assays performed in drug discovery for high-throughput analysis. Assays evaluating changes in cell functions are essential for characterizing test compounds and their potential role as drugs. There are relatively few guidelines and technologies as yet to study 3D cellular models, but in the oncology field there is increasing use of 3D cell models to mimic the complexity of tumors *in vivo*. 2D and 3D models often show significantly different responses to drugs, especially with regard to resistance (Hou 2018; Hongisto 2013).

Using existing microplate readers provides a time- and cost-efficient method for understanding therapeutic effects on 3D cellular models, allowing rapid therapeutic characterization in drug discovery with minimal investment. A recent article on the Cell Culture Dish website addresses 3D cell culture growth and suggests optimized cell viability microplate assays for 3D models (Sargent 2019). It has been reported that 2D cultures show a stronger cytotoxic response in preliminary drug screens than do 3D cultures; these findings were both cell- and drug-dependent and demonstrated that 3D models are more physiologically relevant for drug discovery research (Hou 2018).

Both high-content imaging and fluorescence imaging have been traditionally used to study 3D phenotypic changes, but now there is more interest in quantifying cellular function using microplate readers. Results of high-content imaging and microplate assays have been shown to correlate in cell health assays that utilize spheroids (Figure 6.2). The wide availability of microplate readers and compatible assays offers researchers a range of options to perform preliminary or complementary studies while continuing to use high-content and fluorescence imaging approaches.

Incubation time with gambogic acid	Potency values of gambogic acid (µM)	
	Varioskan LUX multimode reader	CellInsight CX7 HCA platform
2 h	100.4	>60
19 h	56.8	~44.4
48 h	17.8	19.8

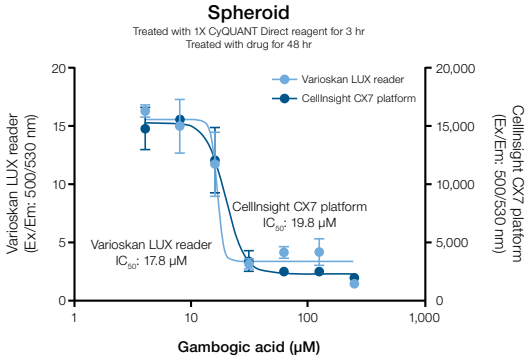

Figure 6.2. Measuring cell health with the Varioskan LUX Multimode Microplate Reader vs. the CellInsight CX7 HCA Platform. Existing solution- and fluorescence-based assays can be analyzed by microplate readers for initial drug discovery questions. Similar IC_{50} values are determined by using existing assays on the microplate reader and high-content system.

Many cellular viability assays are performed using microplate readers and can be adapted to 3D culture. Table 6.4 summarizes some of the assays and reagents used with microplate readers.

Table 6.4. Quantitation of 3D cell health—analysis on different detection platforms.

Cellular function	Reagent or assay	Detection platform	Experimental guidelines	
			Concentration*	Incubation time
Apoptosis	CellEvent Caspase 3/7 Green Detection Reagent	Microplate reader	0.33X	2 hr
		Fluorescence microscopy, high-content screening	1X	1 hr
Mitochondrial health	MitoTracker Orange CMTMRos	Microplate reader	2X	1 hr
		Fluorescence microscopy, high-content screening	1X	30 min–1 hr
Proliferation	Click-iT EdU Cell Proliferation Kits	Fluorescence microscopy, high-content screening	1X	Standard protocol
Viability	CyQUANT Direct Cell Proliferation Assay	Microplate reader	1X dye, 2X background suppressor	45 min–1 hr
	CyQUANT XTT Cell Viability Assay	Microplate reader	2X	5–8 hr
	PrestoBlue HS Cell Viability Reagent	Microplate reader	1X	3–5 hr
	alamarBlue HS Cell Viability Reagent	Microplate reader	1X	3–5 hr
	CyQUANT LDH Cytotoxicity Assay	Microplate reader	1X	30 min
	CyQUANT LDH Cytotoxicity Assay, fluorescence	Microplate reader	1X	10 min
	LIVE/DEAD Viability/Cytotoxicity Kit	Fluorescence microscopy, high-content screening	1X	Standard protocol
Reactive oxygen species	CellROX Deep Red Reagent	Fluorescence microscopy, high-content screening	1X	1 hr
Hypoxia	Image-iT Hypoxia Reagent	Fluorescence microscopy, high-content screening	1X	1 hr

* Go to **thermofisher.com/microplate-viability** for additional product information.

Another technology that has been used in high-throughput screenings for various applications is the **Invitrogen™ QuantiGene™ Plex assay**, which relies on branched DNA technology for signal amplification and Luminex® beads and instruments for readout. One example where researchers have taken advantage of this multiplex gene expression system that does not require RNA extraction is in the development of a method for the 3D culture of primary human airway basal cells called bronchospheres (Danahay 2015). The scientists conducted a high-throughput screen for secreted factors that influence bronchosphere development. Using QuantiGene Plex assays to measure gene expression for up to 80 targets per well including housekeeping genes, they found that developing bronchospheres respond to IL-13 with an increase in the expression of markers of goblet cells and a decline in ciliated cell number.

Section 7

3D cell culture models in disease and physiological research

7.1

Cancer models

Although animal models can replicate many aspects of diseases including cancer, often an *in vitro* representation can aid our understanding of pathophysiology and support drug discovery (Kumar 2019). As well, cell culture models are less expensive, and more easily scaled up than animal model systems. Furthermore, personalized cultures of cancer cells can help identify patient-specific therapies based on the specific markers of cancer cells (Kumar 2019). As discussed in the section on imaging and analysis, 3D cultures present some challenges with regard to high-throughput screening. However, the opportunities presented by 3D cell cultures are expected to outweigh the challenges, as 3D cultures more accurately represent the true biology of disease, especially cancer (Booij 2019).

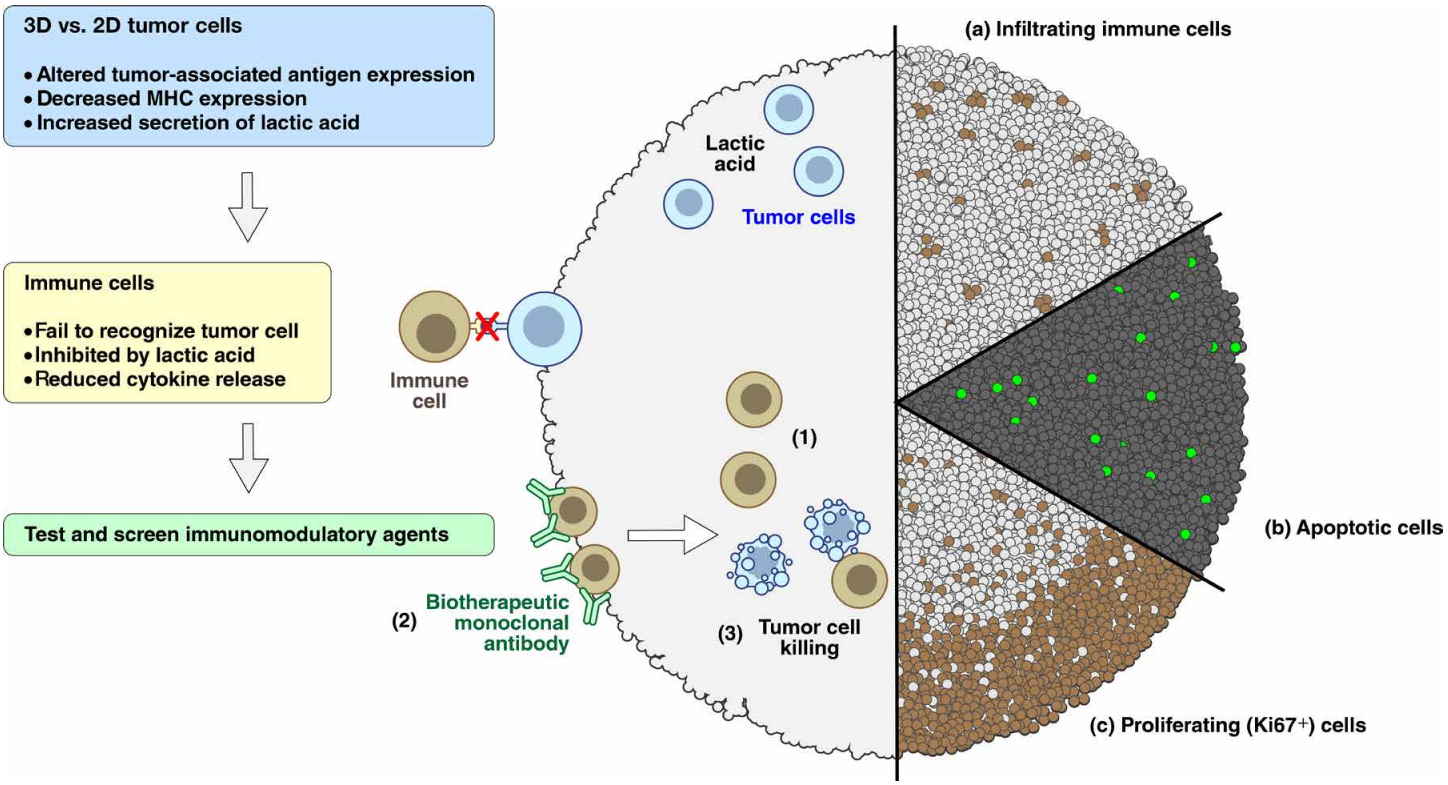

Figure 7.1. Tumor spheroids recapitulate properties of a solid tumor microenvironment. Cells grown in spheroids interact with other cells and the extracellular matrix (ECM) and are exposed to local gradients of nutrients, gases, growth factors, and other secreted factors. All of these interactions affect cell function and response to drugs.

3D cell culture lends itself to studying specific cancer types. Organoids for colorectal cancer research reproduce the physiology, morphology, and cellular composition of the intestinal epithelium *in situ*, making this an ideal system to study the basic and translational research aspects of colorectal cancer. Basic studies include those requiring genetic manipulation of cells and stem cell assays, whereas translational approaches include personalizing treatment from biopsy samples, high-throughput screening of drug candidates, and correction of mutations using gene editing techniques (Young 2016).

Two 3D models of breast cancer were used to evaluate how doxorubicin is transported into tumors, spheroids, and microtissue. Both models were created by co-culturing cancer-associated fibroblasts with the breast cancer cell line MCF-7. The researchers observed that microtissue had a higher diffusion rate with respect to doxorubin than did spheroids; this correlated with high drug-induced toxicity (Brancanto 2017). Such exploratory studies are useful as a means to study novel anticancer drug effects *in vitro*.

As early as 1990, Iwasaki and colleagues created a model showing lymphokine-activated killer (LAK) cell cytolysis of glioma spheroids. In this model, lymphocytes from human peripheral blood were activated by cytokines (at the time called lymphokines), then co-cultured with spheroids of a glioma cell line. Results showed that LAK cells penetrated to the interior of the spheroids and caused cytolysis of tumor cells, whereas unstimulated cells lack the capability to penetrate and kill target cells (Iwasaki 1990).

More recently, Courau and colleagues co-cultured human colorectal tumor spheroids with activated T cells or natural killer (NK) cells to examine the extent of immune-mediated cytotoxicity. They observed rapid destruction of tumor spheroids by apoptosis, and that the process was driven by the surface protein NKG2D, expressed by T cells and NK cells, and ligands of the target cells. T cells and NK cells did not infiltrate the spheroids or induce apoptosis (Courau 2019).

Consistent growth of cells as spheroids would be an important tool in developing cancer models. To this end, Sant and Johnston evaluated two methods of creating spheroids for use in high-throughput screening; these methods included very low–attachment plates and hydrogel in microwell plates (Sant 2017). Neither method had a clear advantage over the other, but both allowed the formation of relatively uniform spheroids.

To aid growth of spheroids from cancer cell lines, very low–attachment plasticware has shown to be useful. **Gibco™ Nunclon™ Sphera™** flasks and plates are designed to enhance spheroid formation; their plastic surfaces are treated to block adsorption of ECM proteins that mediate cell adhesion, so that cell lines grow as spheroids.

Nunclon Sphera 96-well plates have been shown to support formation of spheroids in a variety of cancer types, including those of the breast, colon, and prostate. Spheroids generated in this format allow for characterization before and after treatment (Figure 7.2).

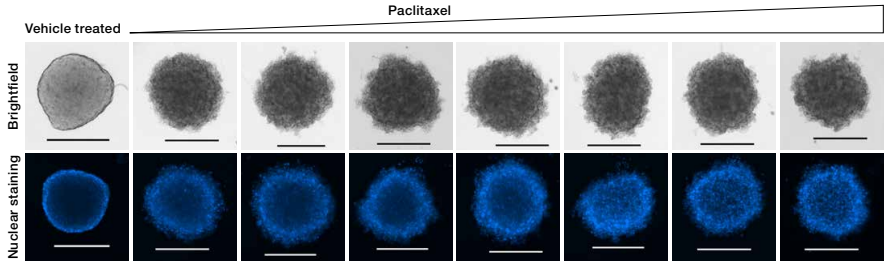

Figure 7.2. Effect of paclitaxel on spheroid integrity. 2,000 T-47D cells were seeded on Nunclon Sphera plates for spheroid generation. On day 6, the spheroids were treated with either DMSO or increasing concentrations (0.625–10 µM) of paclitaxel (a chemotherapeutic drug). Brightfield and fluorescence images at the respective time points were captured with the Invitrogen™ EVOS™ M7000 Imaging System using a 4x objective. Increasing paclitaxel concentration compromises the spheroid integrity, leading to better penetration of the nuclear dye. Scale bar: 400 µm.

7.2

Neural models

3D models in neuronal research have proven useful in a variety of research areas, from Alzheimer's disease to viral infections of the central nervous system (CNS). A system for modeling Alzheimer's disease was described by Kim and colleagues. In this model, neuronal progenitor cells were genetically modified to bear mutations associated with Alzheimer's disease. The progenitor cells were then differentiated in a matrix, and analysis of β-amyloid protein proceeded 6 weeks later. This model system offers a way to study Alzheimer's disease *in vitro*; these findings could be applied to the study of other neurodegenerative diseases as well (Kim 2015a).

D'Aiuto and colleagues devised a system that uses 3D cultures to model viral infections of the CNS. In this model, human induced pluripotent stem cells (iPSCs) grown without an ECM were treated with neuronal factors to induce differentiation. The 3D cultures were then infected with herpes simplex virus type 1, and the effects of the antiviral drug acyclovir were evaluated on the infected cells. The findings are noteworthy because the authors showed that generation of adherent 3D neuronal cultures did not require cells embedded in matrices; rather, the differentiating progeny cells were observed to organize into multilayered structures having some complex features of the ventricular/subventricular zone. Furthermore, the model showed how a 3D neuronal culture could be adapted for high-throughput evaluation of antiviral drug activity (D'Aiuto 2018).

Workflows for generating neural organoids from pluripotent stem cell culture typically follow a specific sequence of steps that begin with standard culture of pluripotent stem cells (Figure 7.3). Brightfield imaging as part of phenotypic analysis of neural organoid cultures reveals development of neuroepithelial structures (Figure 7.4).

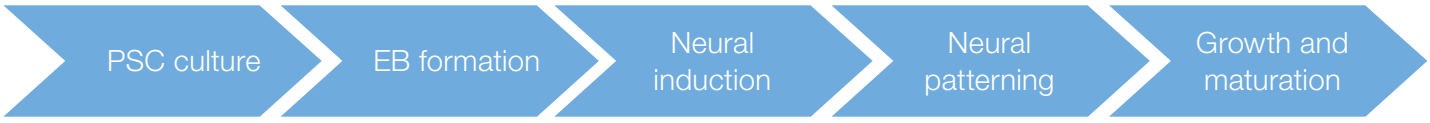

Figure 7.3. The essential steps from pluripotent stem cell to neuronal organoid.

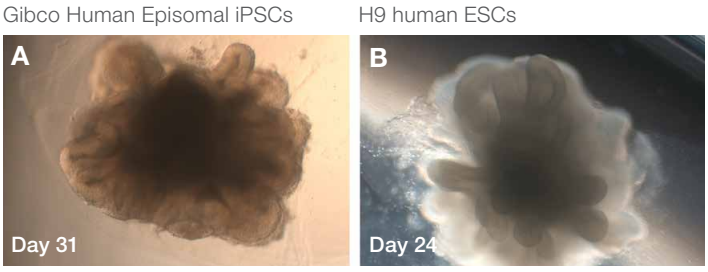

Figure 7.4. Neuroepithelial development in organoid cultures.
Brightfield images of neural organoids on day 31 or day 24 of culture show convoluted neuroepithelial structures.

View the full application note titled "Differentiation of pluripotent stem cells into neural organoids" in the appendix.

7.3

Liver models

3D liver models have applications in various aspects of research, ranging from toxicology to nonalcoholic steatohepatitis (NASH) and insulin resistance (together known as nonalcoholic fatty liver disease, NAFLD). In brief, NASH and NAFLD were modeled *in vitro* by creating spheroid cultures of human primary hepatocytes, which were then treated with fatty acids over time. From these cultures, fatty acid accumulation could be assessed, and gene expression profiling could be performed. In particular, genes associated with insulin resistance were monitored (Kozyra 2018). The researchers observed that initially, the spheroids were sensitive to insulin but that after exposure to fatty acids, the spheroids expressed genes associated with insulin resistance, and furthermore showed physiological hallmarks of resistance to insulin (Kozyra 2018).

In considering *in vitro* cultures, whether 2D or 3D, of liver for ADME (absorption, distribution, metabolism, excretion) and toxicology studies, one must take into account how complex the liver is, that liver cells are polarized, and that liver functionality does not reside solely with hepatocytes.

Of the 3D techniques available, the ones most useful for ADME and toxicology studies are spheroids grown in hydrogels, spheroids grown in synthetic scaffolds, and hepatospheres derived from hepatomas or primary hepatocytes (Godoy 2013). Which system to use ultimately depends on the exact nature of the question to be answered. Groger and colleagues used organ-on-a-chip models to create a liver sinusoid that would allow them to study liver dysfunction. The sinusoid is composed of several cell types—hepatocytes and vascular cells in layers plus non-parenchymal cells—which communicate with each other. Inflammation was induced by several stimuli to study the disruption in normal liver function. In this way the 3D model simulated the liver dysfunction that occurs *in vivo* during sepsis; the model provides a valuable tool for studying the disease and repair process (Groger 2016).

For many studies of the liver, primary human hepatocytes might be the preferred cells with which to start 3D cultures. Available for sale, these cells can be used readily for spheroid cultures in combination with low-attachment plastic U-well plates (Figure 7.5).

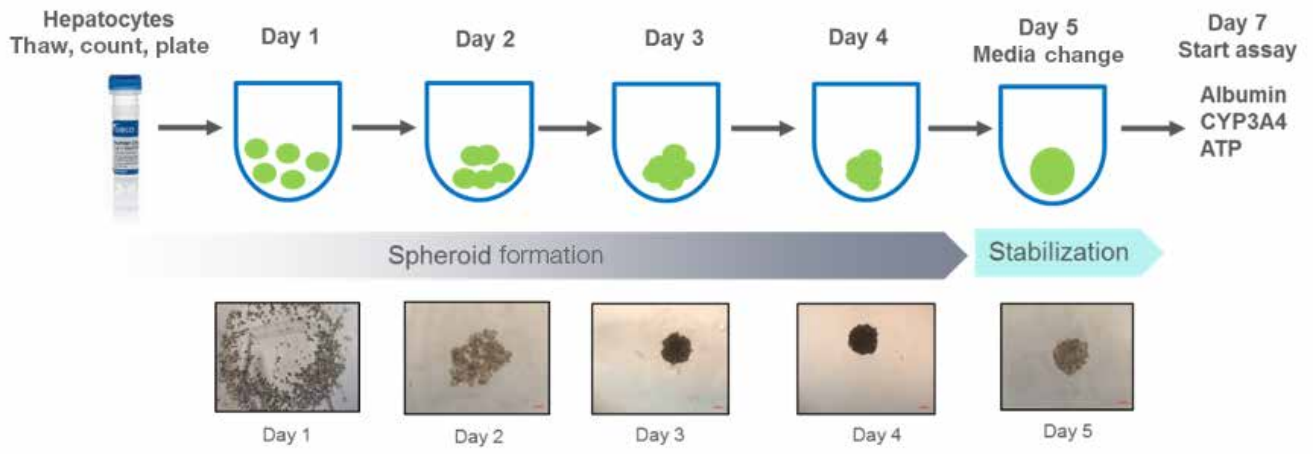

Figure 7.5. Formation of hepatic spheroids from primary human hepatocytes. Primary human hepatocytes from a commercial source are plated in U-wells. Spheroids form in 5 days or less and can be assayed for liver function by day 7.

3D hepatic spheroid culture is suitable for studying drug metabolism. A sufficient assay window for metabolite formation was observed for the CYP450 enzymes studied (Figure 7.6). In general, 3D hepatic cultures were more efficient in drug metabolism compared with 2D cultures.

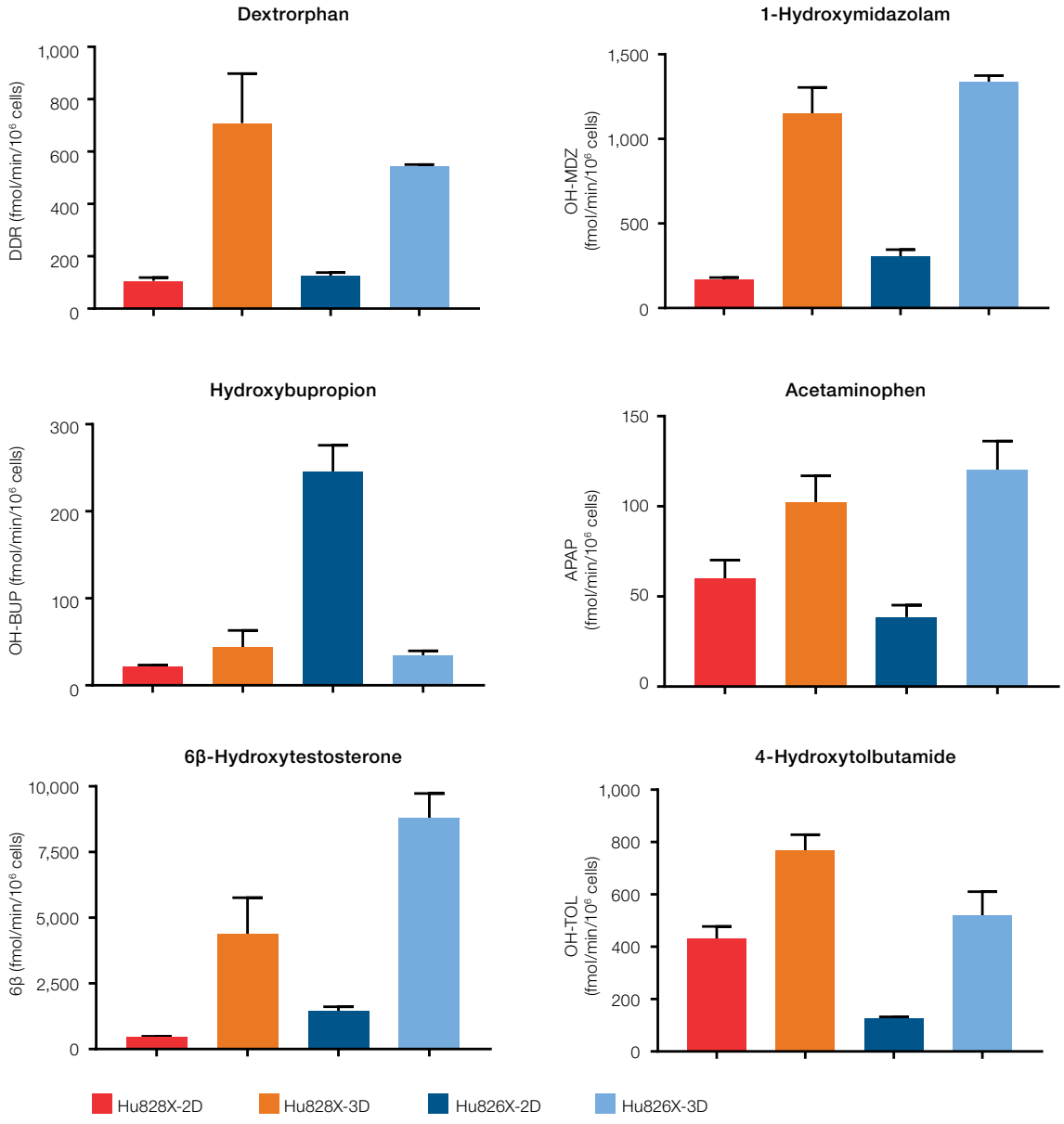

Figure 7.6. Comparison of metabolites between 2D and 3D cultures. The metabolites quantified using high-resolution mass spectrometry (HRMS) were converted to mole amounts based on the standard curves of the respective metabolites. Two different lots of primary human hepatocytes, Hu828X and Hu826X (partially redacted), were used in this assay. Results were normalized to incubation time of individual substrates and number of cells per well in the 2D and 3D cultures. Data are mean ± SD; n = 3.

As researchers migrate to working with more phenotypically stable primary human hepatocyte 3D cultures, it is important to understand how closely gene expression mimics *in vivo* hepatic phenotypes and how levels of gene expression in 3D cultures compare to those in traditional 2D hepatocyte cultures (Figure 7.7).

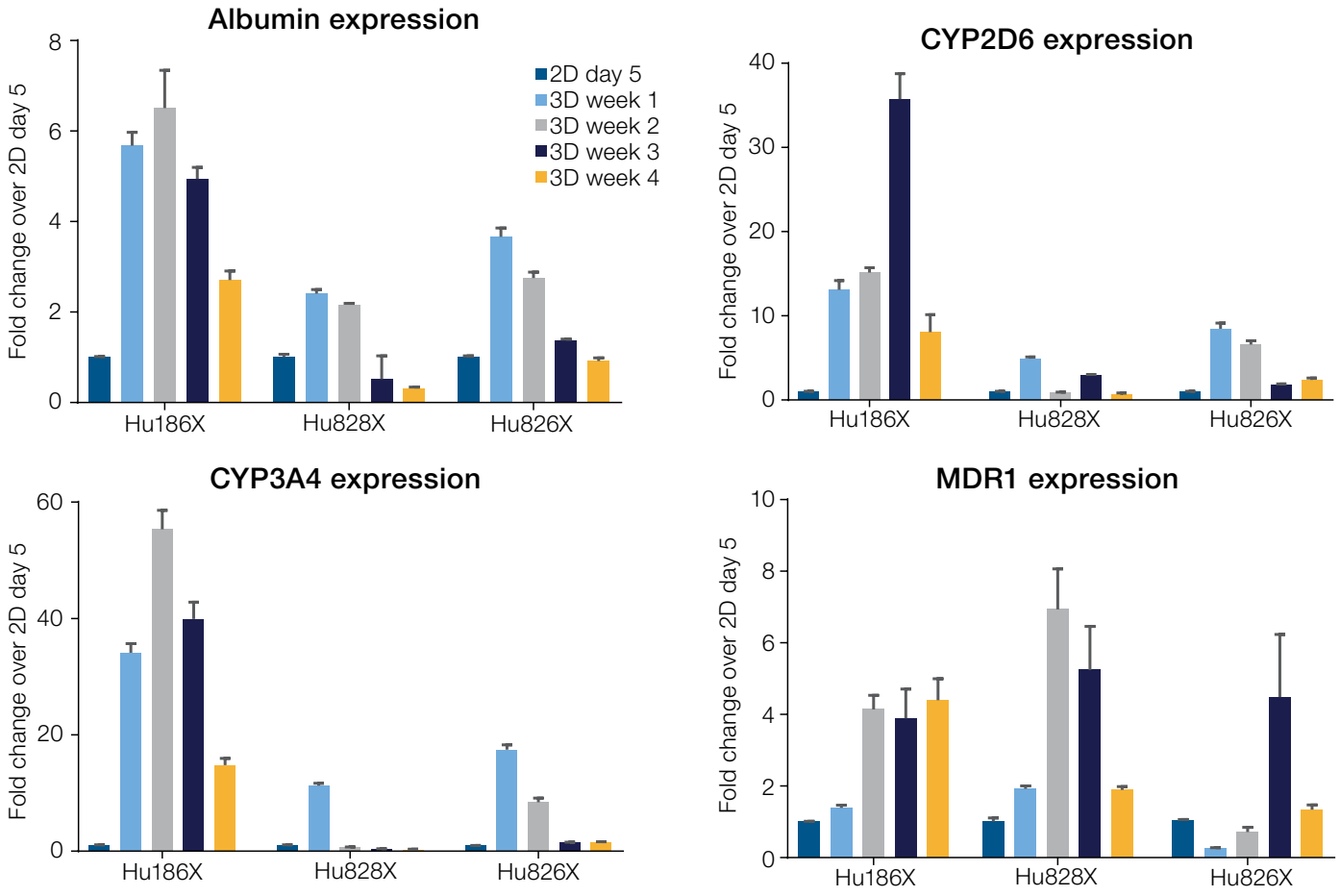

Figure 7.7. Time course evaluation of hepatic gene expression shows elevation in spheroid cultures. qPCR results for albumin, CYP3A4, CYP2D6, and MDR1 mRNA levels of 3 individual lots of Gibco™ Human Spheroid-Qualified Hepatocytes. Gene expression levels of 3D cultures at different time points were normalized to day 5 of 2D culture. Each 3D spheroid sample contained a pool of 16 spheroids. Results are mean ± SEM; n = 3 spheroid pool samples.

Animal spheroids for 3D culture and analysis

Animal (dog and rodent) hepatocytes can be formed into spheroids using **Thermo Scientific™ Nunclon™ Sphera™ U-bottom plates** (Figure 7.8).

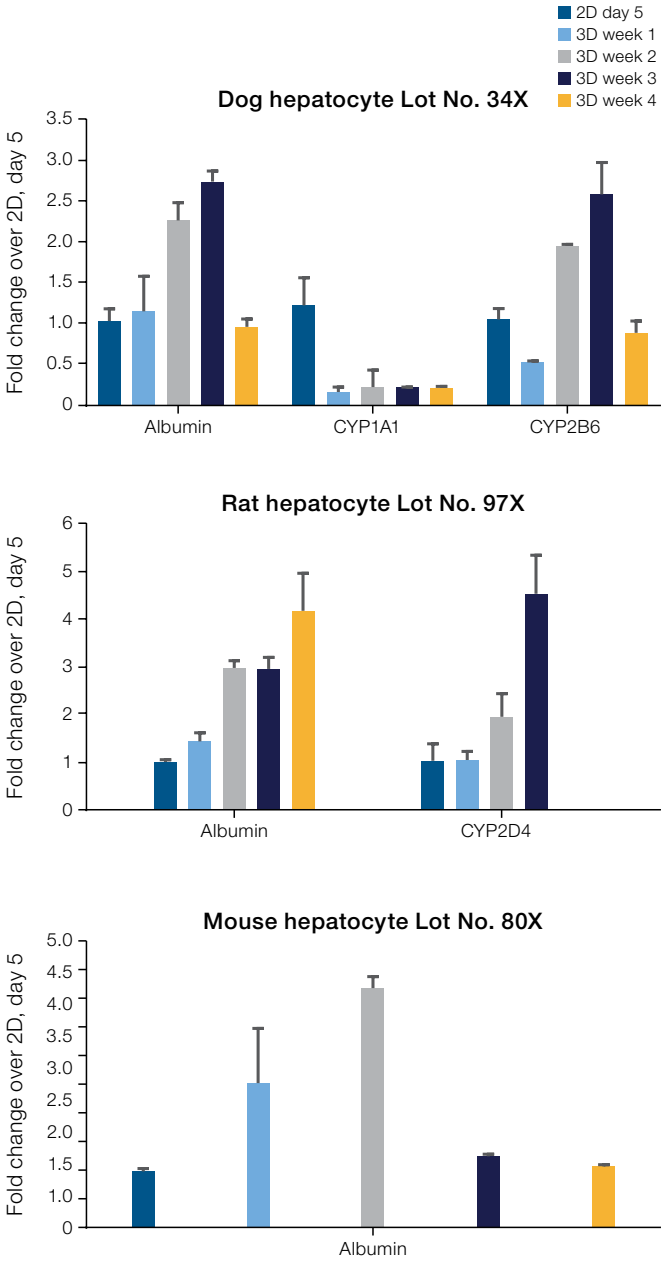

Figure 7.8. Analysis of spheroids formed using animal cells. Gene expression levels were measured by RT-qPCR to compare the levels of gene expression between day 5 of 2D culture and various days of 3D culture.

HepaRG cells for 3D culture and analysis

Gibco™ HepaRG™ cells can be used in 3D modeling for rapid spheroid formations and reproducible results. HepaRG cells easily assemble into viable 3D spheroids in just 2–3 days and produce CYP activity higher than 2D cultures of HepaRG cells (Figure 7.9).

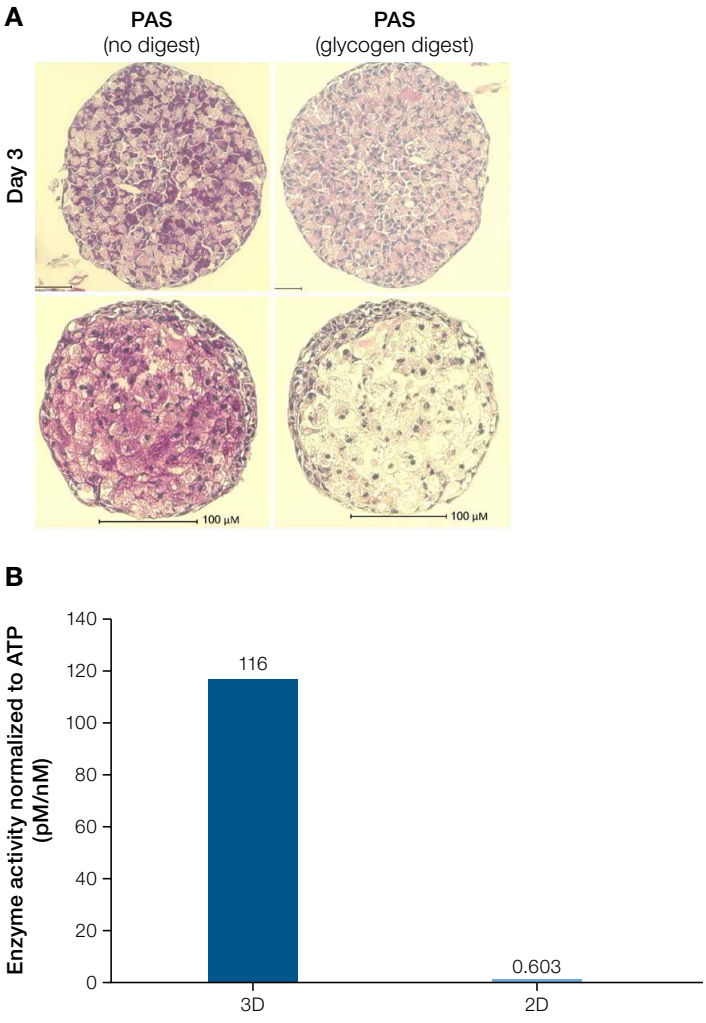

Figure 7.9. HepaRG spheroids show increased glycogen storage and basal CYP activity. (A) Periodic acid–Schiff (PAS) staining of HepaRG cells indicates glycogen storage functionality. HepaRG spheroids show increased glycogen storage over time. **(B)** Basal CYP3A4 activity is ~200 times higher in spheroids than monolayer cultures.

The hepatic spheroids show stable morphology and viability for up to 3 weeks. Moreover, they express normal liver surface markers and liver enzymes and display sensitivity to compounds such as chlorpromazine, meaning they are useful for toxicology and ADME studies. Finally, these spheroids show the formation of bile ducts, a feature not seen with hepatoma-derived spheroid cultures (Figure 7.10).

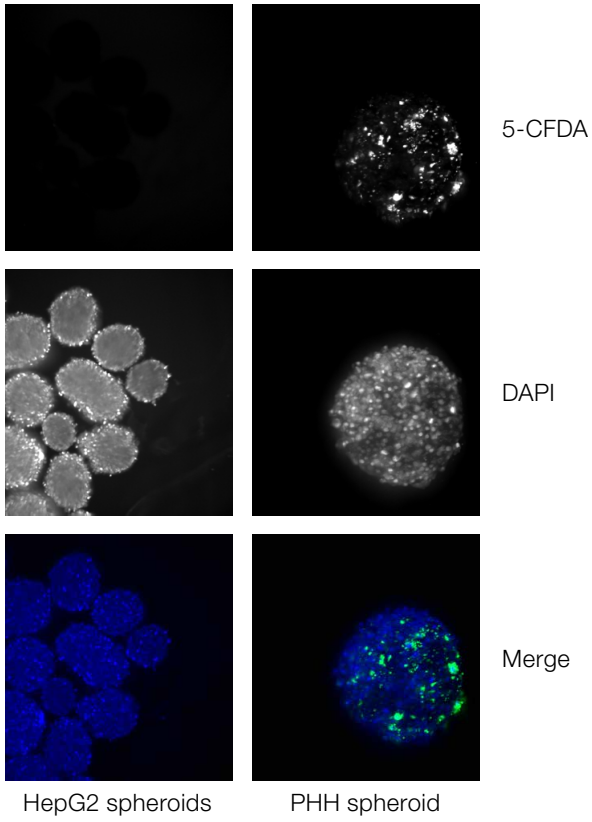

Figure 7.10. Bile duct formation in cultures of hepatic spheroids. HepG2 hepatoma spheroids on day 14 (left) and hepatic spheroids on day 7 (right) were stained with CFDA and DAPI (10x magnification). Hepatic spheroids show clear formation of bile ducts in comparison to the HepG2 spheroids.

7.4 Intestinal models

3D models of the intestines have diverse applications, ranging from understanding the embryonic development and adult homeostasis of the intestinal tract and the etiology of diseases such as colorectal cancer, to exploring the role of the gut microbiome in human health.

In the 1970s, Caco-2 cells were derived from colon adenocarcinoma and became a popular cell model for studying the function of intestinal epithelia. This cell line has been used as a screening tool for drug absorption and permeability, but it lacks the cellular diversity, function, and architecture of normal intestinal epithelium. In 2009, the Clevers and Kuo labs reported the establishment of culture conditions to grow organoids derived from adult intestinal stem cells that recapitulated the structure and function of the small intestine and colon epithelium (Sato 2009; Ootani 2009; Sato 2011; Jung 2011). Following these reports, protocols and techniques to differentiate iPSCs into small intestine and colon organoids were published. Although these organoids may not fully mature *in vitro*, as do those from adult stem cells, these iPSC-derived models may contain an additional mesenchymal component (Spence 2011; Forster 2014; Munera 2017). Furthermore, the culture conditions used to grow adult stem cell–derived organoids have been refined to support the isolation and expansion of colorectal cancer tissue (Sato 2011; van de Wetering 2015; Fujii 2016). These cancer organoids are similarly effective as patient-derived xenograft models at propagating cancer tissue with features of the original tissue, without the need for animal hosts, making them a very attractive method to scale organoids for screening approaches. Indeed, colorectal cancer biobanks have been established and shown to predict responsiveness to therapies (van de Wetering 2015; Ooft 2019).

Human gut-on-a-chip was used by Kim and colleagues to study commensal organisms in an intestinal environment. In addition to the microbiome, peristalsis and inflammation were also studied. The researchers found that when peristalsis was halted, bacterial overgrowth ensued. The resulting inflammation resembled that of human inflammatory bowel disease (Kim 2015b). 3D intestinal culture lends itself to studying the gut microbiome in disease. This aspect is particularly important in veterinary medicine, since livestock are prone to infection by *Salmonella* and other species that cause diarrhea in young animals, with concomitant economic loss. Derricott and colleagues recently used bovine and porcine intestinal organoid cultures to study infection by *Toxoplasma gondii* and *S. enterica*. They found that the viable organoids obtained from abattoirs could be cryopreserved and resuscitated, then infected successfully (Derricott 2019). As *Toxoplasma* and *Salmonella* are human pathogens, these organoid cultures have implications for human health as well. These studies demonstrate multiple uses for this type of 3D intestinal culture.

7.5
Kidney models

3D models for research on kidney physiology have been used for applications ranging from studying nephrotoxicity to disease processes. Organotypic models have been described that mimic the complexity of kidney. This model, derived from adult kidney, differentiates into physiologically active tubules (Jun 2018). The authors postulate their model should be useful in disease research.

An organ-on-a-chip model was used to study gentamycin toxicity; this model used a perfused 3D kidney organoid to study renal clearance. Nephrotoxicity was assessed by looking at the pharmacokinetic profile of gentamycin given either as continuous infusion or as a bolus dose. The researchers found that gentamycin caused less nephrotoxicity when given as a bolus than when given as continuous infusion, where nephrotoxicity was measured as increased cell membrane permeability, decreased cell viability, and decreased cell junctions (Kim 2016). Taken together, these data show the usefulness of perfused organ-on-a-chip models for studying kidney physiology under normal and abnormal conditions.

Finally, understanding complex cell interactions as a basis for drug discovery was the impetus for Nugraha and colleagues to create a 3D co-culture system to understand how kidney fibrosis develops and to screen promising compounds to treat it. This system allows researchers to examine epithelial–mesenchymal crosstalk in a high-throughput system (Nugraha 2017), thus combining basic research with drug discovery.

7.6

Lung models

The lung is a complex organ, one that interfaces with air, mechanically deforms with each breath, and exchanges gases. Yet recent advances have made it possible to reproduce lung function through 3D cell culture technology. Huh and colleagues created an organ-on-a-chip model that captures the alveolar–capillary interface of human lungs. Using this model, the researchers demonstrated that the cells responded to silica particles, bacteria, and other stimuli, including mechanical stress. Although the model does not capture lung function entirely (such as the effect of alveolar macrophages on lung function), it captures enough to allow for screening of novel drugs (Huh 2010).

3D lung models are being used in respiratory disease models as well. In one model, Gercken and colleagues used tissue slices obtained from donors to create 3D models of respiratory disease such as lung fibrosis. By using lung tissue filled with agar, the researchers created models to study various disease processes. A detailed protocol for generating 3D models from resected lung tissue is decribed in the paper (Gerckens 2019).

Deslee and colleagues devised a model for chronic obstructive pulmonary disease (COPD) using primary bronchial epithelial cells obtained from brushings. The cells grew as spheroids, which were then subjected to various stimuli to simulate the chronic inflammation that is part of the process of COPD. This 3D model represents a means to investigate how COPD initiates and progresses (Deslee 2007).

Increased airway smooth muscle (ASM) mass and mast cell infiltration are pathophysiological features of asthma, often called airway remodeling. To study the relationship among airway remodeling, mast cells, and the ECM, Ceresa and colleagues created a 3D model in which airway cells in collagen were cultured alone or with mast cells. They observed that mast cells enhanced airway cell proliferation and production of matrix metalloproteinases, and that the 3D system accurately recapitulated several hallmarks of asthma pathophysiology (Ceresa 2009).

Influenza is a respiratory disease with considerable worldwide morbidity and mortality each year. Zhou and colleagues used lung organoid cultures to study the infectivity of influenza virus. Since influenza strains change through genetic reassortment, such a model will be useful to establish the human infectivity of avian strains or strains emerging in other species. The lung organoids offer a rapid means to assess virus infectivity that can be standardized across laboratories (Zhou 2018).

Lung injury from use of tobacco products remains a major public health concern. To study the effect of cigarette smoke on lungs, Kuehn and colleagues used organotypic 3D cultures to look at various parameters, such as ciliary beating frequency and cytochrome P450 activity following repeated exposure to cigarette smoke, or air as a control. The researchers include a detailed protocol in the paper. Measuring particle deposition in real time allowed smoke exposure to be calibrated. Alterations in the transcriptome were detected following exposure to cigarette smoke, in addition to changes in ciliary beating frequency and cytochrome P450 activity (Kuehn 2015).

Section 8

Services

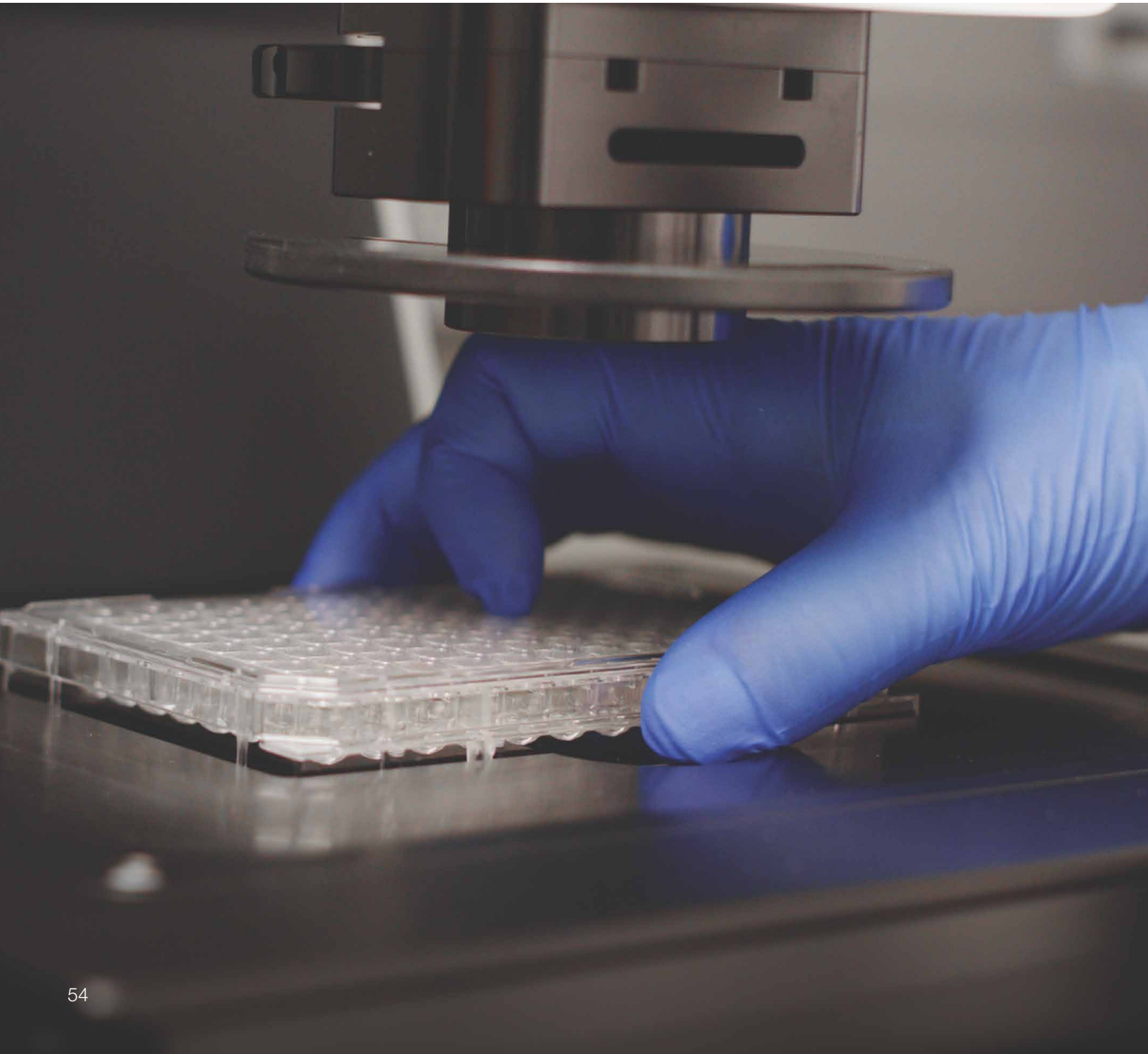

8.1

Custom cell services

Researchers are continuously being asked to transition their studies into more physiologically relevant models, but the path to get there is not always obvious. Whether your team needs help developing the right 3D cell model or is interested in outsourcing steps of the research project, our CellModel™ Services team can help provide a solution tailored to your research needs.

All of the methods and protocols used to make the 3D model are openly shared with the client to ensure a smooth transition at the conclusion of the service. Some of the areas we can collaborate with you on are:

Custom cell lines and the creation of 3D models

Immortalized cell lines

- T47D or MDA-MB-231 (breast)
- HepG2 (liver)
- HCT116 (colon)
- PC3 or LNCaP (prostate)
- A549 (lung)

Primary cell lines and co-cultures

- Primary hepatocytes (human, rat, mouse, dog, monkey)
- Non-parenchymal cell lines (e.g., Kupffer cells, stellate cells)
- Keratinocytes
- Endothelial cells

Stem cells and organoids

- Neuronal models
- Intestinal models

Custom media creation and services

- Throughout the 3D model service, we use Gibco™ media, supplements, and reagents to ensure the highest-quality 3D model
- All of the media and reagents are readily available, allowing you to continue to culture your 3D model in your lab at the conclusion of the service

Characterization and expression services

Standard imaging

- Fixed- or live-cell imaging of your 3D models using the Invitrogen™ EVOS™ M7000 Imaging System

High-resolution imaging (confocal)

- Fixed- or live-cell imaging of your 3D models using the Thermo Scientific™ CellInsight™ CX7 LZR HCA Platform

Gene expression profiling

- Gene expression levels (mRNA) of your 3D models will be analyzed using Applied Biosystems™ TaqMan® Gene Expression Assays

Functional readouts and assessment of functional activity

- Functional assessment of your 3D model using our catalog of Invitrogen™ dyes and reagents

Cell banking

- Scale-up propagation and banking of your 3D model to support screening campaigns; includes the growth of 3D models using Gibco media and supplements

Screening and profiling

- Leveraging our over 20 years of profiling experience, we can perform custom screening projects with your 3D models to help support your drug discovery programs

We are continuously working on expanding our list of available cell lines, as well as developing new and improved methods to grow 3D models. Reach out to our team today to discuss what services, training, or demonstrations we can offer.

Find out more at **thermofisher.com/askdiscovery**

Section 9

References

Section 1: Introduction to 3D models

Aboulkheyr Es et al. *Trends Biotechnol.* 2018;36(4):358–371.
Amann et al. *Sci Rep.* 2017;7(1):2963.
Benien and Swami. *Future Oncol.* 2014;10(7):1311–1327.
Chen et al. *Trends Mol Med.* 2018;24(9):805-820.
Däster et al. *Oncotarget.* 2017;8(1):1725–1736.
Edmondson et al. *Assay Drug Dev Technol.* 2014;12(4):207–218.
Fang and Eglen. *SLAS Discov.* 2017;22(5):456–472.
Horvath et al. *Nat Rev Drug Discov.* 2016;15(11):751–769.
Lv et al. *Oncol Lett.* 2017;14(6):6999–7010.
Mazzoleni et al. *Genes Nutr.* 2009;4(1):13–22.
Mittal et al. *J Cell Physiol.* 2019;234(6):8352–8380.
Petersen et al. *Proc Soc Natl Acad Sci U S A.* 1992;89(19):9064–9068.
Rios and Clevers. *Nat Methods.* 2018;15(1):24–26.
Rossi et al. *Nat Rev Genet.* 2019;19(11):671–687.
Schwank et al. *Cell Stem Cell.* 2013;13(6):653–658.
Takahashi. *Annu Rev Pharmacol Toxicol.* 2019;59:447–462.
Tiriac et al. *Cancer Discov.* 2018;8(9):1112–1129.
Yamada et al. *Makromol Chem Rapid Commun.* 1990;11(11):571–576.
Yang et al. *Biomaterials.* 2005;26(33):6415–6422.
Yang et al. *Biomaterials.* 2007;28(34):5033–5043.
Zhang et al. *Ann Biomed Eng.* 2017;45(1):148–163.

Section 2: Culture overview

Carlson et al. *Curr Protoc Cell Biol.* 2008;Chapter 19:Unit 19.9.
de Souza. *Nat Methods.* 2018;15(1):23.
Dekkers et al. *Nat Med.* 2013;19(7):939–945.
Ding et al. *Nature.* 2012;481(7382):457–462.
Drost et al. *Nat Protoc.* 2016;11(2):347–358.
Editorial. *Nat Cell Biol.* 2018;20(6):633.
Edmondson et al. *Assay Drug Dev Technol.* 2014;12(4):207–218.
Fang and Eglen. *SLAS Discov.* 2017;22(5):456–472.
Fennema et al. *Trends Biotechnol.* 2013;31(2):108–115.
Hoppensack et al. *Tissue Eng Part C Methods.* 2014;20(7):599–609.
Huch and Koo. *Development.* 2015;142(18):3115–3125.
Kaushik et al. *Stem Cells.* 2018;36(9):1329–1340.
Narsinh et al. *Mol Ther.* 2011;19(4):635–638.
Ootani et al. *Nat Med.* 2009;15(6):701–706.
Sachs et al. *Cell.* 2018;172(1–2):373–386.
Sutherland et al. *Cancer Res.* 1981;41(7):2980–2984.
Sutherland et al. *J Natl Cancer Inst.* 1971;46(1):113–120.
Song et al. *Sci Rep.* 2019;9(1):5977.
Srinivasan et al. *J Lab Autom.* 2015;20(2):107–126.
Takahashi and Yamanaka. *Cell.* 2006;126(4):663–676.
Takai et al. *Sci Rep.* 2016;6:21174.
Ude et al. *J Nanobiotechnology.* 2019;17(1):70.
Vlachogiannis et al. *Science.* 2018;359(6378):920–926.
Yan et al. *Sci Rep.* 2019;9(1):1295.

Section 3: Sources for cell lines used in 3D cell models

Baghbaderani et al. *Stem Cell Rev Rep.* 2016;12(4):394–420.

Baptista et al. *Int J Mol Sci.* 2018;19(5):1285.

Bardelli and Moccetti. *Stem Cells Int.* 2017;2017:6406025.

Chen and Pruett-Miller. *Stem Cell Res.* 2018;31:186–192.

Ben Jehuda et al. *Stem Cell Rev Rep.* 2018;14(3):323–336.

Centeno et al. *Mol Neurodegener.* 2018;13(1):27.

Cesarz and Tamama. *Stem Cells Int.* 2016;2016:9176357.

Chonghalle. *Sci Transl Med.* 2018;10(451):eaau7377.

Driehuis and Clevers. *Am J Physiol Gastrointest Liver Physiol.* 2017;312(3):G257–G265.

Dutta et al. *Trends Mol Med.* 2017;23(5):393–410.

Gholami et al. *Cell Rep.* 2013;4(3):609–620.

Gillet et al. *J Natl Cancer Inst.* 2013;105(7):452–458.

Gomez-Lechon et al. *J Cell Physiol.* 1998;177(4):553–562.

Goodspeed et al. *Mol Cancer Res.* 2016;14(1):3–13.

Horii et al. *Int J Mol Sci.* 2013;14(10):19774–19781.

Huch and Koo. *Development.* 2015;142(18):3115–3125.

Hussain. *Genetic Engineering & Biotechnology News.* 2017;37(13).

Jiang et al. *Cell Mol Immunol.* 2014;11(1):17–24.

Kaushik et al. *Stem Cells.* 2018;36(9):1329–1340.

Kelava and Lancaster. *Dev Biol.* 2016;420(2):199–209.

Kropp et al. *Process Biochem.* 2017;59:244–254.

Lancaster et al. *Nature.* 2013;501(7467):373–379.

Malik and Rao. *Methods Mol Bio.* 2013;997:23–33.

Marti et al. *Nat Protoc.* 2013;8(2):223–253.

McCauley and Well. *Development.* 2017;144(6):958–962.

McCracken et al. *Nature.* 2014;516(7531):400–404.

Mesquita et al. *Stem Cells Int.* 2019;2019:9704945.

Mummery et al. *Stem Cells: Scientific Facts and Fiction, Second Edition.* 2014. Academic Press. pp 101–129.

Nagle et al. *Semin Cancer Biol.* 2018;53:258–264.

Namekawa et al. *Cells.* 2019;8(1):74.

Rossi et al. *Nat Rev Genet.* 2018;19(11):671–687.

Sanchez et al. *Front Cell Dev Biol.* 2019;7:44.

Selby et al. *SLAS Discov.* 2017;22(5):473–483.

Skottke et al. *Int J Mol Sci.* 2019;20(8):1998.

Staudt. Human Cancer Models Initiative. 2016. Available at https://www.cancer.gov/about-nci/organization/ccg/blog/2016/human-cancer-models-initiative-launch; accessed October 10, 2019.

Tiriac et al. *Cancer Discov.* 2018;8(9):1112–1129.

Ulrich and Pour. Cell Lines. In: Brenner and Miller (editors), Encyclopedia of Genetics. 2001. Available at https://www.sciencedirect.com/topics/neuroscience/cell-lines; accessed October 10, 2019.

Wang et al. *Oncotarget.* 2018;9(63):32191–32203.

Wilding and Bodmer. *Cancer Res.* 2014;74(9):2377–2384.

Young et al. *Cell Stem Cell.* 2016;18(4):533–540.

Yu et al. *PLoS One.* 2018;13(3):e0193694.

Zhang and Manninen. *Methods Mol Biol.* 2019;1926:77–84.

Section 4: Matrices

Breslin and O'Driscoll. *Drug Discov Today.* 2013;18(5–6):240–249.
Caliari and Burdick. *Nat Methods.* 2016;13(5):405–414.
Chida et al. *Cytotechnology.* 2013;65(6):955–965.
Chittajallu et al. *Nat Methods.* 2015;12(6):577–585.
Diekjürgen and Grainger. *Biomaterials.* 2017;141:96–115.
Dhaliwal. *Mater Methods.* 2012;2:162.
Doyle. *Curr Protoc Cell Biol.* 2016;72:10.20.1–10.20.16.
Franco-Barraza et al. *Curr Protoc Cell Biol.* 2016;71:10.9.1–10.9.34.
Godugu et al. *PLoS One.* 2013;8(1):e53708.
Gupta et al. *Cytotechnology* 2016;68(1):45–59.
Guzman et al. *Biomaterials.* 2017;115:19–29.
Goertzen et al. *Biol Proced Online.* 2018;20:20.
Hayashi and Furue. *Stem Cells Int.* 2016;2016:5380560.
Jongpaiboonkit et al. *Biomaterials.* 2009;29(23):3346–3356.
Knight and Przyborski. *J Anat.* 2015;227(6):746–756.
Morizane et al. *J Neurosci Res.* 2011;89(2):117–126.
Neal et al. *Nanomater Environ.* 2014;2(1):1–12.
Oda et al. *J Biol Chem.* 2010;285(38):29270–29278.
Ovsianikov et al. *Trends Biotechnol.* 2018;36(4):348–357.
Raghavan et al. *Oncotarget.* 2016;7(13):16948–16961.
Rossi et al. *Nat Rev Genet.* 2018;19(11):671–687.
Shimizu et al. *Circ Res.* 2002;90:e40–e48.
Shimomura et al. *J Exp Orthop.* 2018;5(1):2.
Sin et al. *Sci Rep.* 2017;7(1):2585.
Stadler et al. *Cell Mol Life Sci.* 2017;74(10):1907–1921.
Sui et al. *Curr Prot Hum Genet.* 2018;99(1):e68.
Takagi et al. *Sci Adv.* 2016;2(4):e1500887.
Tibbitt and Anseth. *Biotechnol Bioeng.* 2009;103(4):655–663.
Türker et al. *Biomater Sci.* 2018;6(7):1745–1753.
Worthington et al. *Front Oncol.* 2015;5:92.
Xie et al. *Nat Sci Rep.* 2017;7:14070.

Section 5: Media and supplements

Boj et al. *Cell* 2015;160(1–2):324–328.
Clinton and McWilliams-Koeppen. *Curr Protoc Cell Bio.* 2019;82(1):e66.
Diao et al. *Cell Death Dis.* 2019;10(3):238.
Devall et al. *PLoS One.* 2020;15(1):e0227116.
Dowling and Clynes. *Proteomics.* 2011;11(4):794–804.
Dye et al. *Elife.* 2015;4:e05098.
Freedman et al. *Nat Commun.* 2015;6:8715.
Grassi et al. *Cell Death Dis.* 2019;10(3):201.
Guha et al. *Oncotarget.* 2019;10(58):6245–6259.
Huch et al. *Nature.* 2013;494(7436):247–250.
Iefremova et al. *Cell Rep.* 2017;19(1):50–59.
Ísberg et al. *Sci Rep.* 2019;9(1):14843.
Iscove et al. *Blood.* 1971;37(1):1–5.
Kaya et al. *Mol Vis.* 2019; 25:663–678.
Kessler et al. *Nat Commun.* 2019;10(1):1194.
Kim et al. Stem Cell Reports. 2019;12(3):518–531.
Koning et al. *Cell Mol Life Sci.* 2020;77(12):2257–2273.
Lancaster et al. *Nature.* 2013;501(7467):373–379.
Lee et al. *Nat Methods.* 2007;4(4):359–365.
Li et al. *Nat Commun.* 2018;9(1):2983.
Li et al. *Cell Stem Cell.* 2016;19:516–529.
Lucey et al. *Arch Pathol Lab Med.* 2009;133(9):1463–1467.
Morizane et al. *Nat Biotechnol.* 2015;33(11):1193–1200.
Muotri et al. *Stem Cells Dev.* 2018;27(22):1549–1556.
Ootani et al. *Nat Med.* 2009;15(6):701–706.
Pappas et al. *J Vis Exp.* 2019;152:10.3791/60346.
Paşca et al. *Nat Methods.* 2015;12(7):671–678.
Pawitan. *Biomed Res Int.* 2014;2014:965849.
Proctor et al. *Arch Toxicol.* 2017;91(8):2849–2863.
Rodríguez-Hernandez et al. *Int J Curr Res Acad Rev.* 2014;2(12):188–200.
Sachs et al. *Cell* 2018; 172(1–2):373–386.e10.
Sato et al. *Gastroenterology.* 2011;141(5):1762–1772.
Sato et al. *Nature.* 2009;459(7244):262–265.
Simian and Bissell. *J Cell Biol.* 2017;216(1):31–40.
Smits et al. *NPJ Parkinsons Dis.* 2019;5:5.
Spence et al. *Nature.* 2011;470(7332):105–109.
Strikoudis et al. *Cell Rep.* 2019;27(12):3709–3723.
Szvicsek et al. *Cell Mol Life Sci.* 2019;76(12):2463–2476.
Takebe et al. *Cell Rep.* 2017;21(10):2661–2670.
Uchida et al. *JCI Insight.* 2017;2(1):e86492.
Watson et al. *Nat Med.* 2014;20(11):1310–1314.
Wilkinson et al. *Stem Cell Transl Med.* 2017;6:622–633.
Yao et al. *Reprod Med Biol.* 2017;16(2):99–117.
Zhou et al. *Cell Stem Cell.* 2017;21(2):274–283.e5.

Section 6: Imaging and analysis

Almasi et al. *Cell Physiol Biochem.* 2019;52(4):742–757.

Assinger et al. *PLoS One.* 2015;10(4):e0122527.

Burgess et al. *PLoS One.* 2018;13(6):e0197517.

Danahay et al. *Cell Rep.* 2015;10(2):239–252.

Eke et al. *Int J Oncol.* 2016;48(1):313–321.

Freimark et al. *Int J Artif Organs.* 2010;33(4):193–197.

Gieseck et al. *PLoS One.* 2014;9(1):e86372.

Goldshtein et al. *Mol Ther Nucleic Acids.* 2019;16:378–390.

Graf and Boppart. *Methods Mol Bio.* 2010;591:211–227.

Hanson et al. *Tissue Eng Part A.* 2011;17(19–20):2463–2471.

Heng et al. *Biol Proceed Online.* 2009;11:161–169.

Holville and Martin. *Curr Prot Immunol.* 2016;112:14.38.1–14.38.24.

Hongisto et al. *PLoS One.* 2013;8(10):e77232.

Hou et al. *SLAS Discov.* 2018;23(6):574–584.

Huang et al. *Cancer Res.* 2017;77(21):6011–6020.

Kim et al. *Biomater Res.* 2016;20:2.

Lakner et al. *Sci Rep.* 2017;7:42730.

Legrand et al. *Blood.* 2001;97(2):502–508.

Montoya et al. 2019; poster available at: http://assets.thermofisher.com/TFS-Assets/BID/posters/new-improved-cellular-health-evaluation-microplate-reader-assays-poster.pdf

Nunez et al. *Cytometry A.* 2004;61A(1):56–61.

Palmer et al. *J Vis Exp.* 2016;114:e54255.

Piccinini et al. *Biol Proced Online.* 2017;19:8.

Proffitt et al. *Cytometry.* 1996;24(3):204–215.

Richardson and Lichtman. *Cell.* 2015;162(2):246–257.

Rotman and Papermaster. *Proc Nat Acad Sci U S A.* 1966;55(1):134–141.

Sargent. Cell Culture Dish. Spheroid cell culture—practical solutions for frequently asked questions. Available at https://cellculturedish.com/spheroid-cell-culture-practical-solutions-for-frequently-asked-questions/; accessed October 10, 2019.

Sart et al. *Nat Commun.* 2017;8(1):469.

Takeuchi et al. *Sci Rep.* 2014;4:4488.

Tsuji et al. *Cell Transplant.* 2017;26(6):1089–1102.

Wu et al. *Microsyst Nanoeng.* 2018;4:21.

Zhu et al. *Neurosci Bull.* 2017;33(1):95–102.

Section 7: 3D cell culture models in disease and physiological research

Booij et al. *SLAS Discov.* 2019;24(6):615–627.

Brancato et al. *Acta Biomater.* 2017;75:200–212.

Ceresa et al. *Am J Physiol Lung Cell Mol Physiol.* 2009;296(6):L1059–L1066.

Courau et al. *J Immunother Cancer.* 2019;7(1):74.

D'Aiuto et al. *Stem Cell Res Ther.* 2018;9(1):134.

Derricott et al. *Cell Tissue Res.* 2019;375(2):409–424.

Deslee et al. *Respir Res.* 2007;8(1):86.

Forster et al. *Stem Cell Reports.* 2014;3(1):215.

Fujii et al. *Cell Stem Cell.* 2016;18(6):827–838.

Gerckens et al. *J Vis Exp.* 2019;144:e58437.

Godoy et al. *Arch Toxicol.* 2013;87(8):1315–1530.

Groger et al. *Sci Rep.* 2016;6:21868.

Huh et al. *Science.* 2010;328(5986):1662–1668.

Iwasaki et al. *Cancer Res.* 1990;50(8):2429–2436.

Jun et al. *PLoS One.* 2018;13(10):e0206447.

Jung et al. *Nat Med.* 2011;17(10):1225–1227.

Kim et al. *Biofabrication.* 2016;8(1):015021.

Kim et al. *Proc Nat Acad Sc U S A.* 2016;113(1):E7–E15.

Kim et al. *Nat Protoc.* 2015;10(7):985–1006.

Kozyra et al. *Sci Rep.* 2018;8(1):14297.

Kumar et al. *Pathol Oncol Res.* 2020;26(2):1353–1354.

Kuehn et al. *J Vis Exp.* 2015;96:e52325.

Múnera et al. *Cell Stem Cell.* 2017;21(1):51–64.e6.

Nugraha et al. *Sci Rep.* 2017;7(1):14490.

Ootani et al. *Nat Med.* 2009;15(6):701–706.

Ooft et al. *Sci Transl Med.* 2019;11(513):eaay2574.

Phan et al. *Commun Biol.* 2019;2:78.

Sant and Johnston. *Drug Discov Today Technol.* 2017;23:27–36.

Sato et al. *Gastroenterology.* 2011;141(5):1762–1772.

Sato et al. *Nature.* 2009;459(7244):262–265.

Spence et al. *Nature.* 2011;470(7332):105–109.

van de Wetering et al. *Cell.* 2015;161(4):933–945

Young and Reed. *Curr Colorectal Cancer Rep.* 2016;12(5):281–287.

Zhou et al. *Proc Nat Acad Sci U S A.* 2018;115(26):6822–6827.

Appendix

Protocols and applications

A.1

Differentiation of pluripotent stem cells into neural organoids

Introduction

Recent advances in cell culture techniques have focused on creating 3-dimensional (3D) systems in an attempt to represent *in vivo* cell–cell relationships and microenvironments *in vitro*. Various tissue engineering technologies such as bioprinting, microfluidics, and organs-on-chips have been used successfully to generate 3D cultures [1,2]. Remarkable progress has also been made utilizing adult and pluripotent stem cells (ASCs and PSCs) to generate 3D organ-like (i.e., organoid) cell models [3-5]. PSC-based methods frequently start by aggregating cells in suspension culture to form clusters called embryoid bodies (EBs). Cells in these clusters are capable of differentiating into many types and can undergo self-organization and self-morphogenesis to create a complex cell model that better mimics the *in vivo* cell–cell interactions and microanatomy of a given tissue type. Some PSC-based approaches also require the encapsulation of cells within a natural or synthetic extracellular matrix (ECM)-like substrate [6-8]. In all methods, the application of growth factors, small molecules, and other media supplements is used to guide the formation of organoid systems based on principles inferred from studies of embryogenesis and adult stem cell biology. There are now many published methods for generating a variety of organoid types that resemble different parts of the brain, as well as the liver, intestine, and kidney, to name a few.

The unknown compatibility of multiple reagents from different vendors that span the organoid workflow is an issue that many researchers experience. This issue can have dramatic consequences for the successful generation of the desired organoid system and its reproducibility between laboratories. Established workflows for generating neural organoids from PSCs typically follow a specific sequence of steps that begin with standard PSC culture followed by EB formation, neural induction, neural patterning, and organoid growth [7, 9-12] (Figure 1). The composition of the cell culture medium at each of these steps is critical for the successful differentiation of PSCs. Importantly, the differentiation capacity of a given PSC line must be determined empirically, and some optimization of the differentiation method may be needed for the PSC line of choice. In this application note, we demonstrate the use of Gibco™ StemFlex™ feeder-free medium, Gibco™ Geltrex™ matrix, and Thermo Scientific™ Nunclon™ Sphera™ microplates to create neural organoids and spheroids.

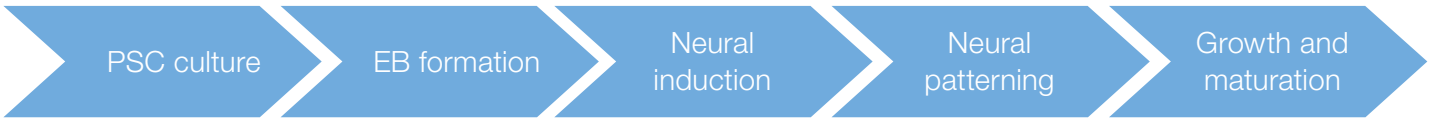

Figure 1. The essential steps of neural organoid formation from PSC cultures.

Experimental details and results

PSC culture

Prior to differentiation, H9 human embryonic stem cells (ESCs) and Gibco™ Human Episomal Induced Pluripotent Stem Cells (iPSCs, Cat. No. A18945) were maintained using StemFlex Medium and grown on Thermo Scientific™ Nunclon™ Delta tissue cultureware coated with a 1:100 dilution of Geltrex LDEV-Free, hESC-Qualified, Reduced Growth Factor Basement Membrane Matrix (Cat. No. A1413301). PSC clumps were routinely passaged using Gibco™ Versene™ Solution (Cat. No. 15040066).

EB formation

PSCs were cultured in feeder-free conditions using StemFlex Medium (Cat. No. A3349401). When PSC cultures reached 70–80% confluency, they were dissociated into single-cell suspensions using Gibco™ StemPro™ Accutase™ Cell Dissociation Reagent (Cat. No. A1110501), Trypsin/EDTA Solution (Cat. No. R001100), or TrypLE™ Select Enzyme (Cat. No. 12563011). Cell counts and viability were determined using Gibco™ Trypan Blue Solution (Cat. No. 15250061) and the Invitrogen™ Countess™ II FL Automated Cell Counter (Cat. No. AMQAF1000). About 6–9 x 10^5 viable cells per well were seeded in StemFlex Medium with Gibco™ RevitaCell™ Supplement (Cat. No. A2644501) in Nunclon Sphera 96-well U-bottom microplates (Cat. No. 174925). Nunclon Sphera microplates exhibit virtually no cell attachment, promoting consistent formation of spheroids. EBs formed overnight equally well with all dissociation methods but most efficiently with the addition of RevitaCell Supplement (Figure 2).

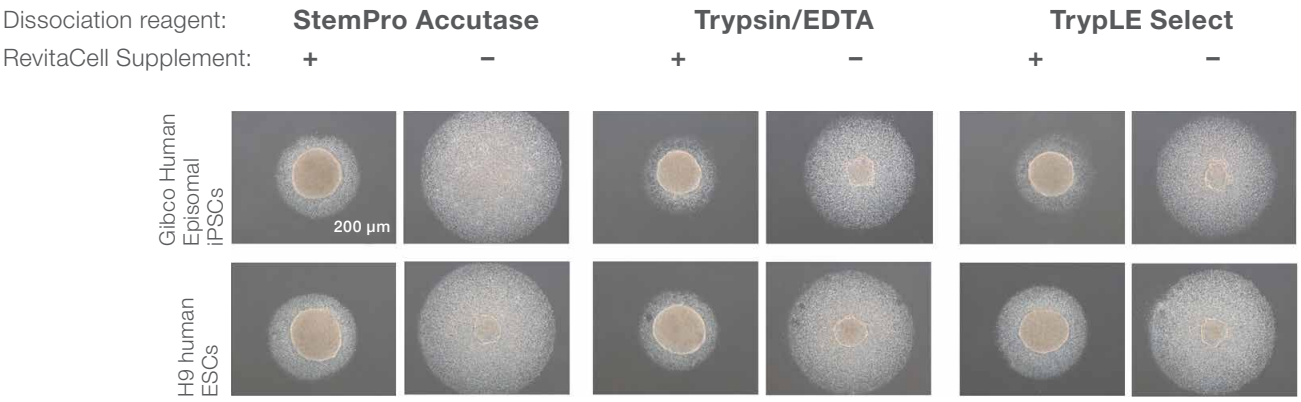

Figure 2. RevitaCell Supplement dramatically improves EB formation. A comparison of EB formation after isolation of PSCs by different methods demonstrated that EBs formed equally well with each dissociation reagent but only if RevitaCell Supplement was included in the culture medium. Cells that do not contribute to the EB are eventually washed away during media changes and do not typically interfere with subsequent steps; here they were not washed away, to illustrate the efficiency of EB formation.

In the absence of RevitaCell Supplement, small EBs did form but with poor efficiency, as most cells either did not survive or did not self-aggregate (Figure 2). EBs were then cultivated for 3–4 days, with a 75% medium change every other day with StemFlex Medium with RevitaCell Supplement. The resulting EBs were of consistent size that was directly proportional to the number of cells seeded (Figure 3).

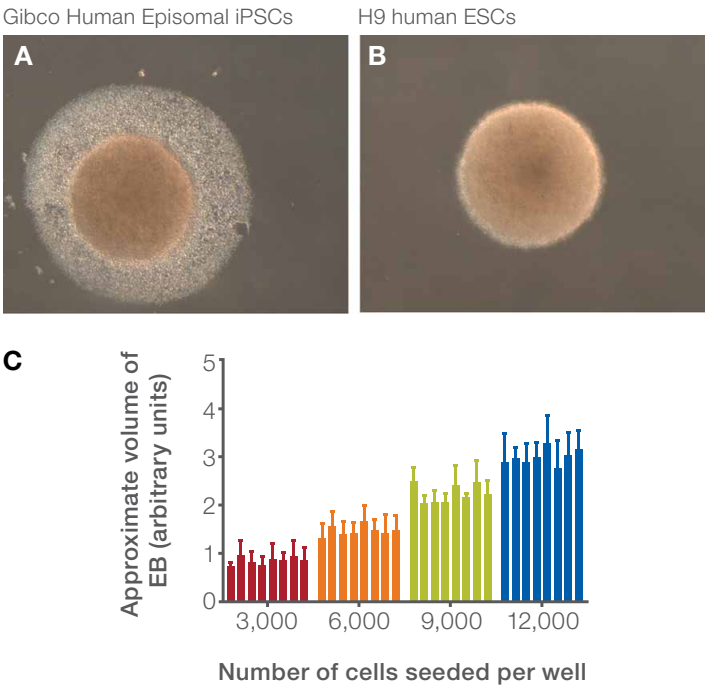

Figure 3. Evaluation of EBs formed in StemFlex Medium with RevitaCell Supplement. (A, B) These images show representative EBs from two different PSC lines after 4 days of culture. **(C)** EB size is directly proportional to the number of cells seeded. The graph shows the consistency in size between 8 replicates for each cell density that was evaluated. Data were calculated by measuring the area of each EB using ImageJ software. The area was then used to calculate the approximate EB volume, which is plotted on the y-axis.

Neural induction and patterning

Following EB formation, the cell aggregates were induced to differentiate into neural lineages by performing 3–4 successive 75% volume medium changes to serially dilute and remove the prior culture medium. Neural induction medium was composed of Gibco™ DMEM/F-12 with GlutaMAX™ Supplement (Cat. No. 10565018) and N-2 Supplement (Cat. No. 17502001). EBs were cultured for 8–9 days with a 75% volume medium change every other day until the outer layers of the EB formed a bright "ring" in contrast to the darker center (Figure 4). By day 10, each EB that displayed this phenotype was encapsulated in undiluted Geltrex LDEV-Free Reduced Growth Factor Basement Membrane Matrix (Cat. No. A1413201) and incubated at 37°C to gel. The use of Geltrex matrix for this application has been independently demonstrated elsewhere [13]. Droplets of Geltrex matrix containing EBs were then transferred to a differentiation medium consisting of DMEM/F-12 with GlutaMAX Supplement (Cat. No. 10565018) and Gibco™ Neurobasal™ Medium (Cat. No. 21103049) with GlutaMAX Supplement (Cat. No. 35050061), MEM with NEAA (Cat. No. 11140050), 2-mercaptoethanol (Cat. No. 21985023), insulin (Cat. No. 12585014), N-2 Supplement (Cat. No. 17502001), and B-27™ Supplement Minus Vitamin A (Cat. No. 12587010). Encapsulated samples were then transferred to Nunclon Sphera 6-well or 24-well plates (Cat. No. 174932, 174930) with a density of 3–5 or 1–2 droplets per well, respectively.

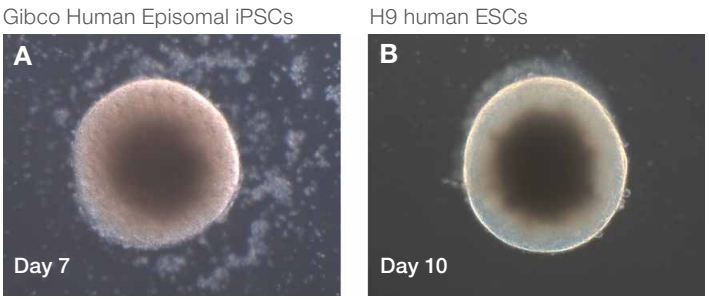

Figure 4. Neural induction and patterning. (A) Brightfield image showing a day 7 EB. **(B)** Day 10 neuralized EB immediately before encapsulation in Geltrex matrix.

Growth and maturation

The samples were cultured in a growth and maturation medium of the same formulation as the previous incubation medium except this medium contained B-27 Supplement (Cat. No. 17504044). From this point on, neural organoids were cultured on an orbital shaker at 80–85 rpm and the medium was changed every 2–3 days. Neuroepithelia become easily visible within about a week. These samples can be continuously cultured for many weeks (Figure 5A, B) or until analysis is performed (e.g., cellular organization, marker expression). For example, Figure 5C indicates the presence of multiple neural cell types present at day 39 of culture. Gene expression analysis shows that these organoids still contain neural stem and progenitor cells, based on *SOX1*, *SOX2*, and *PAX6* expression, as well as immature neuronal markers such as *DCX* and *MAP2*. However, markers of specific neural regions such as *TBR1* (deep layer neurons), *FOXG1* (forebrain tissue), and *SLC6A1* (encodes GABA1 transporter expressed in cerebral cortical tissue, hippocampus, and other tissues) were also detected, indicating the presence of more differentiated cell types.

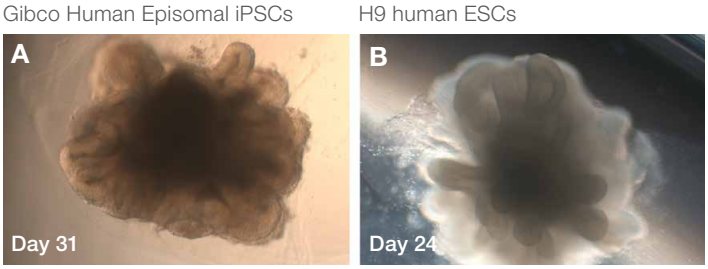

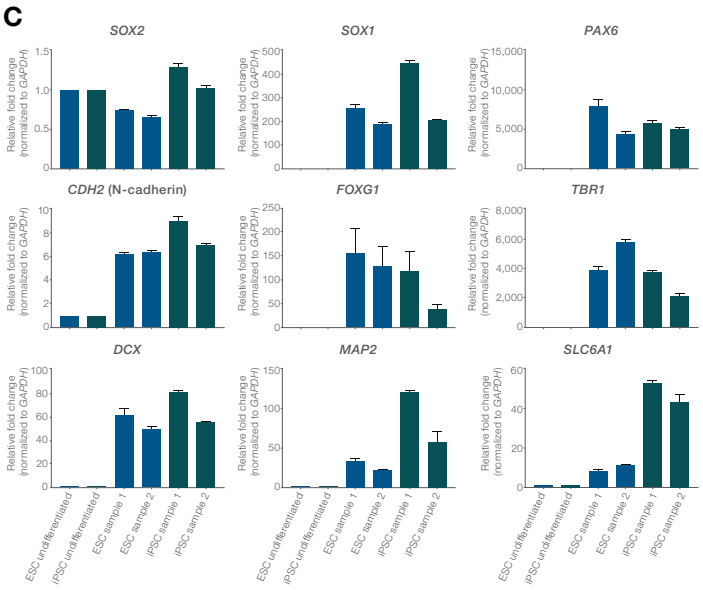

D

Gene	TaqMan Assay	Cells or tissues
SOX2	Hs01053049_s1	Neural stem cells, radial glia
SOX1	Hs01057642_s1	Neural stem cells
PAX6	Hs01088114_m1	Neural stem cells, radial glia
CDH2 (N-cadherin)	Hs00983056_m1	Neural ectoderm
FOXG1	Hs01850784_s1	Forebrain
TBR1	Hs00232429_m1	Deep layer neurons
DCX	Hs00167057_m1	Neurons
MAP2	Hs00258900_m1	Neurons
SLC6A1	Hs01104475_m1	Cerebral cortex, hippocampus

Figure 5. Phenotypic characterization and gene expression analysis of neural organoids. (A, B) Brightfield images of neural organoids on day 31 or day 24 of culture show convoluted neuroepithelial structures. **(C)** Gene expression analyses of day 39 neural organoid cultures indicate the presence of multiple neural cell types, including neural stem cells and neurons. Expression levels were calculated using the $2^{-\Delta\Delta C_t}$ method, relative to undifferentiated H9 human ESCs or Gibco Human Episomal iPSCs. Samples from two experiments are shown. **(D)** Summary of Applied Biosystems™ TaqMan® Assays used for gene expression analysis.

Conclusions

Together, these data demonstrate the compatibility of feeder-free StemFlex Medium and Nunclon Sphera 96-well U-bottom microplates with EB formation and neural organoid differentiation. Furthermore, we demonstrate the effectiveness of Geltrex matrix for the encapsulation and morphogenesis of neural organoids. In all, the results indicate that these three products can be successfully integrated with existing Gibco basal media and supplements that are commonly used for studies involving neural organoids.

References

1. Bhatia SN, Ingber DE (2014) Microfluidic organs-on-chips. *Nat Biotechnol* 32:760–72.
2. Murphy SV, Atala A (2014) 3D bioprinting of tissues and organs. *Nat Biotechnol* 32:773–785.
3. Bartfeld S, Clevers H (2017) Stem cell–derived organoids and their application for medical research and patient treatment. *J Mol Med (Berl)* 95:729–738.
4. Clevers H (2016) Modeling development and disease with organoids. *Cell* 165: 1586–1597.
5. Drost J, Clevers H (2018) Organoids in cancer research. *Nat Rev Cancer* 18:407–418.
6. Sato T, Vries RG, Snippert HJ et al. (2009) Single Lgr5 stem cells build cryptvillus structures *in vitro* without a mesenchymal niche. *Nature* 459:262–265.
7. Lancaster MA, Renner M, Martin CA et al. (2013) Cerebral organoids model human brain development and microcephaly. *Nature* 501:373–379.
8. Gjorevski N, Sachs N, Manfrin A et al. (2016) Designer matrices for intestinal stem cell and organoid culture. *Nature* 539:560–564.
9. Mariani J, Simonini MV, Palejev D et al. (2012) Modeling human cortical development *in vitro* using induced pluripotent stem cells. *Proc Natl Acad Sci U S A* 109:12770–12775.
10. Phillips AW, Nestor JE, Nestor MW (2017) Developing hiPSC derived serum free embryoid bodies for the interrogation of 3-D stem cell cultures using physiologically relevant assays. *J Vis Exp* 125:e55799.
11. Sloan SA, Darmanis S, Huber N et al. (2017) Human astrocyte maturation captured in 3D cerebral cortical spheroids derived from pluripotent stem cells. *Neuron* 95:779–790.e6.
12. Thomas CA, Tejwani L, Trujillo CA et al. (2017) Modeling of TREX1-dependent autoimmune disease using human stem cells highlights L1 accumulation as a source of neuroinflammation. *Cell Stem Cell* 21:319–331.e8.
13. Iefremova V, Manikakis G, Krefft O et al. (2017) An organoid-based model of cortical development identifies non-cell-autonomous defects in Wnt signaling contributing to Miller-Dieker syndrome. *Cell Rep* 19:50–59.

A.2

The use of B-27 Supplement in establishing and characterizing functional 3D neural spheroid models from monolayer-expanded NSCs

Introduction

The expanding application of 3D culture methods to generate stem cell–derived models of neuronal development, maturation, and disease enables the creation of more complex cellular models that more faithfully recapitulate *in vivo* neural architectures and physiology than traditional 2D cultures.

Here we evaluated the differentiation and functional maturity of neural stem cells (NSCs) generated and expanded in monolayer culture, and then transferred them to conditions that promote 3D spheroid formation. Using a range of analysis tools, we demonstrated that our Sox2/Nestin-positive NSCs are capable of forming 3D spheroids that could be matured to generate electrically active neurons with robust expression of genes related to functional synapses and neurotransmitter trafficking.

Currently, many approaches to create 3D models rely on reagents and tools designed for 2D monolayer systems. In our study, multiple specialty cultureware, media combinations, culture conditions, and reagents were assessed for optimal differentiation of NSCs to neurons and the influence these many variables had on proliferation, gene expression, and maturation.

Our results clearly demonstrate the feasibility of transitioning from a 2D NSC culture system to a 3D system and the importance of optimizing several key culture system parameters in order to reproducibly generate neural spheroids and influence the rate of maturation. Defining the relative benefits of modeling and analyzing neural biology in 2D versus 3D systems is an area of active investigation in which our study highlights several points of consideration.

Materials and methods

Gibco™ Human Episomal iPSC Line (Cat. No. A18945) or H9 hESCs were differentiated to NSCs using Gibco™ PSC Neural Induction Medium (Cat. No. A1647801) (Figure 1). Cells at P6 were cryopreserved, and upon thaw seeded into neural expansion medium in Gibco™ Nunclon™ Sphera™ 96U-well microplates (Cat. No. 174925). After 7 days in culture, spheroids were transitioned to maturation medium consisting of either Gibco™ Neurobasal™ Medium (Cat. No. 21103049) with B-27™ Supplement (Cat. No. 1750404) or the Gibco™ B-27™ Plus Neuronal Culture System (Cat. No. A3653401) with or without the addition of Gibco™ CultureOne™ Supplement (Cat. No. A3320201)

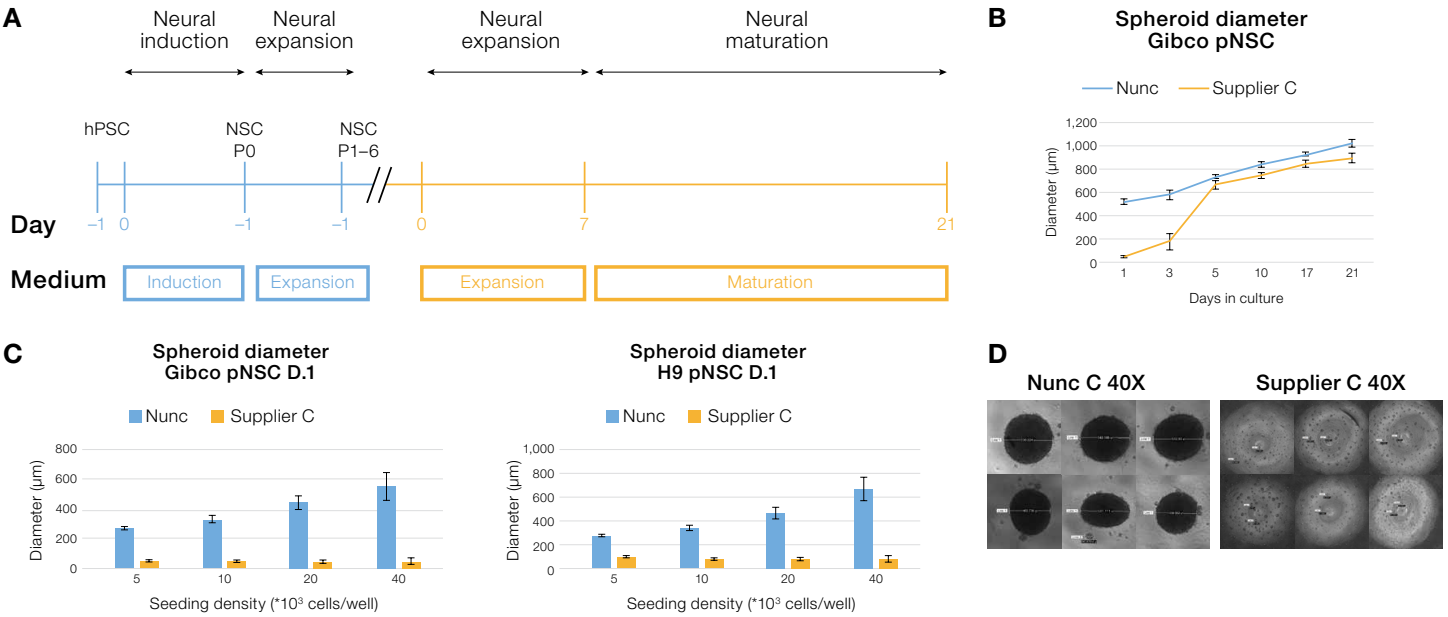

Figure 1. Establishing neural spheroid models. (A) Workflow for generating and maturing neural spheroid models. **(B, D)** Compared to products from other suppliers, NSCs seeded in Nunclon Sphera plates rapidly establish uniformly sized spheroids. **(C)** NSCs generated from two PSC lines (iPSCs left panel, ESCs right panel) seeded at a range of densities formed single spheroids within 24 hr. **(D)** Phase-contrast images of neural spheroids at 1 day in culture captured on an Invitrogen™ EVOS™ FL Auto Imaging System. Equivalent exposure settings were used for both plates. Differences in plate dimensions affect image brightness.

Results

Maturation medium containing either B-27 or B-27 Plus Supplement yielded spheroids of similar size and shape (Figure 2). Addition of CultureOne Supplement resulted in smaller spheroids with a more compact morphology, likely due to reduced progenitor proliferation. Addition of CultureOne Supplement elevates the expression level of genes related to functional synapses and neurotransmitter trafficking (Figure 3). Culture in B-27 Plus Supplement and CultureOne Supplement resulted in high levels of PVALB expression, suggesting increased numbers of this subtype of GABAergic neurons. Spheroids matured in the B-27 Plus Neuronal Culture System with CultureOne Supplement appear to contain denser and more structured neurite networks. Neural spheroids are electrically active and contain a mixed population of excitatory and inhibitory neurons (Figure 4).

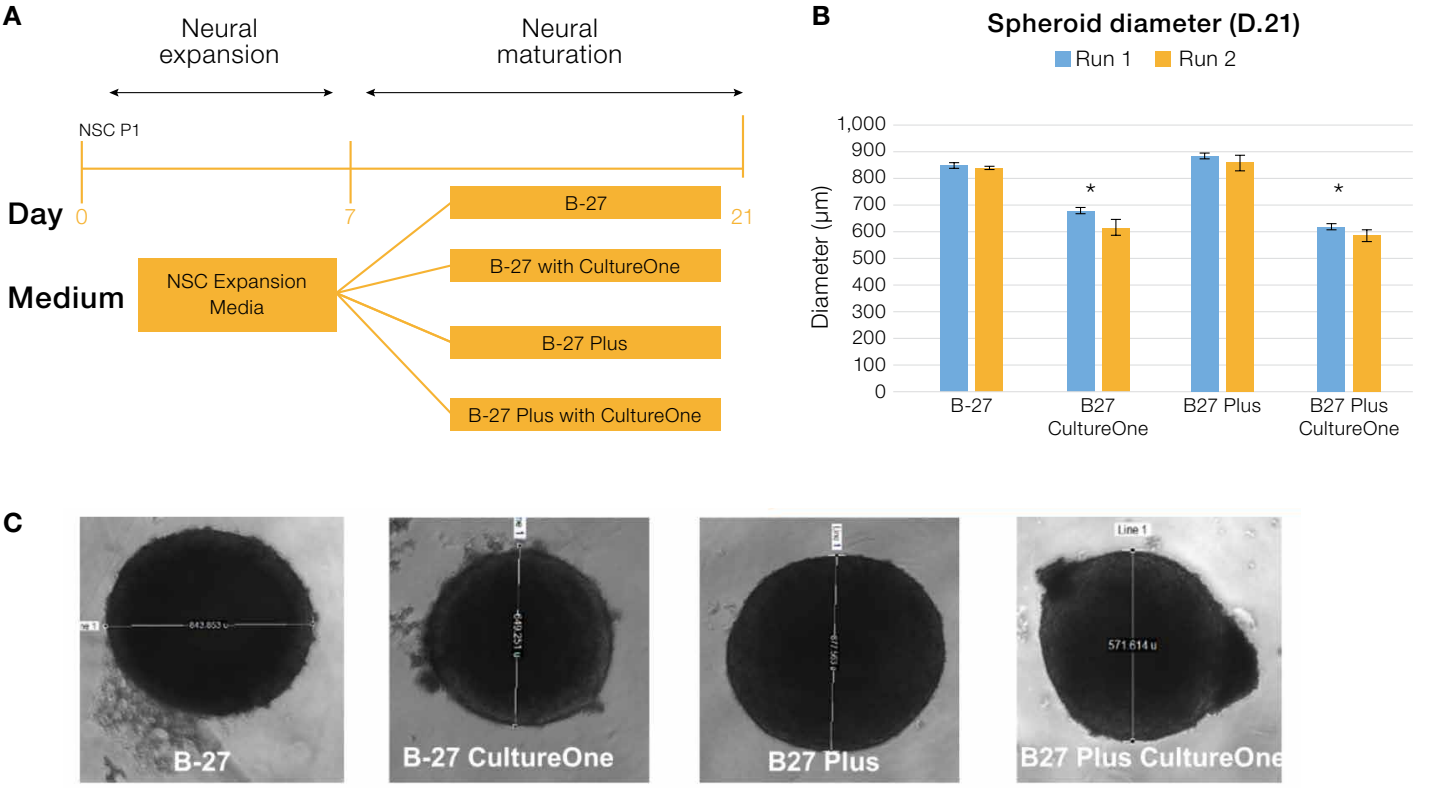

Figure 2. Maturation of neural spheroids. (A) After 7 days in culture, spheroids were transitioned to 4 different maturation media (indicated). **(B)** Phase-contrast images of neural spheroids at 21 days in culture captured on an EVOS FL Auto Imaging System show morphological changes observable in spheroids cultured in the presence of CultureOne Supplement. **(C)** Spheroid diameter using measurement tools on the EVOS FL Auto Imaging System from two independent experiments. Differences observed with the addition of CultureOne Supplement is statistically significant (Student's *t*-test, P value <0.001).

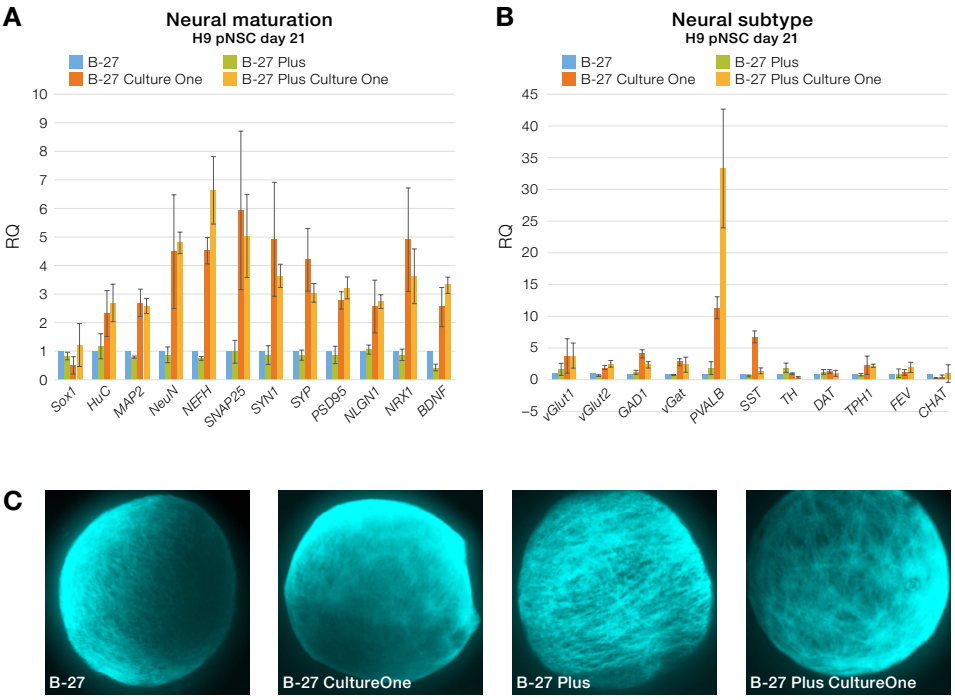

Figure 3. Characterization of neural spheroids. Gene expression analyses of **(A)** neural maturation and **(B)** subtype markers from spheroids at 21 days in culture assessed using Applied Biosystems™ TaqMan® Assays. **(C)** Spheroids stained with Invitrogen™ Tubulin Tracker™ Deep Red (Cat. No. T34077) to label neuronal processes. Images were acquired using the Thermo Scientfic™ CellInsight™ CX7 LZR HCA Platform.

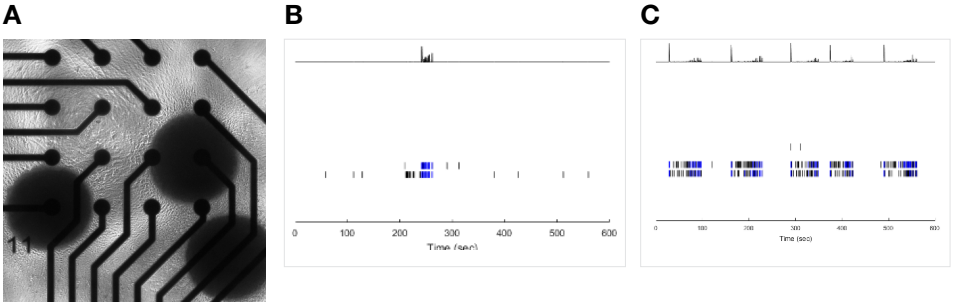

Figure 4. Functional assessment of neural spheroids. Multi-electrode array (MEA) analysis using the Axion Biosystems Maestro platform. **(A)** Phase-contract image of neural spheroid attached to MEA surface. Raster plots of spiking activity **(B)** before and **(C)** after treatment with 1 µm picrotoxin (GABA antagonist).

Summary

- Existing reagents are compatible with the generation of 3D neural spheroid cultures
- Addition of CultureOne Supplement modulates the rate of proliferation and maturation of neural spheroids
- Spheroids matured in the B-27 Plus Neuronal Culture System develop complex neurite networks and are electrically active

A.3

3D modeling of PSC-derived dopaminergic neurons

Introduction

Accurate *in vitro* modeling of neurological diseases requires multiple cell types of the brain to interact and develop toward mature functionality. When human pluripotent stem cells (PSCs) undergo neural differentiation in 3D, self-organization of progeny cells results in organoids with brain-like structures and functions that are not observed in 2D culture. However, the increased complexity of neural organoids often comes with the costs of low throughput and poor reproducibility. Disease models for drug discovery may therefore have to temper self-organized complexity with inductive specification of desired cell types.

To model Parkinson's disease (PD), we have explored methods for differentiation of human PSCs to midbrain dopaminergic (DA) neurons in 3D. In order to compare physical influences on organoid structure, we have used a single set of media previously optimized for midbrain floor plate specification, expansion, and maturation in 2D culture. This media kit worked to specify floor plate and differentiate dopaminergic neurons in suspension culture, although the time requirements for specification and differentiation in 3D could be significantly reduced.

We tested physical parameters including rotation vs. static suspension, and encapsulation within extracellular matrix (ECM) vs. dilute addition of ECM molecules to the medium. Surprisingly, static suspension cultures with addition of dilute ECM could reproduce some of the known benefits of ECM encapsulation, such as morphological complexity and faster neuronal maturation, without the difficulty and low throughput of encapsulation methods.

To apply these promising steps toward a reproducible 3D model for Parkinson's disease, we have generated midbrain organoids from an iPSC line engineered via CRISPR-Cas9 technology to carry the PD-linked A30P mutation in alpha-synuclein (SNCA) and an unaltered wild-type (WT) line from the same editing process. Here, we describe our testing of the response of these mutant and wild-type organoids to oxidative stressors.

To be useful for drug screening, *in vitro* disease models must be reproducibly generated at large scale. As a first step toward this goal, we tested whether 3D organoid models of the ventral midbrain could be produced using the simple and scalable Gibco™ PSC Dopaminergic Neuron Differentiation Kit. The increased complexity of organoid models has been reported to depend upon cell interactions with basement membrane. We explored methods of organoid formation with or without added extracellular matrix (ECM) for effects upon complexity and neuronal maturation.

Methods

2D specification with the kit occurs in attached culture, followed by multiple passages in expansion medium until day 21 (Figure 1). Floor plate cells are then passaged onto a poly-D-lysine/laminin surface for differentiation of dopaminergic neurons up to day 35. The method of 3D midbrain organoid formation begins with PSCs in rotating suspension culture. These cells are dissociated and seeded into suspension culture for floor plate specification, then changed into expansion medium and maturation medium while in suspension without further passaging. The duration of specification and expansion can be shortened for 3D culture with equivalent expression of floor plate markers.

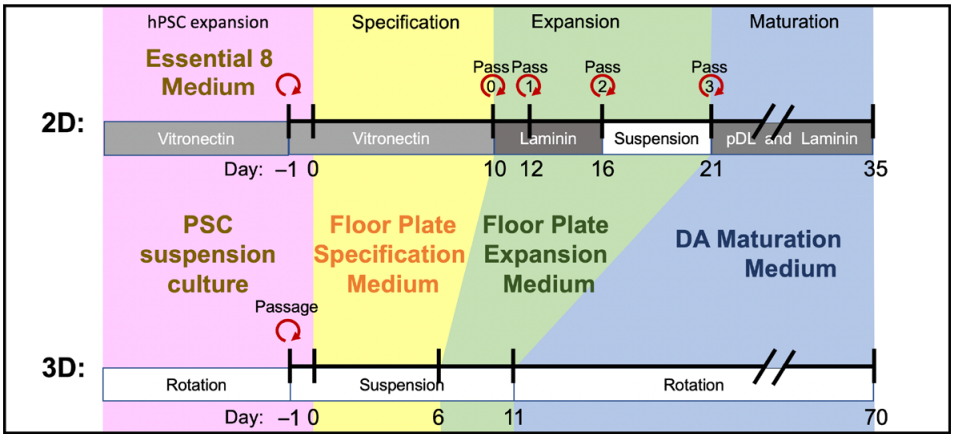

Figure 1. Workflow for the floor plate derivation process using the three media in the PSC Dopaminergic Neuron Differentiation Kit.

Results

We compared the morphology of organoids grown without ECM to organoids grown with ECM and in U-well microwell plates. ECM encapsulation or U-bottom microplate expansion boosts the formation of midbrain floor plate organoids (Figure 2). Furthermore, the addition of ECM during floor plate specification in microwell plates alters the architecture of microwell organoids (Figure 3).

Further analysis verified maturation and functional activity of midbrain organoids. When formed with ECM or in microwells, midbrain organoids have a more complex epithelial morphology and earlier outgrowth of dopaminergic neurons (Figure 4). Earlier detection of neuromelanin in microwell organoids with dilute Geltrex matrix also suggests more rapid maturation of dopaminergic neurons (Figure 5). Microelectrode array (MEA) analysis confirmed that midbrain organoids formed in multiwell plates with dilute Geltrex matrix can produce coordinated dopaminergic activity in as little as five weeks (Figure 6).

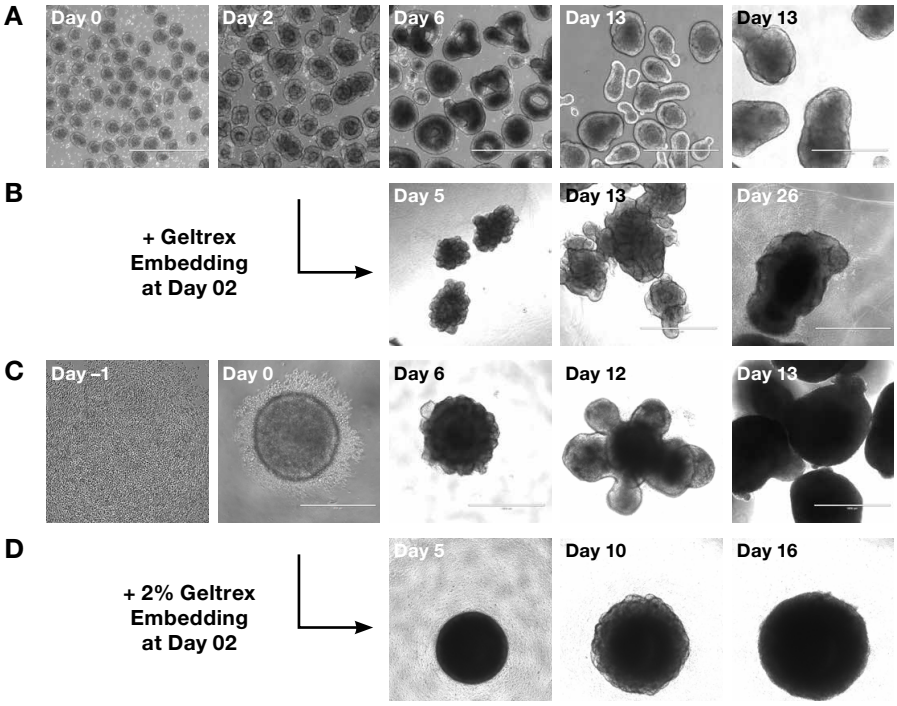

Figure 2. Organoid formation is boosted by ECM. (A) Floor plate specification and expansion of hPSCs in rotating suspension culture without ECM. Numbering of days and passages correspond to the schematic in Figure 1. **(B)** ECM encapsulation at day 2 in 50% Gibco™ Geltrex™ LDEV-Free Reduced Growth Factor Basement Membrane Matrix during floor plate specification in rotating suspension culture. **(C)** Static suspension culture for floor plate specification and expansion in Thermo Scientific™ Nunclon™ Sphera™ U-bottom microwell plates without ECM. Spheroids are transferred to rotating culture for maturation. **(D)** Static suspension culture in microwells using Floor Plate Specification Medium supplemented with 2% Geltrex matrix at day 2. All other medium changes remain as above. Scale bars: 1,000 µm.

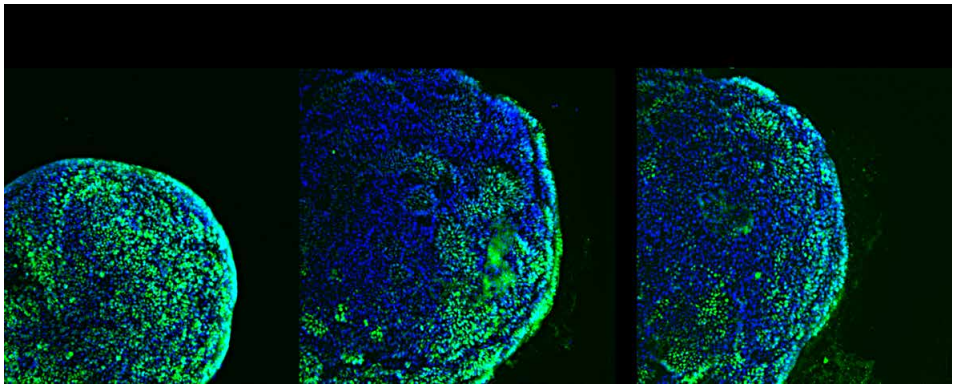

Figure 3. Added ECM supports prominent rosette-like structures in early organoids. Static microwell organoids after specification by method C (no ECM), supplemented at day 2 with 200 µg/mL laminin (LAM), or supplemented with 2% Geltrex (GTX) matrix. Organoids were fixed on day 7 and stained with N-cadherin antibody and DAPI. Maximal intensity projections of 8 µm optical sections were imaged on the Thermo Scientific™ CellInsight™ CX7 LZR High Content Analysis Platform.

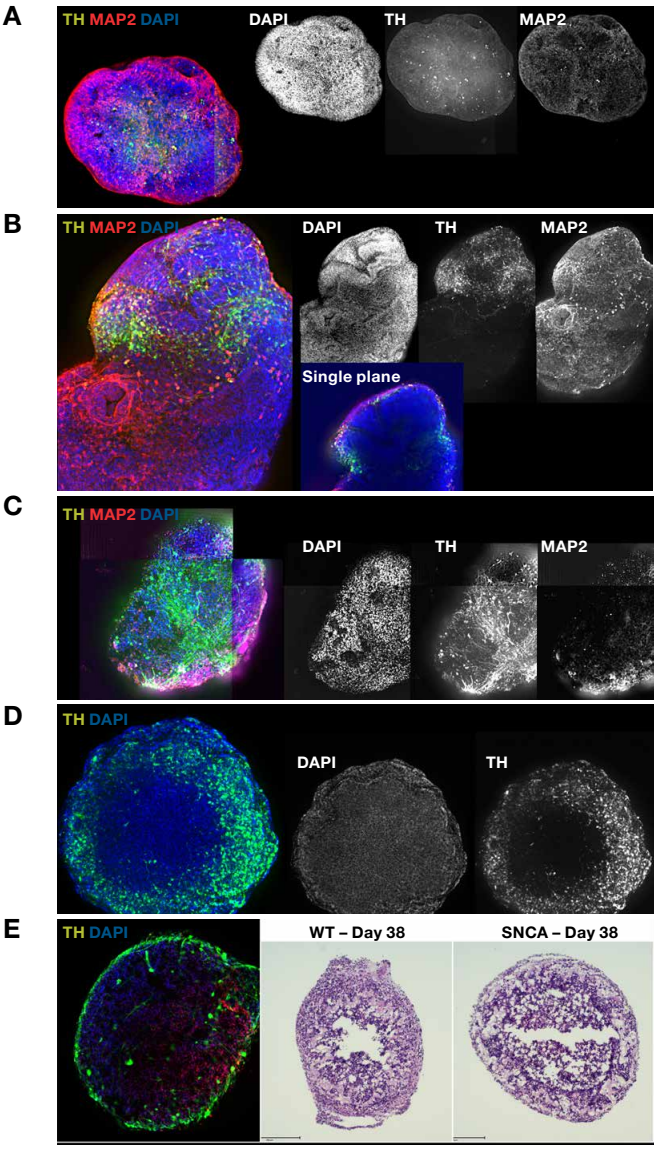

Figure 4. ECM encapsulation and U-bottom microplates increase organoid complexity and yield of dopaminergic neurons. Maximal intensity projections of optical sections after antibody staining were acquired on the CellInsight CX7 LZR High Content Analysis Platform. **(A)** Rotating suspension organoid (method A) at day 19 (early maturation) stained with MAP2 and tyrosine hydroxylase (TH) antibodies. **(B)** Encapsulated organoid (method B) at day 19 stained with MAP2 and TH antibodies. **(C)** Microwell organoid (method C) at day 19 stained with MAP2 and TH antibodies. **(D)** 23-day microwell organoid specified in the presence of 2% Geltrex matrix at day 2 (method D) and stained with TH antibody. (E) Hematoxylin and eosin staining of sections of 5-week-old microwell organoids specified in 2% Geltrex matrix. Staining reveals thick bands of cells at the outside of the organoids surrounding a dense core of degraded cells.

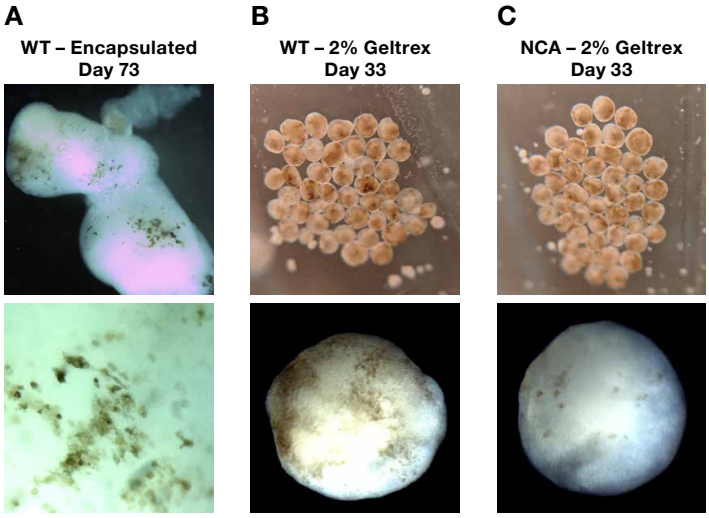

Figure 5. ECM promotes maturation of floor plate organoids. **(A)** Encapsulated organoid (method B) imaged at day 73 without stains or dyes. Reddish-brown color suggests presence of neuromelanin, a pigment that is a by-product of dopamine synthesis [1]. **(B)** Microwell organoids at day 33 specified in 2% Geltrex matrix (method D) from a SNCA wild-type CRISPR iPSC line. **(C)** Microwell organoids at day 33 specified in 2% Geltrex matrix (method D) from a SNCA A30P mutant CRISPR iPSC line.

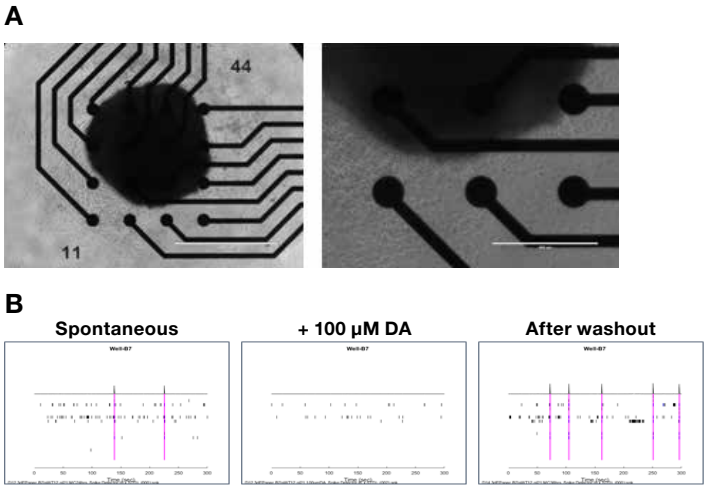

Figure 6. Floor plate organoids mature functionally. **(A)** Microwell organoid specified in 2% Geltrex matrix and cultured in suspension until day 21 and in attached culture on a poly-D-lysine/laminin–coated MEA for 14 days. **(B)** Raster plots of MEA recordings from the plated microwell organoid. Each plot shows 300 seconds of activity, first in maturation medium, second after addition of 100 µM dopamine, and third following washout of the dopamine. Vertical pink bars indicate detected network bursts.

This 3D culture technique was adapted to model oxidative stress in midbrain organoids derived from iPSCs. Results confirmed that midbrain organoids can be generated from disease-relevant iPSC lines and used to model responses to environmental stresses (Figure 7).

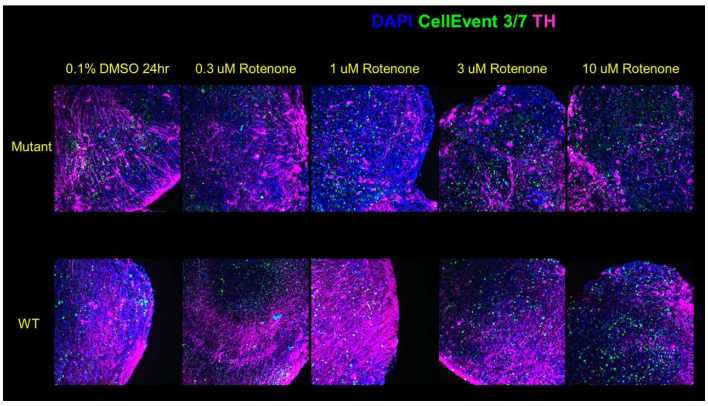

Figure 7. Modeling oxidative stress in floor plate organoids. Oxidative stress test on 5-week midbrain organoids derived in multiwell plates with dilute Geltrex matrix from two CRISPR-engineered iPSC lines. Organoids were treated with rotenone for 20 hr while in rotating suspension. Treated organoids were fixed and serially permeabilized with methanol and Triton™ X-100 solution, then stained for active caspase-3 and TH. Whole-mount organoids were then cleared with Invitrogen™ CytoVista™ 3D Cell Culture Clearing Reagent and imaged on the CellInsight CX7 High Content Analysis Platform. Quantitation of active caspase-3 staining in TH-positive neurons can be performed to measure stress sensitivity.

Summary

- Midbrain organoids formed in ECM or microwells show greater complexity than organoids in free suspension.
- ECM or microwells promote increased differentiation of dopaminergic neurons within organoids
- The combination of microwells and dilute ECM during floor plate specification contributes to earlier maturation and functional activity of dopaminergic neurons
- This combined ECM and microwell method offers higher throughput than encapsulation methods for generation of disease-model brain organoids

Reference

1. Jo J, Xiao Y, Sun AX et al. (2016) Midbrain-like organoids from human pluripotent stem cells contain functional dopaminergic and neuromelanin-producing neurons. *Cell Stem Cell* 19(2):248–257.

A.4

High-throughput fluorescence imaging and analysis of spheroids

Tips, tricks, and tools to efficiently grow, stain, image, and analyze 3D cell cultures

Introduction

As cells do not grow in isolation, traditional two-dimensional (2D) cell culture monolayer models lack physiologically relevant environmental conditions and can have drastic differences in terms of their physical and biochemical features, compared to intact biological systems. Since more physiologically relevant animal studies are time consuming and expensive, there is a need for experimental models that span the gap between *in vitro* cell-based assays and *in vivo* animal studies. To satisfy this need, researchers have been turning to three-dimensional (3D) organoid and tumor spheroid systems that mimic an *in vivo* setting while maintaining the ease of manipulation of cell-based assays. These 3D model systems have several features that allow them to more closely resemble the environment of cells in an intact organism, including cell-to-cell interactions, cell-to-matrix interactions, relevant gene expression profiles, and gradients of oxygen, nutrients, and metabolites [1] (Figure 1). Because 3D spheroids share features with tumors, such as functionally different zones with apoptotic or necrotic regions in the core and proliferative cells along the periphery, they are an excellent model for cancer biology and drug discovery assays. Their features allow better investigation of chemoresistance in the core of tumors to improve drug delivery, along with more relevant drug screening and pharmacology assays [2-4].

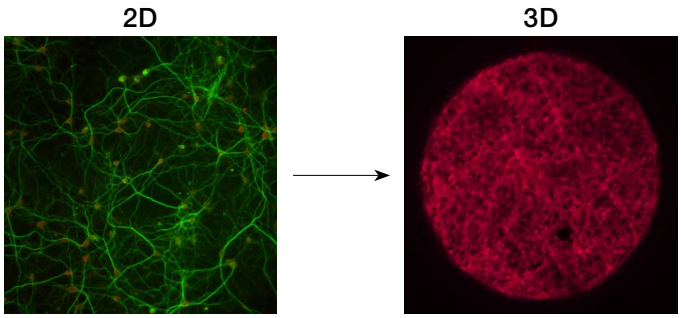

	2D monolayer	3D spheroid
Cellular interactions	Cell to cell	Cell to cell, cell to extracellular matrix
Cellular activity	Cellular adhesion, proliferation, and modified genes	Proliferative ring; apoptotic or necrotic core
Microenvironment	Relatively uniform	Gradients of oxygen, metabolites, and nutrients

Figure 1. Comparison of 2D and 3D cellular models. Working in 3D systems involves the formation of spheroids. Spheroids are aggregates of cells that can be either grown in suspension, encapsulated, or grown on top of a 3D matrix. Compared to 2D cell models, 3D spheroids have cellular interactions, zones of cellular activity, and microenvironments that more closely resemble *in vivo* systems, allowing more relevant pharmacology studies and better tumor models.

3D cell culture and analysis workflow

Using optimal techniques and cell culture reagents, 3D spheroids can easily be grown in the lab and stained with a variety of fluorescent reagents to examine molecular localization and various cellular functions. Fluorescently labeled spheroids can be imaged and analyzed using microplate readers, fluorescence microscopy, or high-content imaging systems. Invitrogen™ and Thermo Scientific™ cell culture systems, reagents, instrumentation, and analysis software are available for a complete 3D cell culture workflow from growth and staining of cells to imaging and quantitation of results (Figure 2). These products enable robust 3D cell cultures with accurate imaging and analysis for more physiologically relevant drug discovery and cancer biology applications.

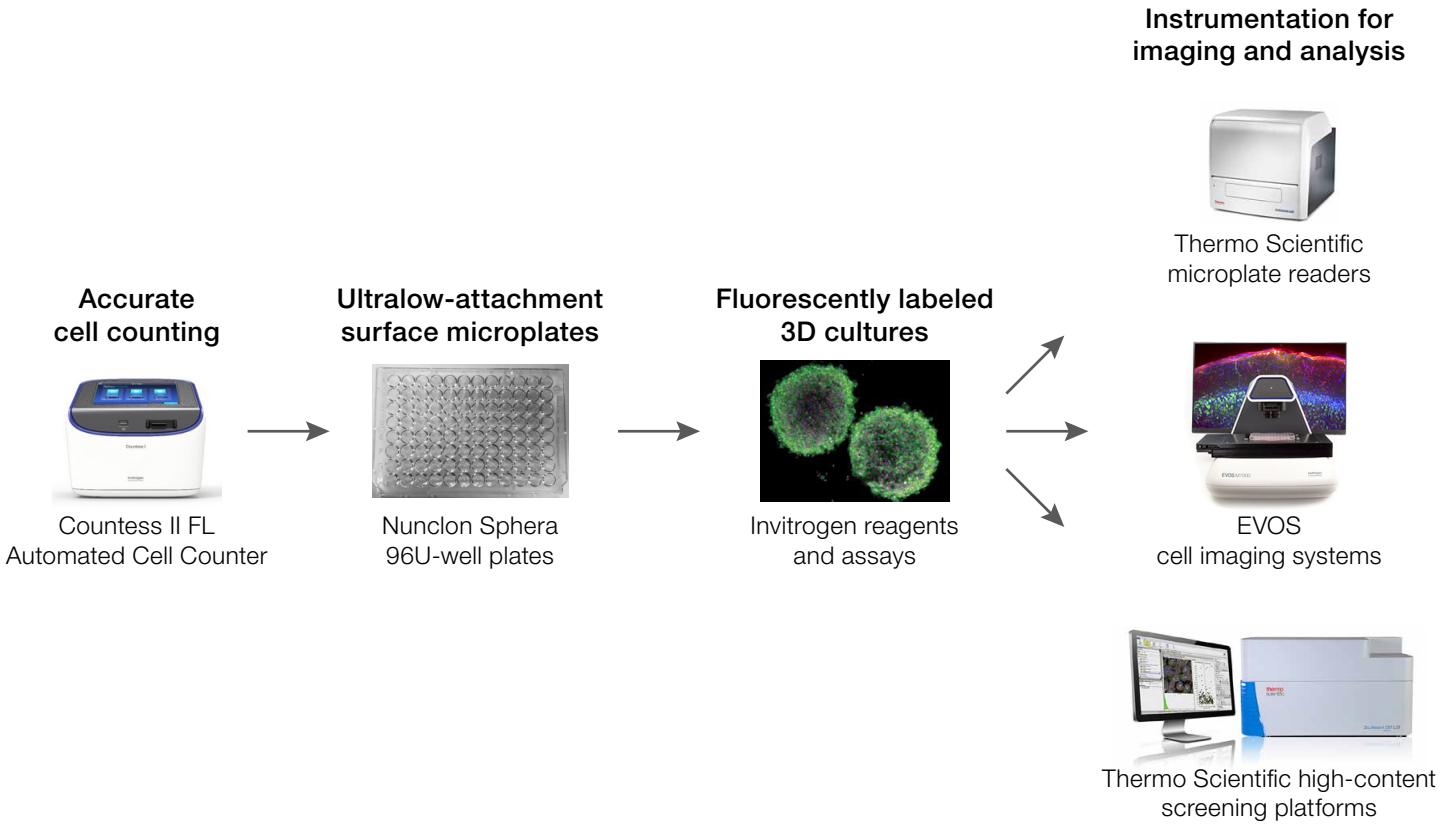

Figure 2. Workflow for spheroid growth, staining, imaging, and quantitation. Accurate cell counting with the Invitrogen™ Countess™ II FL Automated Cell Counter enables cell seeding at the appropriate density for spheroid growth on Thermo Scientific™ Nunclon™ Sphera™ 96U-well plates, which have an ultralow-attachment surface optimal for spheroid growth. Spheroids can then be stained with Invitrogen™ fluorescent reagents and assays followed by imaging and analysis on several fluorescence platforms, including Thermo Scientific™ microplate readers, Invitrogen™ EVOS™ cell imaging systems, and Thermo Scientific™ high-content screening (HCS) platforms.

How to grow spheroids

Although growing cells in a 3D assembly is more challenging than monolayer culturing techniques, spheroid growth of many cell types can easily be accomplished using optimized tools and methods. To efficiently grow spheroids in culture, it is important to seed cells at the appropriate cell density and use cell culture plates that are optimized for 3D growth. These plates have an ultralow-attachment surface compared to traditional tissue culture–treated plates, which encourages cells to grow together in a 3D assembly instead of on a single surface. Nunclon Sphera 96U-bottom plates have an ultralow-attachment, round-bottom surface, which minimizes monolayer cell adhesion and promotes the growth of single spheroids rather than multiple spheroids or satellite 3D cultures, compared to other types of plates (Figure 3). The Countess II FL Automated Cell Counter can be used to accurately count cells so that they are seeded on 3D culture plates at the appropriate density for growing into a 3D spheroid. Growth of cells into 3D cell culture can also be aided by briefly centrifuging the plate after the appropriate number of cells are plated.

Because cells grown in 3D culture are growing together in a free-floating 3D structure instead of attaching to a surface, gentle pipetting is required to change the medium without disturbing or aspirating the spheroid. This can be more easily accomplished by growing the spheroid in a relatively large volume of medium (for instance, 200 µL per well in a 96-well plate) and replacing half the medium every other day rather than removing the entire volume of medium. The use of media and supplements optimized and verified for 3D cell culture also enables spheroids to form more quickly, which can minimize the number of medium changes and allows faster maturation of cells with mature phenotypes. Some cells may also need external factors such as cadherin to grow into a 3D complex.

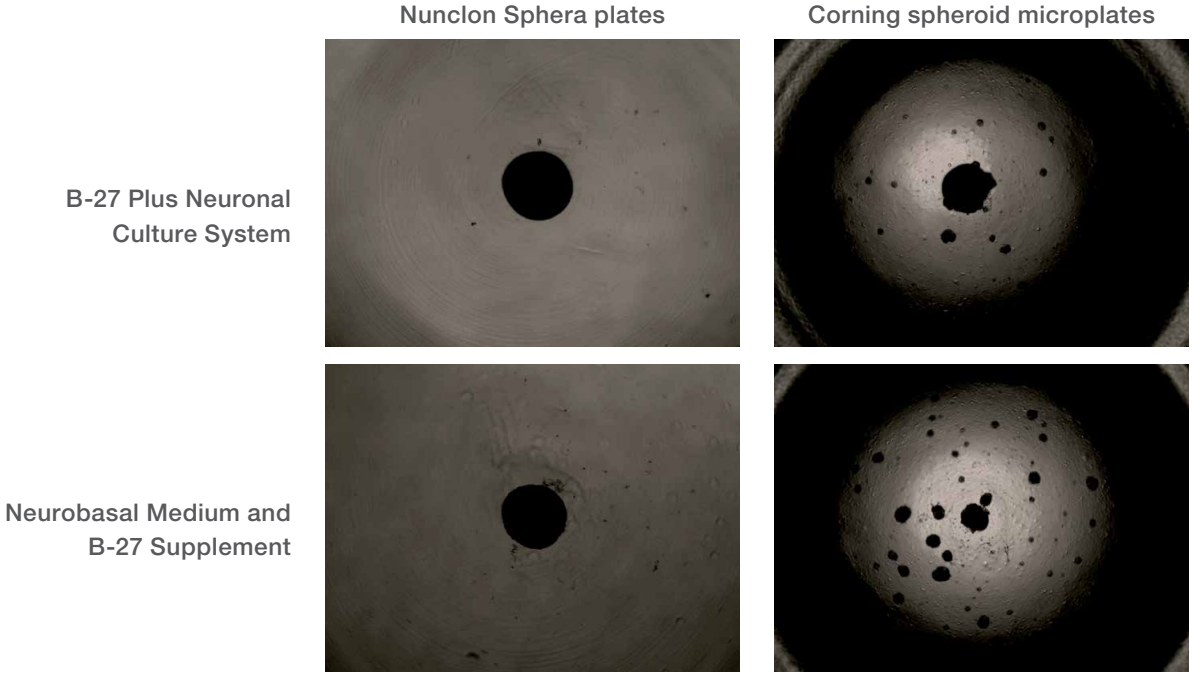

Figure 3. Optimal growth of spheroids on Nunclon Sphera 96U-well plates. Neural stem cells (NSCs) were seeded at 5,000 cells per well on Nunclon Sphera 96U-well plates or Corning™ 96-well Ultra-Low Attachment (ULA) Spheroid Microplates and grown for 10 days in the Gibco™ B-27™ Plus Neuronal Culture System or Gibco™ Neurobasal™ Medium and B-27™ Supplement. Imaging on an Invitrogen™ EVOS™ XL Core Imaging System showed that NSCs grown on Nunclon Sphera plates formed single, tight neurospheroids while NSCs grown on other plates formed multiple spheroids with satellite cultures.

How to stain spheroids

Spheroids can be stained with a variety of fluorescent reagents to examine localization and abundance of molecules within the 3D cell culture, along with viability, apoptosis, mitochondrial health, and other cellular functions (Table 1). Many fluorescent stains and probes developed for 2D cell culture staining can also be used to stain spheroids. However, because 3D cell cultures are denser than monolayers, concentration and incubation time may need to be optimized to allow stains to fully penetrate into the center of the 3D culture, and the duration of wash steps may need to be increased to reduce background. When immunostaining fixed and permeabilized spheroids, adding 5% DMSO to the antibody staining solution can help reduce background.

Table 1. Fluorescent reagents and assays for spheroid staining and analysis on different detection platforms.

Cellular function	Reagent or assay	Detection platform	Experimental guidelines	
			Concentration*	Incubation time
Apoptosis	CellEvent Green Caspase-3/7	Microplate reader	0.33X	2 hr
		Fluorescence microscopy, high-content screening	1X	1 hr
Mitochondrial health	MitoTracker Orange	Microplate reader	2X	1 hr
		Fluorescence microscopy, high-content screening	1X	30 min–1 hr
Proliferation	Click-iT EdU	Fluorescence microscopy, high-content screening	1X	Standard protocol
Viability	CyQUANT Direct Green	Microplate reader	1X dye, 2X background suppressor	45 min–1 hr
	CyQUANT XTT	Microplate reader	2X	5–8 hr
	PrestoBlue HS	Microplate reader	1X	3–5 hr
	alamarBlue HS	Microplate reader	1X	3–5 hr
	CyQUANT LDH Cytotoxicity Assay	Microplate reader	1X	30 min
	CyQUANT LDH, fluorescence	Microplate reader	1X	10 min
	LIVE/DEAD Viability/Cytotoxicity Kit	Fluorescence microscopy, high-content screening	1X	Standard protocol
Reactive oxygen species	CellROX Deep Red	Fluorescence microscopy, high-content screening	1X	1 hr
Hypoxia	Image-iT Hypoxia Reagent	Fluorescence microscopy, high-content screening	1X	1 hr

* Concentration recommended for 3D staining relative to the manufacturer's recommended working conditions for 2D staining.

Imaging and analysis of spheroids

Once spheroids are stained with the fluorescent reagents of choice, there are a variety of ways to image and analyze them to obtain data from 3D cellular models. Microplate assays can be used to quickly assess the general cell health of the entire spheroid, while more complex imaging and analysis allows optical sectioning to visualize cells within the spheroid core and assess individual cells in the 3D culture. Depending on the type of readout and level of detail needed, fluorescently labeled spheroids can be detected and analyzed with microplate readers, fluorescence microscopes, and high-content screening systems. Poor imaging in the core of a 3D cell culture is often thought to be due to reagent penetration issues; furthermore, light scattering can cause significant limitations in spheroid imaging. Selection of the optimal imaging and analysis system enables fluorescence detection throughout the entire spheroid, increasing the quality of 3D culture images and data.

Tissue clearing reagents, such as Invitrogen™ CytoVista™ 3D Cell Culture Clearing Reagent, can improve imaging of 3D cultures. Treatment of spheroids with this reagent improves visualization of cells in the core of 3D spheroids to enable better fluorescence detection and analysis of cells inside the spheroid (Figure 4).

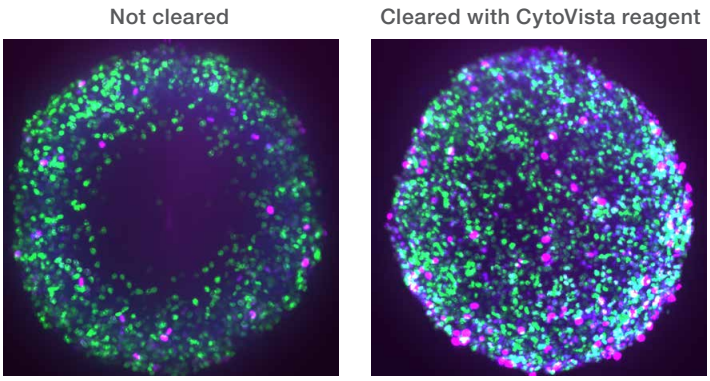

Figure 4. Improved imaging and resolution of a spheroid core cleared with CytoVista 3D Cell Culture Clearing Reagent. A549 spheroids were grown on Nunclon Sphera 96U-well plates at a density of 5,000 cells per well. Spheroids were pulsed with 10 µM 5-ethynyl-2′-deoxyuridine (EdU) for 1 hr. Spheroids were fixed and permeabilized, and then labeled with the Invitrogen™ Click-iT™ EdU Alexa Fluor™ 488 HCS Assay following the kit protocol. Spheroids were also stained with Invitrogen™ Hoechst 34580 and Ki67 mouse monoclonal antibody that was labeled using the Invitrogen™ Zip Alexa Fluor™ 647 Rapid Antibody Labeling Kit. The spheroids were then treated with CytoVista 3D Cell Culture Clearing Reagent for 1 hr or left untreated. The spheroids were imaged with the Thermo Scientific™ CellInsight™ CX7 LZR High Content Analysis Platform using confocal mode. The image is a maximum-intensity projection of 100 optical sections of 2 µm each.

Microplate readers

Microplate assays can be used to quickly assess cell viability and health as a preliminary measurement before downstream applications such as drug characterization. Spheroids require higher drug concentrations for effectiveness, resulting in different IC_{50} values compared to those obtained for the same drug in 2D cultures. IC_{50} values obtained from drug-treated spheroids analyzed by microplate readers and high-content analysis systems are similar, indicating that microplate readers can be used to quickly screen spheroid drug responses and provide similar data as cell-by-cell quantitation (Figure 5).

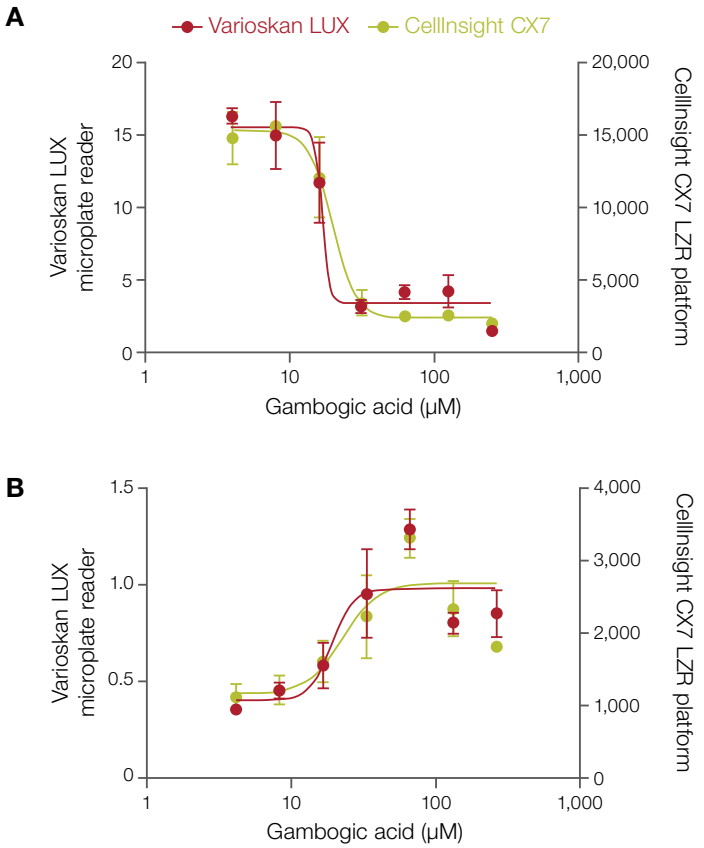

Figure 5. Drug dose response in 3D spheroids. A549 spheroids were treated with various concentrations of gambogic acid for 48 hr, then stained using the **(A)** Invitrogen™ CyQUANT™ Direct Cell Proliferation Assay or **(B)** Invitrogen™ CellEvent™ Caspase-3/7 Green Detection Reagent for analysis of apoptosis. Fluorescence (500 nm excitation, 530 nm emission) was read on the Thermo Scientific™ Varioskan™ LUX Multimode Microplate Reader or the CellInsight CX7 LZR High Content Analysis Platform. For each reagent, similar IC_{50} values were obtained on both the microplate reader and high-content analysis platform, indicating that fluorescence-based assays can be analyzed with microplate readers for initial drug discovery questions.

Fluorescence microscopy

When imaging 3D cultures with fluorescence microscopy, optimization of microscope settings and the use of advanced features can improve image quality and allow better visualization into the spheroid core. Selection of the appropriate objective improves axial resolution and focus, while microscopes with z-stacking capabilities can be used to image throughout entire spheroids. EVOS cell imaging systems are high-performance, easy-to-use imaging systems with z-stacking capabilities that can be used to produce high-resolution images of 3D cultures. These images can then be analyzed on an image analysis platform such as Invitrogen™ Celleste™ Image Analysis Software for quantitation of spheroid size and general intensity measurements of the entire spheroid (Figure 6).

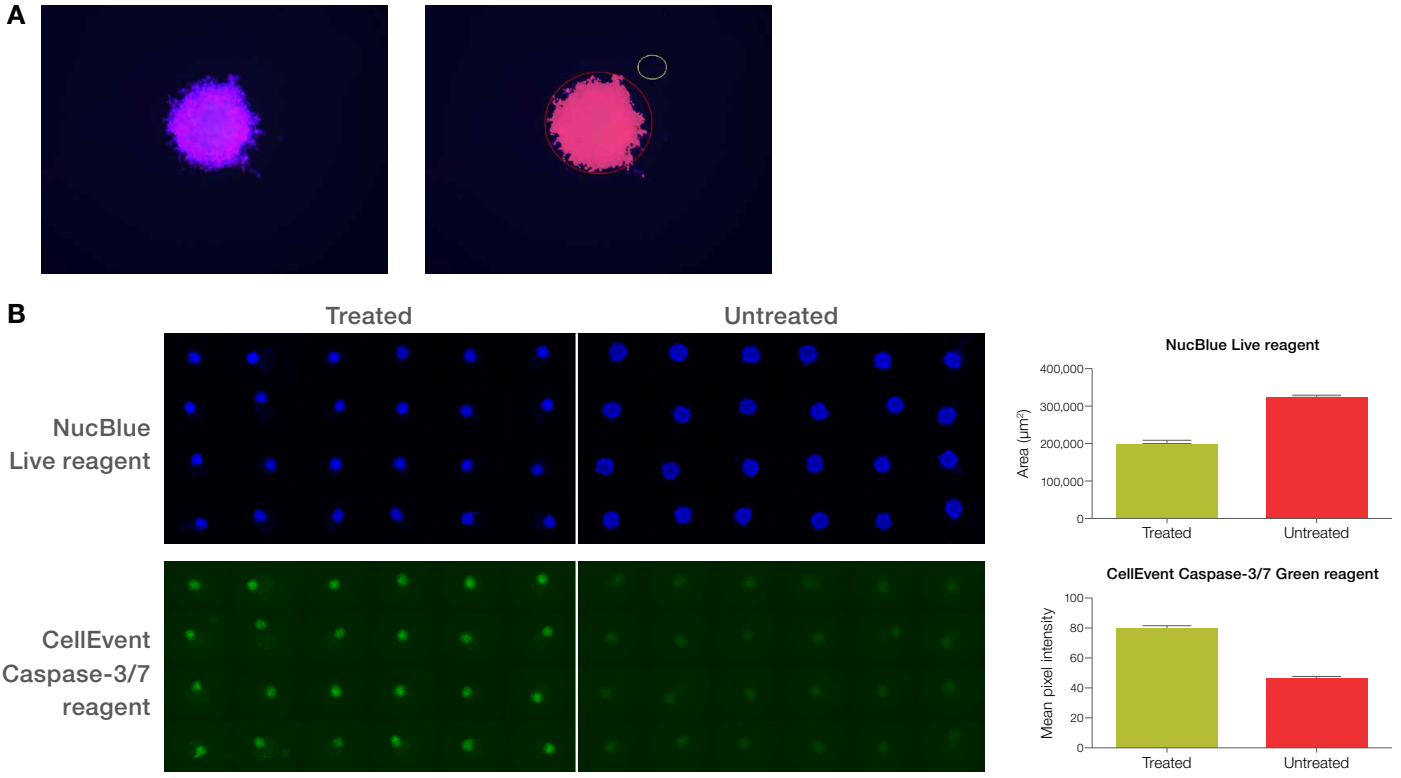

Figure 6. Spheroid imaging on the Invitrogen™ EVOS™ FL Auto 2 Imaging System and segmentation with Celleste Image Analysis Software. **(A)** A549 cell spheroids were cultured in Nunclon Sphera 96U-well plates and subsequently labeled with Invitrogen™ NucBlue™ Live, MitoTracker™ Orange, and CellEvent Caspase-3/7 Green reagents, followed by imaging on the EVOS FL Auto 2 Imaging System using an Olympus™ 4x super-apochromat objective with DAPI, RFP, and GFP filter cubes. Images were imported into Celleste 4.1 software for automated analysis of spheroid morphology and staining intensity using smart segmentation functionality, shown as red (object of interest) and yellow (background) regions of interest. Upon defining the two regions, Celleste 4.1 software is able to automatically detect objects and successfully segment the spheroid versus background. **(B)** Representative montage images showing A549 spheroids that were treated with 40 µM niclosamide or DMSO control. Half the plate was treated, and the other half was untreated. Figures show that treated spheroids are smaller in size, as determined by measuring the area defined by staining with NucBlue Live reagent, and that they have an increase in apoptotic activity, as determined by staining with CellEvent Caspase-3/7 Green reagent. Data were generated by segmenting the spheroids using the smart segmentation inputs defined in (A) and applying the analysis to the 48 wells shown in the representative images. Each bar represents the mean ± SEM for 24 spheroids.

High-content screening

High-content screening offers the benefits of rapid and high-throughput cell imaging and analysis of large cell populations with robust quantitation and statistics. The CellInsight CX7 LZR High Content Analysis Platform has several features that make it an ideal platform for high-content imaging and analysis of 3D cell cultures. This system incorporates high-resolution imaging and the ability to obtain z-stacks, along with a low scanning time and confocal mode. Its laser-based excitation source results in reduced light scatter, deeper penetration, and improved signal-to-noise ratios, compared to LED-based excitation sources.

Thermo Scientific™ HCS Studio™ 3.1 Cell Analysis Software enables cell-by-cell analysis of these high-resolution 3D culture images. The software can segment individual cells within the 3D spheroid and measure cell-by-cell intensity and other features to provide detailed analysis of each cell within the 3D structure (Figure 7).

Conclusion

With optimal cell culture reagents, robust fluorescent reagents and assays, and high-performance fluorescence imaging and detection systems, switching from 2D to 3D cell culture can be easily accomplished even in standard laboratory settings. Because 3D spheroids have a cellular environment and other features that more closely resemble tumors and *in vivo* models, research on these cultures can provide more relevant data and findings that apply to intact biological systems, enhancing research in drug discovery, cancer biology, and other critical areas.

References

1. Baker BM, Chen CS (2012) Deconstructing the third dimension: how 3D culture microenvironments alter cellular cues. *J Cell Sci* 125(Pt 13):3015–3024.
2. Huang BW, Gao JQ (2018) Application of 3D cultured multicellular spheroid tumor models in tumor-targeted drug delivery system research. *J Control Release* 270:246–259.
3. Patel NR, Aryasomayajula B, Abouzeid AH et al. (2015) Cancer cell spheroids for screening of chemotherapeutics and drug-delivery systems. *Ther Deliv* 6(4):509–520.
4. Fang Y, Eglen RM (2017) Three-dimensional cell cultures in drug discovery and development. *SLAS Discov* 22(5):456–472.

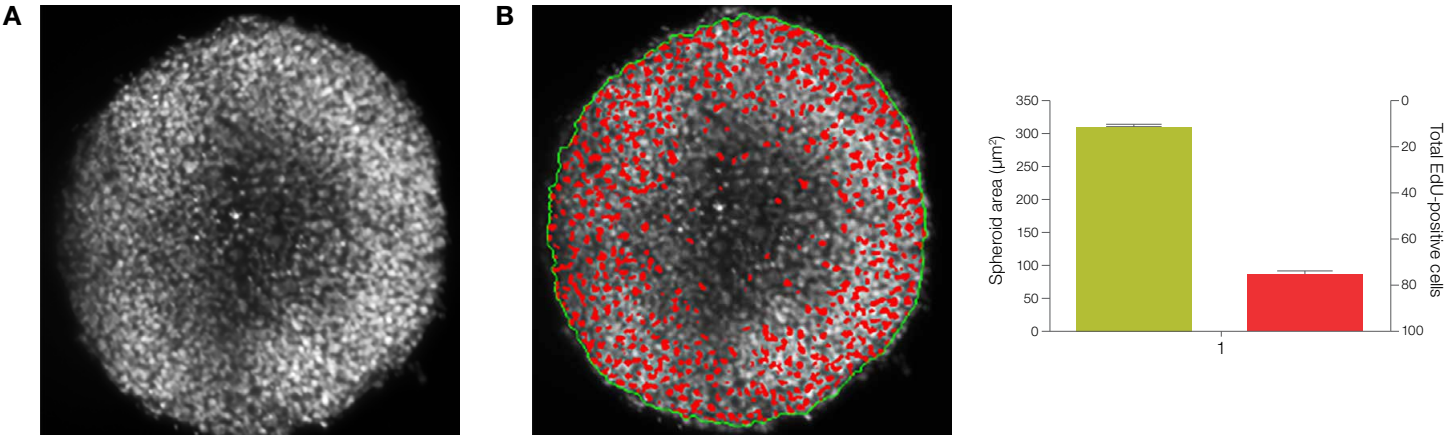

Figure 7. Quantitation of cell proliferation in spheroids using high-content screening. A549 cells were plated at a density of 5,000 cells per well on a Nunclon Sphera 96U-well microplate and incubated for 24 hr in a CO_2 incubator. EdU was added to a final concentration of 10 µM and incubated for 1 hr. The spheroids were then fixed with 4% formaldehyde, permeabilized with 0.25% Triton™ X-100 surfactant, and stained for EdU using the Click-iT EdU Alexa Fluor 488 HCS Assay, following the kit protocol. **(A)** The plate was imaged on the CellInsight CX7 LZR High Content Analysis Platform with a 4x objective using confocal mode. The image is a maximum-intensity projection of 200 optical z-slices of 1 µm each. **(B)** Quantitation was done with HCS Studio software using the Morphology Explorer bio-application. The spheroid was segmented as one object, and EdU-positive cells were counted as spots within the spheroid.

A.5

3D spheroid culture as a tool for studying drug metabolism

Introduction

The primary human hepatocyte (PHH) three-dimensional (3D) culture model developed by Thermo Fisher Scientific holds promise for disease modeling and functional studies. As the liver is the principal site of metabolism for most drugs, primary hepatocytes have become the most popular *in vitro* tool to evaluate hepatic drug metabolism. However, the efficiency of 3D hepatic spheroids for assessing drug metabolism is relatively unknown. One major difference between 3D hepatic culture and conventional two-dimensional (2D) culture is the number of cells per well. A single hepatic spheroid typically consists of 1,000 to 3,000 cells, whereas there are between 50,000 (96-well plate) and 400,000 (24-well plate) cells per well in a conventional 2D culture. Hence, it is expected that metabolites synthesized in 3D culture will be present at lower concentrations relative to those found in 2D culture. However, we have observed that relative gene expression levels for certain **cytochrome P450 (CYP) enzymes** are higher in 3D hepatic spheroids than in their 2D counterparts. As CYP proteins are critical phase I enzymes for drug metabolism, we measured CYP activities for 6 different enzymes with distinct substrates via high-resolution mass spectrometry, directly comparing the activities of 2D and 3D cultures. Our data demonstrate the utility of 3D hepatic spheroid models derived from Gibco™ hepatocytes for studying drug metabolism.

Materials and methods

Spheroid culture

Hepatic spheroids were generated using **Gibco™ cryopreserved spheroid-qualified human hepatocytes (Cat. No. HMCPSQ)** following the **user guide** [1]. Each well contained 3,000 PHHs. The spheroids formed within 5 days of cell seeding. Starting on day 5, half of the plating medium was changed every 48–72 hours. On day 9 of spheroid culture, 2D hepatocytes were seeded in a collagen-coated 96-well plate at 50,000 PHHs per well following **published guidelines** [2].

Metabolic assay

On day 10, the media of both 2D and 3D cultures were replaced with an incubation medium containing **Gibco™ Williams' E Medium** and **Gibco™ Primary Hepatocyte Maintenance Supplements**. Six compounds of interest were added to both 2D and 3D PHH cultures in serum-free Williams' E Medium. The compounds were selected such that several CYP enzymes that are important for hepatic drug metabolism could be interrogated. Table 1 lists the identity of each compound, the CYP enzymes primarily responsible for their metabolism, the metabolites analyzed, and the drug concentrations tested. Of the six compounds used, all except tolbutamide are known as high-turnover compounds with fast intrinsic clearance rates. The incubation time (Table 2) for each compound for both 2D and 3D studies was previously determined to be within the linear range of the assay. The medium was collected without disturbing the cells and stored at –80ºC for later analysis.

Analysis of metabolites

Cell culture samples collected from both 2D and 3D hepatic cultures were analyzed for metabolite formation using the **Thermo Scientific™ Q Exactive™ Plus Hybrid Quadrupole-Orbitrap™ Mass Spectrometer** (Table 3). This allowed for accurate, high-resolution mass measurement, as well as fast scanning for metabolites (quantitative and/or qualitative) in complex matrices.

Liquid chromatography–mass spectrometry (LC-MS)
The **Thermo Scientific™ Vanquish™ Flex Binary UHPLC system** was used for liquid chromatography (LC) analysis. LC separation was performed on a **Thermo Scientific™ Hypersil™ BDS C18 column** using mobile phases A (H_2O/0.1% formic acid) and B (ACN/0.1% formic acid) at a flow rate of 400 µL/min with gradient (5% to 90% in 15 min). The media collected from both 2D and 3D samples containing the respective metabolites were directly injected into the Vanquish system for LC-MS analysis on the Q Exactive Plus mass spectrometer. High-resolution full scan and HCD MS2 data were collected in a data-dependent fashion with polarity switching. The metabolites were readily identified and quantified using full scan mass with resolution 35,000. The various specifications of the mass spectrometer are provided in Table 3.

Table 1. Cytochrome P450 enzymes assayed and compounds analyzed in the metabolic assays.

CYP enzyme assayed	Compound used	Metabolite analyzed	Molecular weight of metabolite (m/z)
CYP2D6	Dextromethorphan	Dextrorphan	258.1852
CYP3A4	Midazolam	1-Hydroxymidazolam	342.0804
CYP1A2	Phenacetin	Acetaminophen	152.0706
CYP2B6	Bupropion	Hydroxybupropion	256.1099
CYP3A4	Testosterone	6β-Hydroxytestosterone	305.2111
CYP2C9	Tolbutamide	4-Hydroxytolbutamide	287.1060

Table 2. Concentration of compounds used and incubation time for 2D and 3D cultures.

Compound used	Concentration (µM)	Incubation time (hr)	
		2D	3D
Dextromethorphan	150	2	8
Midazolam	100	2	8
Phenacetin	200	2	8
Bupropion	500	2	8
Testosterone	400	2	8
Tolbutamide	500	4	16

Table 3. Specifications for Q Exactive Plus Hybrid Quadrupole-Orbitrap Mass Spectrometer.

Category	Specification
Ion source	Thermo Scientific™ Heated Electrospray Ionization (HESI-II) Probe
Ionization mode	ESI positive/negative switching
Sheath gas flow rate	50 units N_2
Auxiliary gas flow rate	10 units N_2
Spray voltage	+3.2/–3.0 kV
Ion transfer tube temperature	300°C
S-lens radio-frequency level	50.0
Heater temperature	425°C

Conclusions

PHH 3D spheroids provide many benefits compared to 2D cultures, including histotypic and phenotypic longevity. However, production of 3D hepatocyte culture is achieved with a small number of cells per spheroid, raising concerns regarding a sufficient assay window for studying drug metabolism. The current study assessed differences in CYP450 enzyme activities in 2D and 3D PHH cultures.

From the data presented, the following conclusions can be reached:

1. Metabolites produced by the 3D hepatic spheroids can be easily identified and quantified using a high-resolution mass spectrometer such as the Q Exactive Plus mass spectrometer (Figure 1).
2. 3D hepatic spheroid culture is suitable for studying drug metabolism. A sufficient assay window for metabolite formation was observed for the CYP450 enzymes studied (Figures 1 and 2).
3. In general, 3D hepatic cultures were more efficient in drug metabolism compared to 2D cultures. This finding is consistent with our previous **observation** that 3D hepatic spheroids express various CYP450 genes and albumin at higher levels than are found in 2D cultures [3]. Previously, we also found higher CYP3A4 activity in 3D cultures using a luminescence-based assay.
4. Based on the data generated, we conclude that 3D hepatic spheroid culture is a suitable system for high-throughput drug screening and metabolic assays.

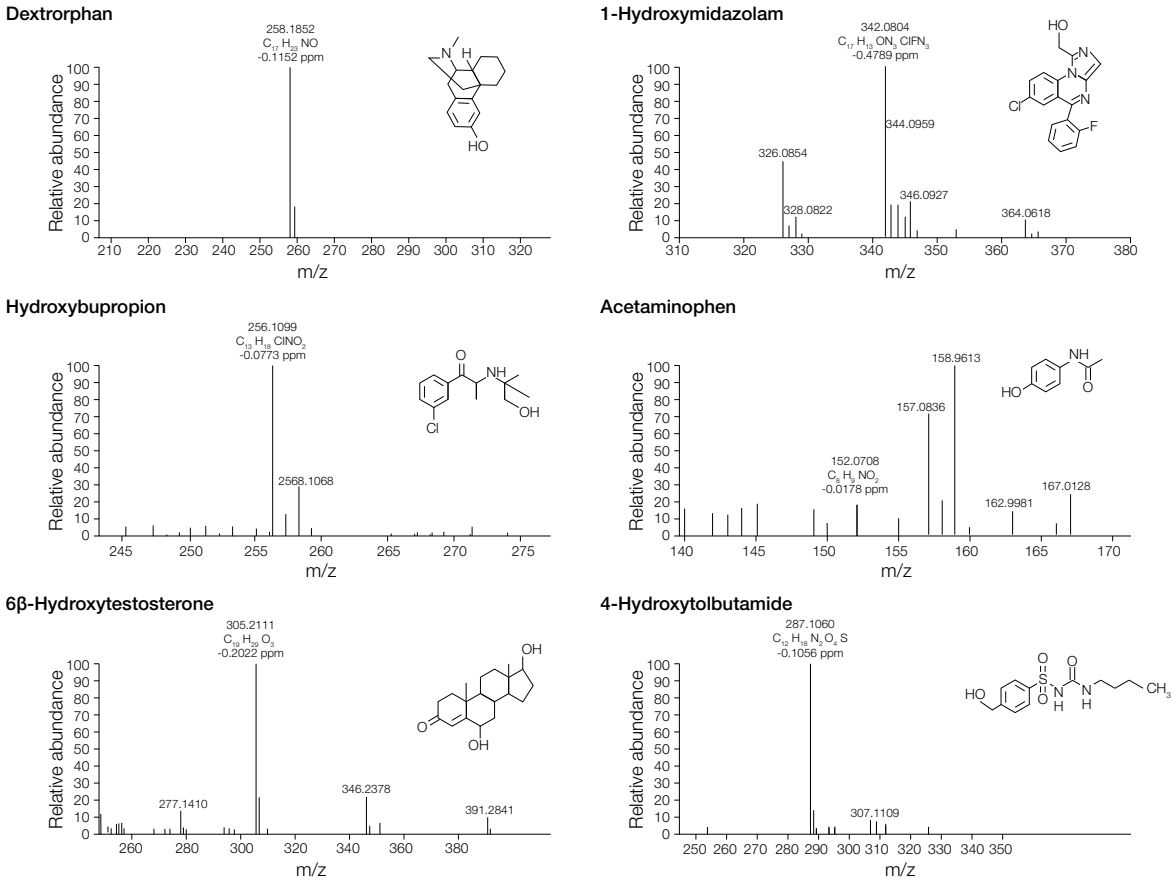

Figure 1. Identification of marker metabolites. The marker metabolites synthesized from the respective compounds were identified and quantified using high-resolution mass spectrometry (HRMS). HRMS readily identified the metabolites secreted from a single spheroid consisting of only 3,000 cells.

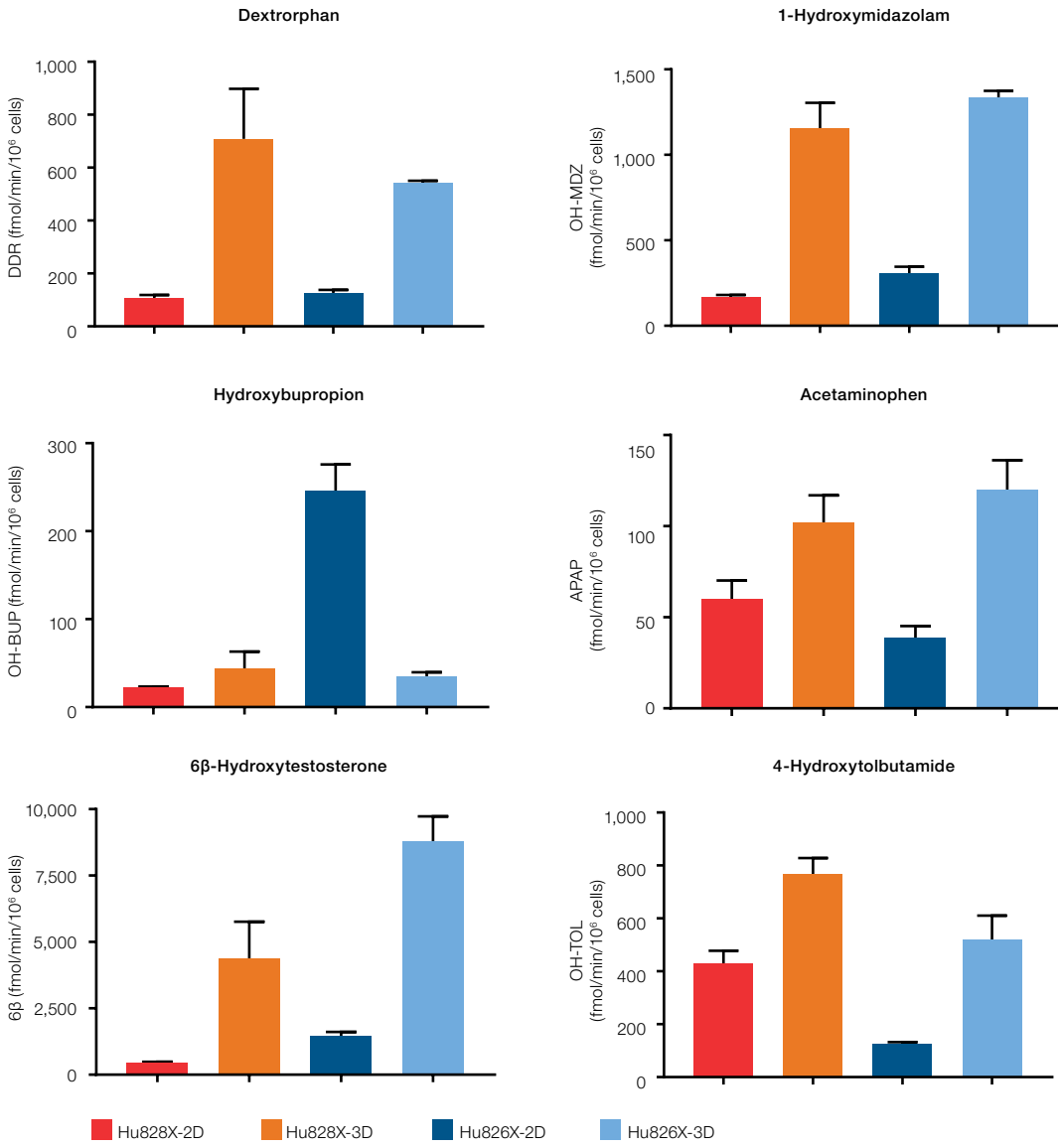

Figure 2. Comparison of metabolites between the 2D and 3D cultures. The metabolites quantified using HRMS were converted to mole amounts based on the standard curves of the respective metabolites. Two different lots of PHH, Hu828X and Hu826X, were used in this assay. Results were normalized to incubation time of individual substrates and number of cells per well in the 2D and 3D cultures. Data are mean ± SD; n = 3.

References

1. Thermo Fisher Scientific. User Guide: Cryopreserved 3D-Spheroid Qualified Human Hepatocytes. Pub. No. MAN0018280.
2. Thermo Fisher Scientific. Thawing and Plating Cryopreserved Hepatocytes. Protocol available at thermofisher.com/us/en/home/references/protocols/drug-discovery/adme-tox-protocols/thawing-and-plating-hepatocytes-protocol.html.
3. Thermo Fisher Scientific. Primary Human Hepatocyte 3D Spheroids for Studying Hepatic Function and Drug Toxicity. Poster available at assets.thermofisher.com/TFS-Assets/BID/posters/human-hepatoctye-3d-spheroids-hepatic-function-drug-toxicity-poster.pdf.

A.6

In vitro evaluation of hepatic function using a primary human hepatocyte 3D spheroid culture system

Introduction

The conventional method of **culturing primary human hepatocytes** (PHH) in a 2-dimensional (2D) monolayer presents limitations in the study of hepatic biology, liver function, and drug-induced hepatotoxicity. Traditional 2D hepatocyte cultures dedifferentiate, resulting in the loss of specific hepatic function in approximately 5 days. We have developed and characterized a PHH 3-dimensional (3D) spheroid culture system that preserves hepatic function and promotes culture longevity.

Gibco™ 3D spheroid–qualified human hepatocytes can easily be assembled into a 3D spheroid culture in 5 days using **Thermo Scientific™ Nunclon™ Sphera™ low-attachment 96-well U-bottom microplates** and **Gibco™ plating medium and plating supplements**. The 3D spheroid hepatocyte culture requires a significantly lower number of cells than its 2D counterpart, allowing this system to better support high-throughput assays. Moreover, the PHH in the 3D spheroid culture are functionally viable for at least 3 weeks, enabling long-term studies of hepatocyte function.

Application 1: PHH 3D spheroid formation

1. Plating medium was made by adding **Gibco™ Primary Hepatocyte Thawing and Plating Supplements (Cat. No. CM3000)** to **Gibco™ Williams' E Medium (Cat. No. A1217601)**. The plating medium and **Gibco™ Hepatocyte Thaw Medium (HTM) (Cat. No. CM7500)** were warmed in a 37°C water bath.

2. Gibco™ Human Spheroid-Qualified Hepatocytes (Cat. No. HMCPSQ) were thawed quickly in a 37°C water bath, and the contents of the tube were transferred to the tube of HTM.

3. The cells were centrifuged at 100 x *g* for 10 min, and the cell pellet was gently resuspended in 3 mL of the plating medium.

4. After counting the hepatocytes, 1,500 cells/well were plated in the *Nunclon Sphera 96-well microplate (Cat. No. 174925)*.

   Note: 1,500 cells in 200 µL of medium (7,500 cells/mL) can be added to each well; or, after pre-wetting the plate with 100 µL of plating medium, 1,500 cells in 100 µL of medium (15,000 cells/mL) can be added to each well.

5. After plating the cells, the plate was centrifuged at 200 x *g* for 2 min to pellet cells to the bottom of the plate.

6. The seeded cells were placed in a 37°C incubator with 5% CO_2 and allowed to incubate for 3–5 days undisturbed before changing the medium.

   Note: It is important to place the plate in an incubator that is not being used with frequent opening for other cultures, and to gently close the incubator door to avoid disturbing the spheroid formation.

7. The spheroids formed within 5 days. No earlier than day 7, biochemical assays and characterization were performed. Hepatocyte maintenance medium (prepared by adding Gibco™ Hepatocyte Maintenance Supplement (Cat. No. CM4000) into Williams' E Medium (Cat. No. A1217601)) was used for 50% medium exchanges every 48–72 hours (Figure 1). Medium exchanges can be completed using the **Thermo Scientific™ Wellwash™ Versa Microplate Washer (Cat. No. 5165010).**

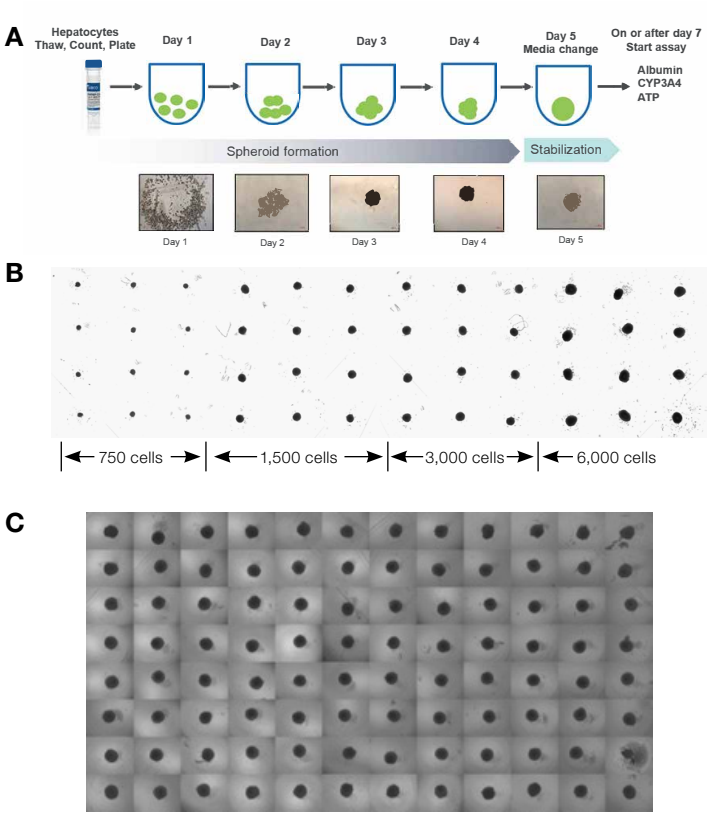

Figure 1. Workflow of assembly and characterization of primary hepatocytes in 3D spheroid culture. (A) Spheroids were imaged in phase at 10x magnification. These images show spheroid formation by day 5 of culture. **(B)** Spheroid size is directly proportional to the number of cells seeded. Spheroids were imaged using the **Invitrogen™ EVOS™ FL Auto 2 Cell Imaging System (Cat. No AMAFD2000)** at 4x. **(C)** Plating of hepatocyte spheroids in a Nunclon Sphera 96-well U-bottom microplate shows consistency in spheroid formation across the plate.

Application 2: Analysis of formation of bile canaliculi in 3D hepatic spheroids

1. Using Application 1, a 3D spheroid culture of hepatocytes was established.
2. A working solution of 5 µM Invitrogen™ 5-carboxyfluorescein diacetate, acetoxymethyl ester (5-CFDA, AM; Cat. No. C1354), was prepared. 5-CFDA is used to visualize formation of bile canaliculi in the 3D spheroids. 5-CFDA permeates intact functional hepatocytes and is hydrolyzed to 5-carboxyfluorescein (5-CF), which is secreted out of the hepatocytes, accumulates in bile canaliculi, and exhibits strong fluorescence.
3. During week 1, the medium was removed from the 3D hepatic spheroids, and they were treated with 100 µL of 5 µM 5-CFDA stock solution and incubated for 1 hr at 37°C.
4. The wells were washed 3 times with hepatocyte maintenance medium, and the cells were imaged using transmission electron microscopy with GFP/FITC settings (Figure 2).

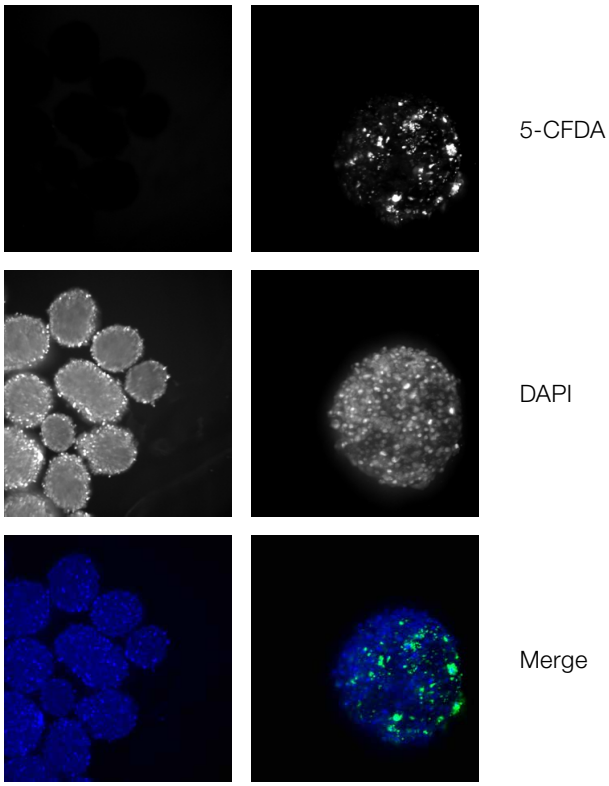

Figure 2. Evaluation of formation of bile canaliculi in hepatic spheroids. HepG2 spheroids during week 2 (left) and hepatic spheroids during week 1 (right) were stained with 5-CFDA and DAPI and imaged using the Thermo Scientific™ CellInsight™ CX7 platform at 10x magnification. Hepatic spheroids show clear formation of bile canaliculi in comparison to the HepG2 spheroids (used as the negative control).

Application 3: Measurement of albumin produced by 2D or 3D spheroid hepatic cultures

1. Using Application 1, a 3D spheroid culture of hepatocytes was established. Additionally, a 2D culture of hepatocytes was started.
2. On day 5 of the 2D hepatocyte culture and on various days of the 3D hepatic spheroid culture, 120 µL of the cell culture medium from each of the wells of the 2D and 3D cultures were collected for analysis of albumin secretion.
3. The cell culture medium was centrifuged at 3,000 x *g* for 10 min, and the supernatant was collected for an ELISA assay using the Abcam Human Albumin ELISA Kit (Figure 3).

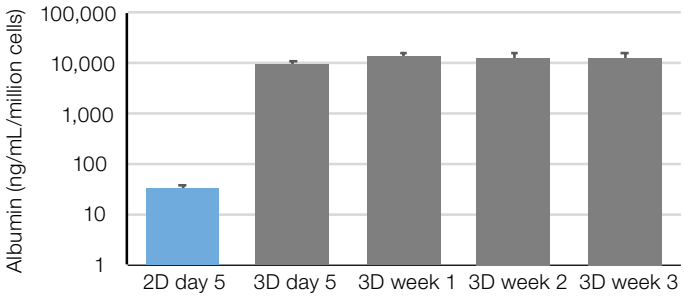

Figure 3. Albumin secretion in 2D and 3D spheroid hepatic cultures. The concentration of albumin secreted is normalized to the total number of cells per well.

Application 4: Activity in 2D or 3D spheroid hepatic cultures

1. Using Application 1, a 3D spheroid culture of hepatocytes was established.
2. On day 5 of the 2D hepatocyte culture and on various days of the 3D spheroid culture, a total of 8 hepatic spheroids were transferred to a single well on a **Thermo Scientific™ Nunclon™ Delta™ 24-well plate (Cat. No. 142475).**
3. The hepatocyte maintenance medium remaining in the 24-well plate after transfer of the spheroids was carefully removed by pipette and replenished with 500 µL of fresh hepatocyte maintenance medium.
4. Activity of the liver enzyme CYP3A4 was measured on the day of the culture indicated in Figure 4, using the protocol for the Promega P450-Glo™ CYP3A4 Assay with Luciferin-IPA.

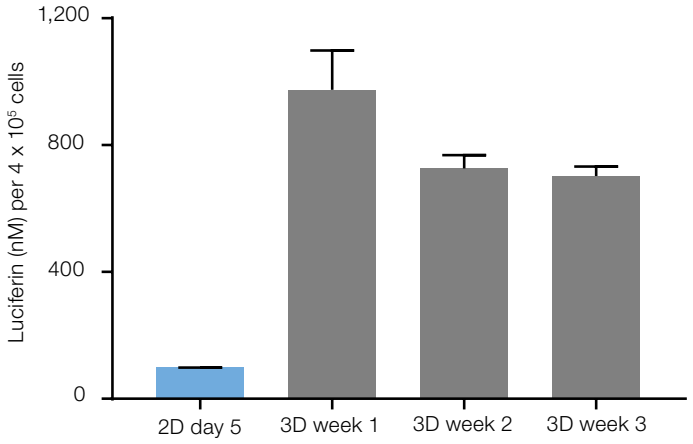

Figure 4. CYP3A4 activity in 2D and 3D spheroid hepatic cultures. CYP3A4 activity was measured using the Promega P450-Glo CYP3A4 Assay with Luciferin-IPA. CYP3A4 activity was found to be significantly higher in the 3D spheroids than in the 2D culture. The data presented are the mean ± SEM (n = 3 for the 2D culture, n = 8 for the 3D spheroids).

Application 5: ATP synthesis by 3D spheroid hepatic cultures

1. Using Application 1, a 3D spheroid culture of hepatocytes was established.
2. During week 1, ATP synthesis was measured in 3 replicates (Figure 5) using the Promega CellTiter-Glo™ 3D Cell Viability Assay.

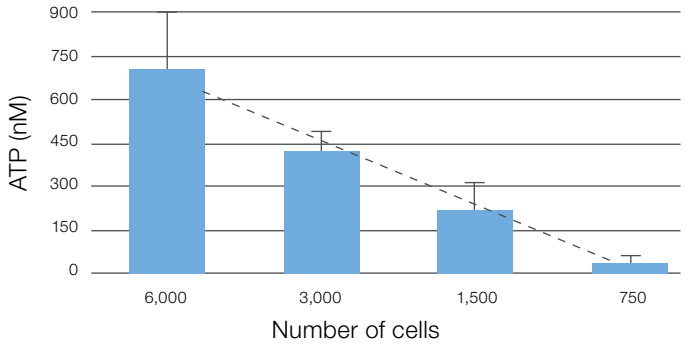

Figure 5. ATP synthesis by 3D spheroid hepatic cultures is proportional to the number of cells. Using the CellTiter-Glo 3D Cell Viability Assay in 3 replicates, ATP synthesis by individual spheroids was measured during week 1.

Application 6: Assay of drug-induced cytotoxicity using 3D spheroid hepatic cultures

1. Using Application 1, a 3D spheroid culture of hepatocytes was established.
2. During week 2 of culture, 3D spheroids were treated with variable levels of the antipsychotic drug chlorpromazine and the anti-inflammatory drug diclofenac, in 4 replicates.
3. Cell viability was assayed 24 hours posttreatment using the protocol for the CellTiter-Glo 3D Cell Viability Assay. Nonlinear regression was performed for variable slope of log (inhibitor) vs. response using GraphPad Prism™ 7 Software (Figure 6). Table 1 shows that 2D and 3D spheroid hepatic cultures have comparable IC_{50} values.

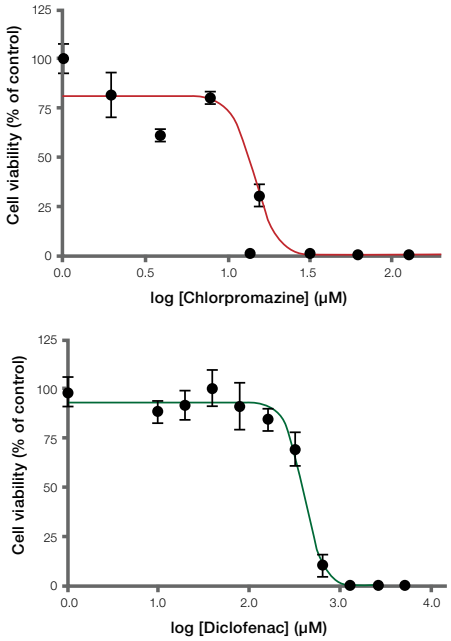

Figure 6. Drug-induced cytotoxicity assayed using 3D spheroid hepatic cultures.

Table 1. IC_{50} of drug-induced cytotoxicity for 2D hepatocytes and 3D spheroid hepatic cultures.

Drug	IC_{50} (2D culture)	IC_{50} (3D culture)
Chlorpromazine	34 µM	14 µM
Diclofenac	331 µM	396 µM

Conclusion

Collectively, these data confirm that cultures of 3D spheroid–qualified human hepatocytes have been characterized to show stable morphology, viability, and hepatocyte-specific functions for at least 3 weeks. We have demonstrated that our 3D spheroid–qualified hepatic cultures are functional, as indicated by formation of bile canaliculi as well as sustained albumin secretion. In comparing CYP3A4 activity on day 5 of 2D hepatic cultures and during week 1 of 3D spheroid hepatic cultures, we have shown that 3D spheroid cultures have significantly higher activity (Figure 4). We also show that this 3D spheroid hepatic culture system can be used to analyze drug-induced cytotoxicity in hepatocytes. Ultimately, these data indicate that the reduced number of cells required for 3D spheroid formation as well as the sustained longevity of these cultures may better support high-throughput assays and long-term studies of hepatocyte functions.

A.7

Formation of uniform and reproducible 3D cancer spheroids in a high-throughput plate format

Introduction

Cells grown on flat two-dimensional (2D) tissue culture substrates can differ considerably from physiological three-dimensional (3D) environments. There is growing evidence that 3D cancer spheroids are more representative of tumors *in vivo* and exhibit several physiological traits including similar morphology, the formation of cell–cell contacts, decreased proliferation, increased survival rates, and a hypoxic core. However, variability in cancer spheroid formation has been a persistent problem for researchers. This is linked to medium composition and volume, cell density, duration in culture, and most importantly, the cellular interactions with the culture dish itself. More consistent results can be achieved using a high-quality cultureware with low cell binding characteristics.

In this application note, we discuss the Thermo Scientific™ Nunclon™ Sphera™ polymer-coated surface, which minimizes cell attachment and supports the formation of cancer spheroids *in vitro*. The Nunclon Sphera cell culture surface inhibits the binding of extracellular matrix (ECM) that usually mediates cell adhesion. Cancer spheroids form quickly in Nunclon Sphera 96-well U-bottom plates without satellite colonies, demonstrating quality superior to that of spheroids formed in methylcellulose-containing media on nontreated plates. Cancer cell viability and spheroid cell health can be conveniently evaluated *in situ* by fluorescence- and colorimetric-based assays directly on the Nunclon Sphera plate. To further convey the physiological relevancy of the cancer spheroids, the hypoxic cores of the spheroids are assessed by immunocytostaining. The consistent formation of uniform and reproducible cancer spheroids in the Nunclon Sphera plate makes it an ideal platform for modeling 3D tumor growth for many cell-based drug discovery procedures, co-culture studies, and high-throughput screening.

Materials and methods

Cancer spheroid culture

Cancer cell lines were maintained in Thermo Scientific™ Nunc™ cell culture flasks before they were subjected to spheroid culture. To form cancer spheroids, cells were seeded in Thermo Scientific™ Nunclon™ Sphera™ 96-well U-bottom plates at densities of 100–5,000 cells/well in 200 µL/well DMEM with GlutaMAX™ Supplement, 10% FBS, 1X MEM Non-Essential Amino Acids, 100 U/mL Penicillin-Streptomycin, and 25 mM HEPES (all Gibco™ medium, serum, and reagents). Nontreated plates were similarly seeded in the complete DMEM containing 3% methylcellulose. The plates were briefly centrifuged at 250 x *g* for 5 minutes. The cells were then incubated at 37°C and 5% CO_2, and re-fed every 72 hr by carefully removing 100 µL of medium from each well and replenishing with 100 µL of fresh growth medium using a multichannel pipette. The formation and growth of spheroids were imaged under the microscope.

Spheroid cell health assessment

The well-being of A549 and HCT 116 spheroids was evaluated *in situ* using Invitrogen™ PrestoBlue™ Cell Viability Reagent. Briefly, 12–13 days after spheroid culture, 20 µL/well of 10X PrestoBlue Cell Viability Reagent was added to the Nunclon Sphera plates. The plates were then incubated at 37ºC and 5% CO_2 for an additional 2–5 hr before being read on a fluorescence-based microplate reader (Ex/Em: 560/590 nm). The fluorescence reading was normalized against spheroid size for better quantitative comparison—higher ratio indicates healthier spheroids.

Spheroid cell viability assessment

After 12–13 days of culturing A549 and HCT 116 spheroids in Nunclon Sphera plates, Invitrogen™ LIVE/DEAD™ cell viability reagents were added to each well. Plates were incubated at room temperature for 30–45 min. The spheroids were rinsed at least 3 times by half-volume changes of DPBS before imaging under a fluorescence microscope. Data were analyzed using ImageJ analysis software.

Detection of hypoxic cores in spheroids

HeLa cells (250 cells/well) were cultured on Nunclon Sphera 96-well U-bottom plates for 2 days in complete medium. The spheroids were stained *in situ* with 5 µM Invitrogen™ Image-iT™ Green Hypoxia Reagent and incubated for an additional 3 hr. Invitrogen™ NucBlue™ Live ReadyProbes™ Reagent was used as nuclear counterstain. The stained spheroids were then transferred by pipetting using wide-bore pipette tips to a Thermo Scientific™ Nunc™ Glass Bottom Dish, and images were taken on a confocal microscope.

ECM protein nonspecific binding assay

Nunclon Sphera 96-well plates and Nunc 96-well plates were coated with 100 µL/well FITC–bovine collagen type I conjugate (24 µg/mL in DPBS) and incubated for 24 hr at 2–8°C. Another set of plates were coated with a TAMRA™ dye conjugate of fibronectin (20 µg/mL in DPBS) and incubated for 16 hr at room temperature. All plates were washed 3 times with 200 µL/well PBS containing 0.05% Tween™ 20 surfactant. The fluorescence intensity was read for FITC dye (Ex/Em: 495/525 nm) or TAMRA dye (Ex/Em: 543/570 nm).

Results

Extremely low adsorption of ECM to the Nunclon Sphera surface

In order for anchorage-dependent or adherent cells to form spheroids in suspension, the culture vessel must promote the aggregation of cells through cell–cell binding by preventing ECM from binding to the culture surface. In this study, we demonstrate that both collagen I and fibronectin adsorption was minimal on the Nunclon Sphera surface when compared to that on the Nunclon Delta surface (Figure 1). This suggests that unlike the standard cell culture–treated surface, the Nunclon Sphera surface has minimal binding interactions with the ECM, consequently discouraging the cells from attaching to the cultureware.

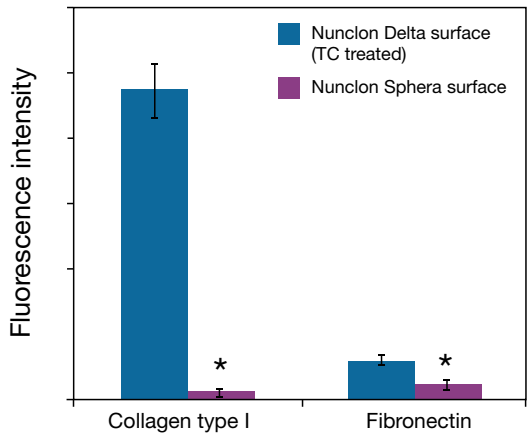

Figure 1. Binding of nonspecific proteins. The adsorption of collagen I and fibronectin to the Nunclon Sphera surface is extremely low compared to the standard cell culture–treated surface (* = Student's *t* test, $P < 0.01$).

The Nunclon Sphera surface is superior for culturing cancer spheroids

HCT 116 human colon carcinoma cells were seeded into Nunclon Sphera 96-well U-bottom plates in complete DMEM. Similarly, cells were seeded into nontreated 96-well U-bottom plates in complete DMEM containing 3% methylcellulose. HCT 116 cancer spheroid formation in the Nunclon Sphera plate demonstrates fewer satellite colonies at the various seeding densities with much cleaner background than the nontreated plate, leading to higher-quality images of the spheroid culture (Figure 2A). At the lowest seeding density of 100 cells/well, the HCT 116 cancer spheroids formed earlier in the Nunclon Sphera plate after only 18 hours of incubation (Figure 2B). Single spheroids with better-defined edges and shapes can be observed in the Nunclon Sphera plates throughout the duration of the culture.

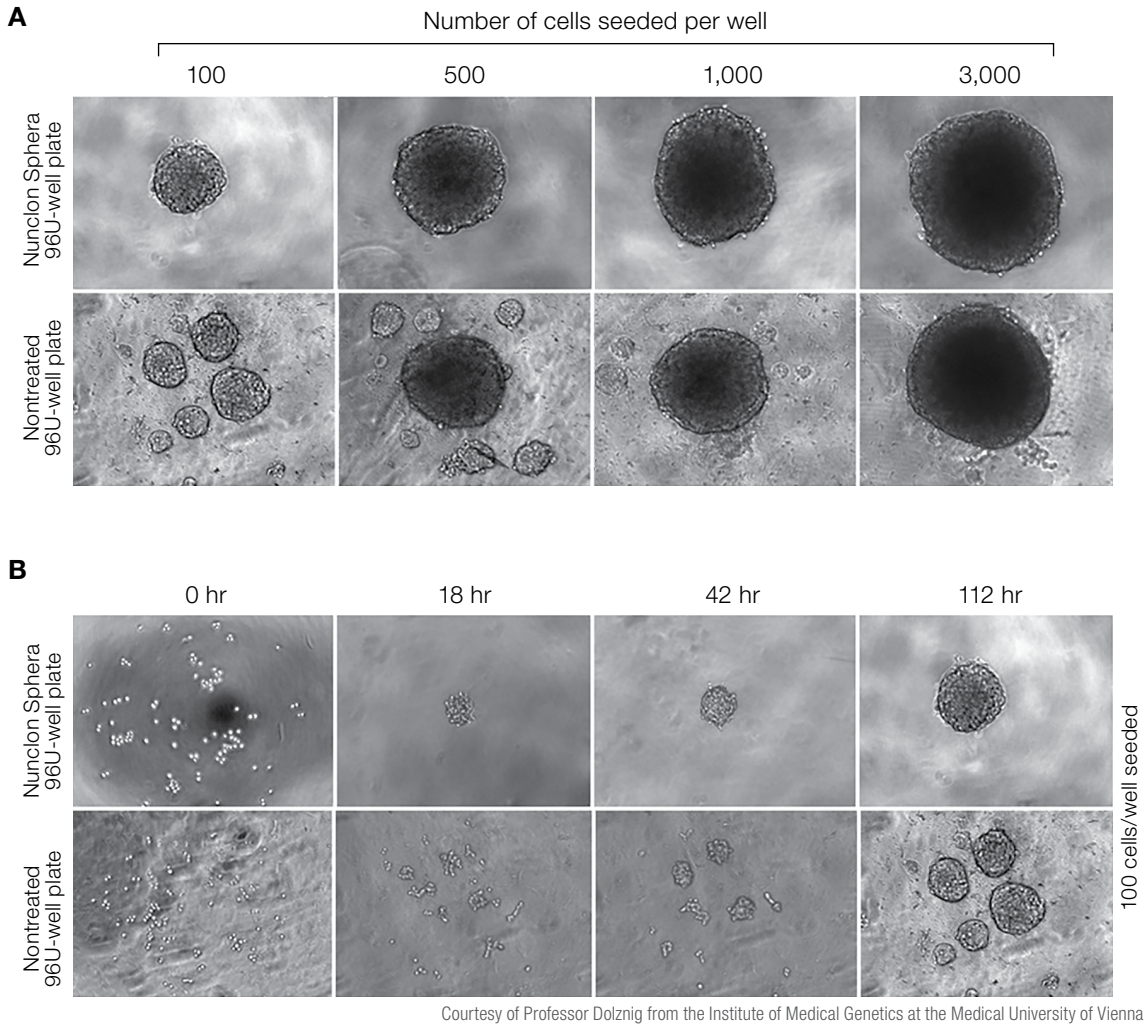

Courtesy of Professor Dolznig from the Institute of Medical Genetics at the Medical University of Vienna

Figure 2. Advantages of Nunclon Sphera plates over nontreated plates and methylcellulose-containing medium. (A) High and consistent quality of cancer spheroids grown in Nunclon Sphera plates. **(B)** Early formation of single cancer spheroids in the Nunclon Sphera 96-well U-bottom plate. (Courtesy of Professor Dolznig from the Institute of Medical Genetics at the Medical University of Vienna.)

Cancer spheroids grown on Nunclon Sphera plates are in excellent condition

To demonstrate spheroid growth, A549 and HCT 116 cancer cell lines were cultured at different densities in Nunclon Sphera plates for 2 weeks. Both cell types show adequate spheroid growth as demonstrated by size measurements (Figure 3A). Additionally, the cell health of A549 and HCT 116 spheroids were assessed using PrestoBlue Cell Viability Reagent (Figure 3B). Data are normalized against spheroid size for better quantitative comparison—higher ratio indicates healthier spheroids. Cell viability of cancer spheroids are further confirmed by staining with LIVE/DEAD reagents (Figure 3C). All parameters indicate that cancer spheroids grown on Nunclon Sphera plates are healthy and robust, and the Nunclon Sphera 96-well U-bottom plate is a reliable and convenient tool for both routine and high-throughput cancer spheroid applications.

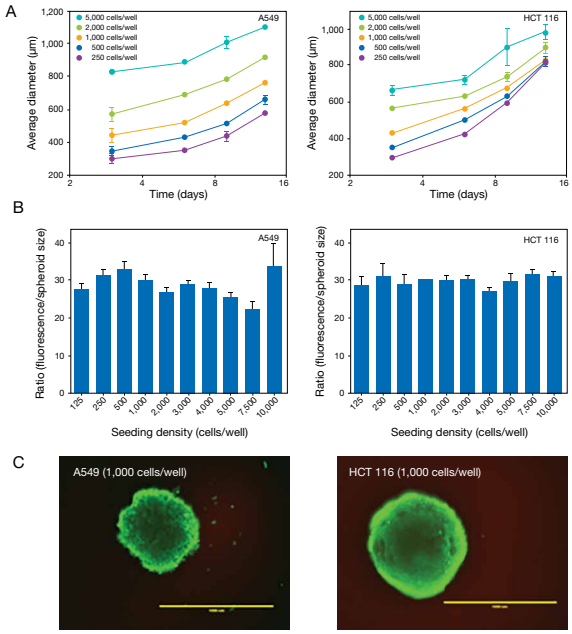

Figure 3. Assessments of spheroid growth, cell health, and viability on Nunclon Sphera plates. (A) Growth kinetics of A549 and HCT 116 cancer spheroids on Nunclon Sphera plates evaluated over a period of 13 days. Data represent the mean ± SD of 3 replicates for each cell number. **(B)** Spheroid cell health assessment on Nunclon Sphera plates performed using the PrestoBlue Cell Viability Reagent, with data normalized by spheroid size. **(C)** Spheroid cell viability evaluated by staining live (green) and dead (red) cells. Scale bar: 1,000 µm.

Hypoxia staining provides supporting evidence for hypoxic cores in cancer spheroids

The low-oxygen core, also known as the hypoxic core, is one of the most distinct characteristics of 3D cancer spheroid growth as opposed to flat monolayer culture. It faithfully imitates the *in vivo* situation of solid tumors where cells rapidly outgrow the blood supply, leaving the center of the tumor in extremely low oxygen concentration. To visualize this spheroid feature, HeLa cells were cultured on Nunclon Sphera 96-well U-bottom plates for 2 days. The evidence of a hypoxic core in the cancer spheroid is shown by hypoxia staining beyond the spheroid surface, mimicking the physiological conditions in a tumor (Figure 4).

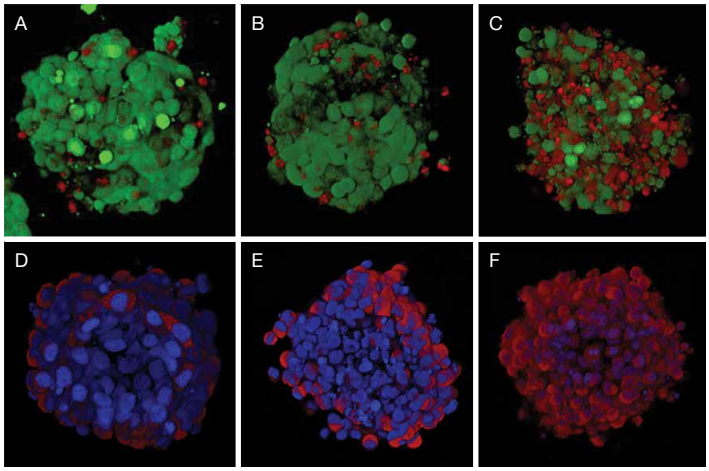

Figure 4. Assaying cell viability and oxidative stress in drug-treated HeLa spheroids. HeLa cells were grown in Gibco™ MEM, seeded at 600 cells/well in a Nunclon Sphera 96-well U-bottom plate, centrifuged at 200 x *g* for 5 min, and cultured for 3 days to allow spheroid formation. One set of HeLa spheroids was **(A)** left untreated, or treated with **(B)** 100 nM niclosamide or **(C)** 10 µM niclosamide for 24 hr, and then stained using the Invitrogen™ LIVE/DEAD™ Cell Imaging Kit. A second set of HeLa spheroids was **(D)** left untreated, or treated with **(E)** 100 nM menadione or **(F)** 10 µM menadione for 1 hr at 37°C to induce oxidative stress, and then stained with NucBlue Live ReadyProbes Reagent and Invitrogen™ CellROX™ Deep Red Reagent. After staining, spheroids were transferred to Thermo Scientific™ Nunc™ glass-bottom dishes with 200 µL pipette tips (with tip ends cut off) and imaged on a Zeiss™ LSM 710 confocal microscope with EC Plan-Neofluar™ 10x/0.3 objective and 488 nm and 561 nm lasers, in addition to the 488/561 nm main beam splitter; stacks were projected using 3D shadow rendering. **(A–C)** In the spheroids assayed with the LIVE/DEAD Cell Imaging Kit, live cells fluoresce green, and dead cells with permeable membranes fluoresce red. **(D–F)** In the spheroids stained with CellROX Deep Red Reagent and NucBlue Live ReadyProbes Reagent, cells showing oxidative stress fluoresce red, and live-cell nuclei fluoresce blue.

A.8

Gene expression profiling of drug metabolism pathways for drug discovery and development using 3D spheroid culture

Introduction

Cell-based assays are a crucial element of the drug discovery process. In comparison to traditional two-dimensional (2D) cell cultures, three-dimensional (3D) cell cultures have been shown to recapitulate *in vivo* biology and microenvironmental factors more closely in terms of complexity, morphology, and phenotype. Thus, 3D cultures may serve as superior preclinical models with higher value for predicting clinical outcomes.

Since the liver is the principal site of metabolism for the majority of drugs, identifying the induction of drug-metabolizing enzymes in the liver is a key step along the drug discovery pipeline. Primary human hepatocytes (PHHs) are considered the gold-standard *in vitro* model for studying hepatic biology, liver function, and drug-induced hepatotoxicity. However, PHHs grown in traditional 2D monolayer cultures rapidly de-differentiate and lose the hepatic-specific functions within a week. Recently developed 3D spheroid cultures, on the other hand, mimic the hepatic microenvironment and maintain hepatic function for at least 5 weeks. Thus, 3D *in vitro* models have been shown to more accurately reflect *in vivo* liver biology [1]. Cytochrome P450 (CYP450) enzymes are essential for the detoxification of foreign chemicals and the metabolism of drugs by the liver. Drugs may interact with the CYP450 system in several ways; they may be metabolized by only one CYP450 enzyme or by multiple enzymes. Three key CYP450 enzymes are commonly used as markers for the 3 major nuclear receptor pathways often used to identify hepatic induction. These include: (1) CYP1A2 for aryl hydrocarbon receptor (AHR) activation, (2) CYP2B6 for constitutive androstane receptor (CAR), and (3) CYP3A4 for pregnane X receptor (PXR). However, a broader assessment of gene signaling pathways offers the potential for improved characterization of drug–drug interactions and prediction of clinical outcomes [2]. In this study, we used the Invitrogen™ QuantiGene™ Plex assay to probe 57 genes related to drug absorption, distribution, metabolism, and excretion (ADME) and housekeeping genes in 3D spheroids cultured from PHH samples.

Materials and methods

Hepatocyte spheroid culture and *in vitro* drug treatments

Hepatic spheroids were formed in 3D culture using Gibco™ Human Spheroid-Qualified Hepatocytes (Cat. No. HMCPSQ) following the user guide [3]. Each well contained 3,000 PHHs. The spheroids formed within 5 days of cell seeding. Starting on day 5, half of the plating medium was changed every 48–72 hours. On day 5 of the 3D culture, 2D hepatic cultures were initiated in collagen I–coated 24-well plates using the same lots of PHHs and following the user manual [4].

Prototypical ligands were used to induce the 3 major nuclear receptor pathways commonly associated with drug metabolism in the liver. 2D and 3D cultures were treated with either 50 µM omeprazole (AHR ligand), 1 mM phenobarbital (CAR ligand), 10 µM rifampicin (PXR ligand), or DMSO (vehicle control). 2D cultures were treated on days 2 and 3, whereas 3D cultures were treated on days 6 and 7.

QuantiGene Plex assay

The QuantiGene Plex assay was used to quantitate a custom panel of 57 genes, including 42 ADME genes, 7 apoptosis genes, and 8 housekeeping genes (Figure 1). Target-specific capture extenders and label extenders were incubated overnight at 54°C with the cell lysates and Luminex® MagPlex® beads. The beads are coated with capture probes specific to the capture extenders, thus hybridizing each target gene to a specific bead (Figure 2). After overnight incubation, the branched DNA signal amplification "tree" was built through a series of 3 sequential 1 hr hybridizations at 50°C with single-stranded DNA oligos called PreAmplifier, Amplifier, and Label Probe. The beads were washed prior to each hybridization. After the hybridization with biotinylated Label Probe and an additional wash, the beads were incubated at room temperature for 30 min with the detection reagent streptavidin phycoerythrin (SAPE). Finally, the beads were washed, resuspended in SAPE buffer, and read on a **Luminex® FLEXMAP 3D® instrument**.

Data analysis

Data exported from the FLEXMAP 3D instrument was analyzed with **Invitrogen™ QuantiGene™ Analysis Software** integrated with **Applied Biosystems™ Transcriptome Analysis Console (TAC) Software 4.0.2**.

CYP1A1	*CYP3A4*	*CYP1A2*	*CYP2C19*	*ABCB11*	*ACTB*	*SLCO1B1*	*ABCB1*	*AOX1*	*CYP3A5*
MAOB	*CYP2C9*	*CYP2D6*	*UGT1A9*	*SULT2B1*	*SLC22A1*	*ABCG2*	*UGT1A4*	*HPRT1*	*TBP*
SLC10A1	*SULT2A1*	*CYP2J2*	*UGT1A1*	*XDH*	*UGT1A6*	*GAPDH*	*UGT2B7*	*CYP2A6*	*SULT1A1*
FMO3	*GUSB*	*POLR2A*	*CYP2E1*	*UGT1A3*	*SLC3A1*	*HMGB1*	*SLC2A1*	*SLCO2B1*	*CYP2C8*
PGK1	*ABCC2*	*FMO1*	*ABCA1*	*CASP9*	*FMO5*	*PPIB*	*SLCO1B3*	*MAOA*	*CYP2B6*
ABCC1	*UGT2B15*	*RIPK1*	*BAX*	*TP53*	*BCL2*	*CASP3*			

Figure 1. The custom QuantiGene Plex assay panel of 57 genes. ADME genes: green; apoptosis genes: blue; housekeeping genes: yellow.

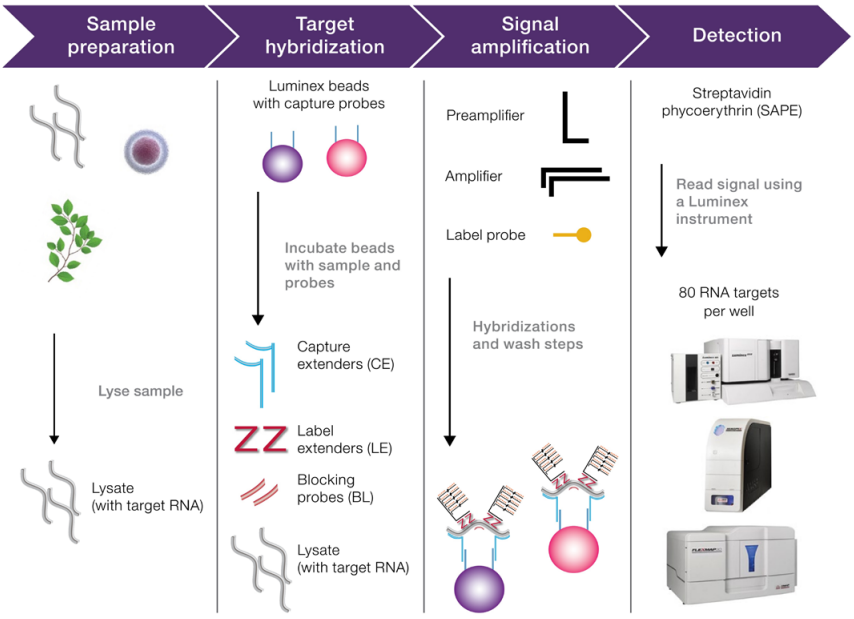

Figure 2. The QuantiGene Plex assay workflow.

Results

Self-assembly of PHHs into 3D spheroids and drug treatments

Gibco™ Human Spheroid-Qualified Hepatocytes (**Cat. No. HMCPSQ**) isolated from a single donor were seeded in Thermo Scientific™ Nunclon™ Sphera™ 96-well U-bottom microplates (**Cat. No.174925**), where they self-assembled into 3D spheroids by day 5 as shown in Figure 3. Spheroids were then treated with various CYP450 inducers on days 6–7, and lysates were prepared on day 8 using the Invitrogen™ QuantiGene™ Sample Processing Kit for cultured cells (**Cat. No. QS0100**).

Gene expression measurements of 3D cultures in response to drug treatments—correlation of qPCR results with QuantiGene Plex assays

CYP3A4 and CYP2D6 mRNA levels in 3 individual sample lots of PHHs (Hu186X, Hu828X, and Hu826X) were analyzed using qPCR and QuantiGene Plex assays. Target gene expression was normalized to the geometric mean of the housekeeping genes. Fold change (Δ) in expression levels of 3D cultures was calculated relative to day 5 of the 2D culture. QuantiGene Plex assay and qPCR data demonstrated good correlation detecting increased transcript expression in all 3D PHH cultures when compared to their 2D counterparts (Figure 4).

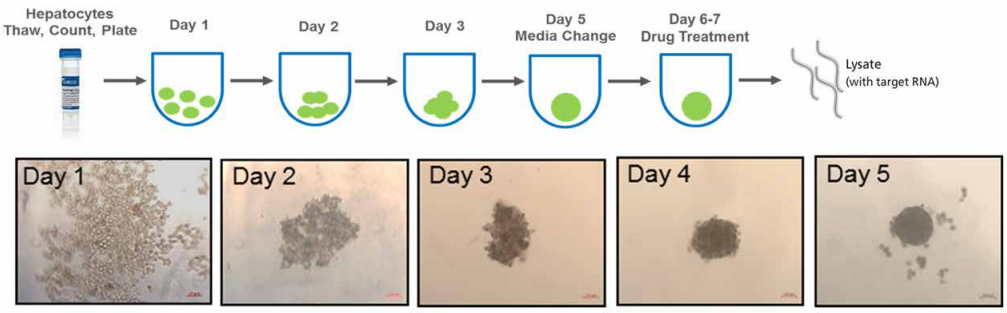

Figure 3. Primary human hepatocytes self-assemble into 3D spheroids after 5 days.

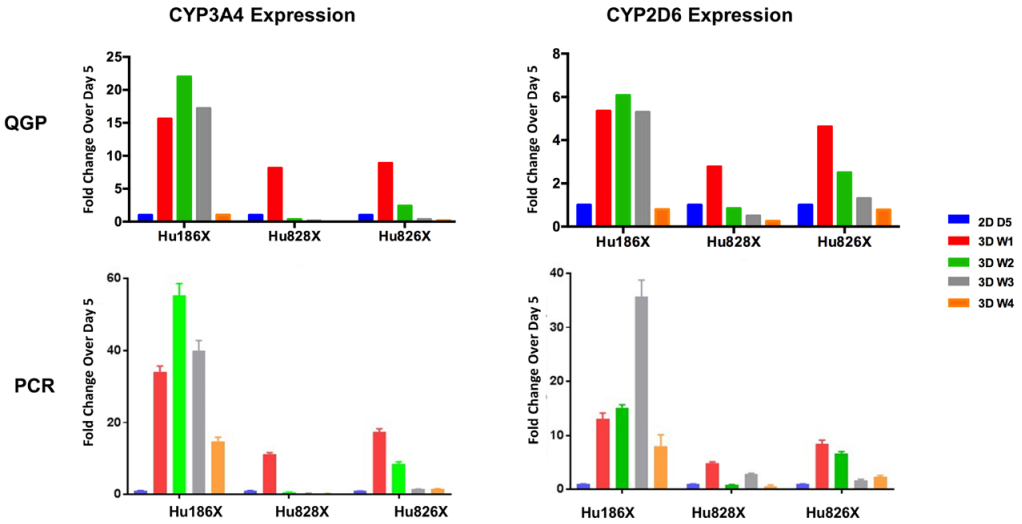

Figure 4. Elevated gene expression in 3D PHH cultures detected by QuantiGene Plex assay (top panel) and qPCR (bottom panel).

Differential changes in drug-induced gene expression in 3D vs. 2D cultures

Data generated using the QuantiGene Plex assay can be loaded into TAC Software 4.0.2 to allow for advanced data visualization such as volcano plots. This type of scatter plot enables for the quick identification of changes in large datasets by plotting fold change vs. *P* value (significance). Volcano plots shown in Figure 5 demonstrate $\log_2$ fold changes in gene expression in 2D and 3D PHH cultures (lot Hu828X) treated with omeprazole compared to DMSO controls (*P* value <0.05, one-way ANOVA). Genes upregulated >2-fold are highlighted in red, and genes downregulated >2-fold are highlighted in green. Similar analyses were performed for 2D and 3D cultures treated with phenobarbital and rifampicin (data not shown). Gene expression profiles of 2D and 3D PHH cultures differed significantly following induction with the 3 ligands, indicating different cellular responses for drug toxicities between 2D and 3D culture conditions.

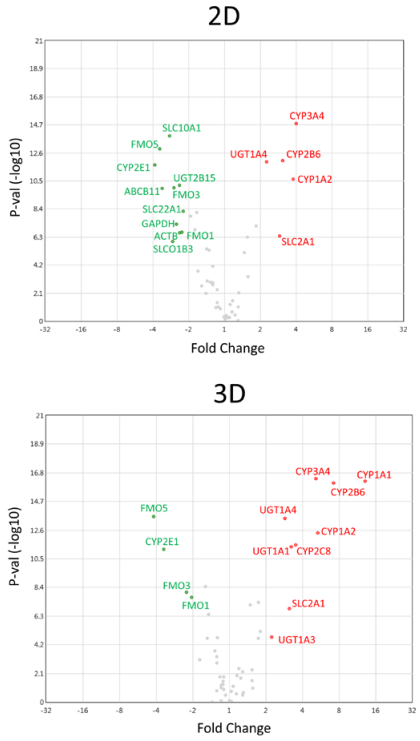

Figure 5. Volcano plots showing differential ADME gene expression in 2D versus 3D PHH cultures treated with omeprazole (data for phenobarbital and rifampicin treatments not shown).

Multiplex gene expression profiling of individual human sample lots of spheroid-qualified hepatocytes

Venn diagram visualization of QuantiGene Plex assay data using TAC Software 4.0.2 demonstrates single-donor lot-to-lot variation in spheroid-qualified hepatocytes. Shared (circle overlap) and treatment-specific (no overlap) differentially expressed genes across the different inducers in 3D spheroids cultured from PHH samples (lots Hu828X and Hu826X) are shown in Figure 6. Genes listed demonstrated log2 fold change >2 (P value <0.05, one-way ANOVA). CYP1A2, known to be a marker of AHR activation, was specifically upregulated by the AHR ligand omeprazole. However, CYP2BP6 and CYP3A4, markers used for CAR and PXR activation, respectively, were found to be upregulated by all 3 ligands.

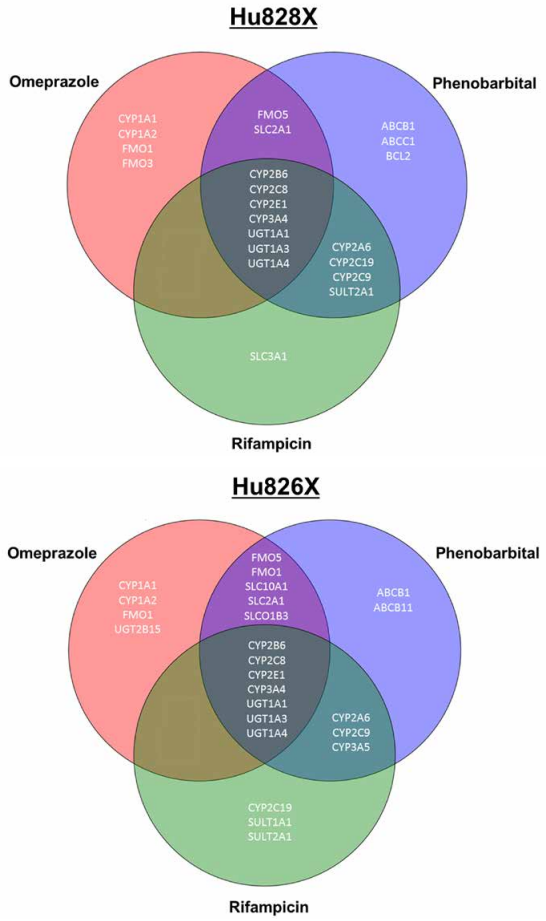

Figure 6. Differentially expressed ADME genes specific to each inducer in 3D spheroid cultures.

In addition to various visualizations, TAC software searches the WikiPathway database and allows you to visualize data on the pathway diagrams and calculate pathway metrics. Metapathway biotransformation phase I and phase II was identified as the primary pathway induced by all 3 ligands. Genes upregulated by rifampicin are highlighted in yellow (Figure 7).

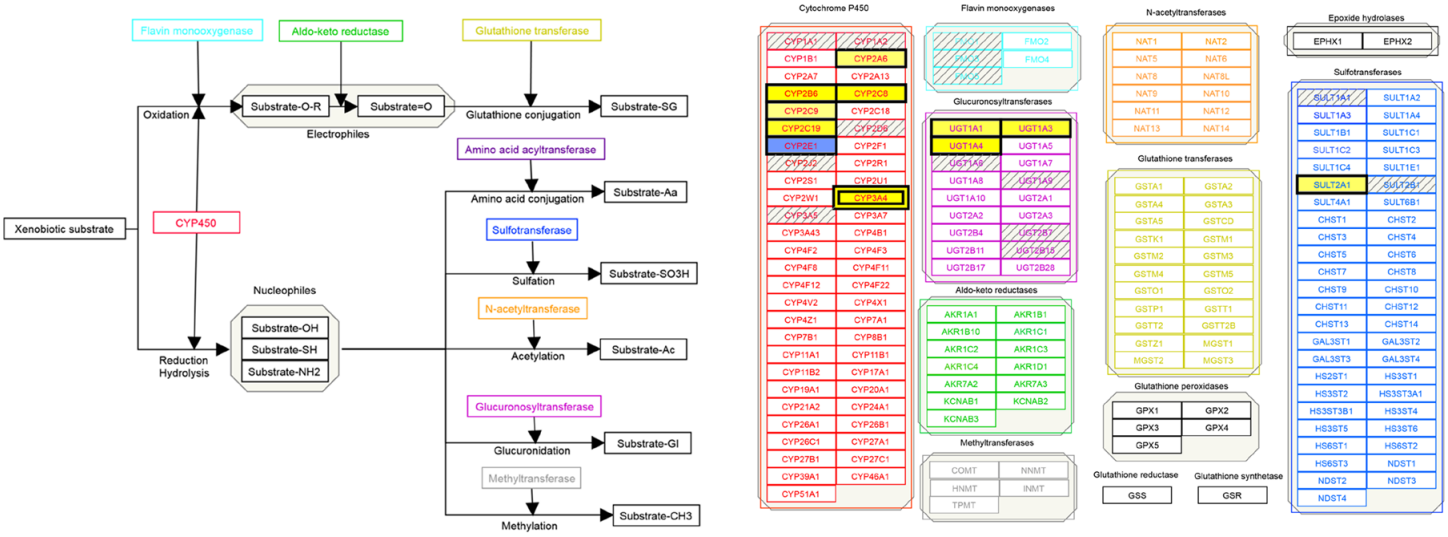

Figure 7. Metapathway biotransformation for phase I and II of drug metabolism.

Conclusions

Human Spheroid-Qualified Hepatocytes can be easily assembled into a 3D culture in 5 days using either the Gibco™ Hepatic Spheroid Kit or Nunclon Sphera 96-well U-bottom microplates and Gibco™ plating media supplements. QuantiGene Plex assay data showed increased CYP3A and CYP2D expression in 3D spheroids, which corroborated gene expression data obtained by qPCR analysis. The changes in ADME gene expression following induction with prototypical ligands differed significantly between 2D and 3D PHH cultures. ADME signaling pathway analysis and the identification of secondary markers or a set of specific gene signatures using the QuantiGene Plex assay may provide a more comprehensive characterization of drug–drug interactions in the liver.

References

1. Bell CC, Hendriks DF, Moro SM et al. (2016) Characterization of primary human hepatocyte spheroids as a model system for drug-induced liver injury, liver function and disease. *Sci Rep* 6:25187.
2. Thermo Fisher Scientific. Application note: Transcript regulation of 18 ADME genes by prototypical inducers in human hepatocytes. Pub. No. COL21791 0417.
3. Thermo Fisher Scientific. User guide: Cryopreserved 3D-Spheroid Qualified Human Hepatocytes. Pub. No. MAN0018280.
4. Thermo Fisher Scientific. User bulletin: Thawing and use of plateable and suspension cryopreserved hepatocytes. Pub. No. MAN0018379.

A.9

Establishing human skin tissue on Nunc Cell Culture Inserts in Carrier Plate Systems

Abstract

Thermo Scientific™ Nunc™ Cell Culture Inserts provide an excellent cell growth system for growing tissues that require an air–liquid interface, especially when used in conjunction with their corresponding carrier plate. The carrier plate has multiple positions to place the inserts to facilitate the handling of the inserts and reduce contamination risk. These multiple positions can be used to increase the volume of medium used for culturing, which can extend the interval between required changes of the medium during tissue growth. Here we examine the effectiveness of the Thermo Scientific™ Nunc™ Cell Culture Inserts in Carrier Plate Systems for producing 3D epidermal skin models.

Key words

Epidermal, 3D tissue, human skin model, cell culture inserts, carrier plate, air–liquid interface, feeding interval, TEER

Introduction

Artificially grown skin models have become an important substitute for actual skin to simulate the effects of different conditions (e.g., acute toxicity, allergenicity, inflammation) on epidermal tissues. Inducing keratinocytes to differentiate into the various layers of epidermis requires direct exposure to air as well as to the culture medium that supplies the nutrients for cell growth and differentiation. This type of air–liquid interface culture can be accomplished by growing cells on a porous membrane carefully positioned in the culture well, allowing the upper surface of the cells to be exposed to the air, while the lower surface of the cells is fed and wetted by medium through the pores of the growth membrane.

The Nunc Cell Culture Insert is a porous membrane device that is commonly used for small-scale 3D skin growth. Cells are seeded in the cell culture insert, and the insert is submerged in medium in a multiwell plate. Once the cell layer is established on the insert's porous membrane, the medium above the membrane is removed, exposing the upper surface of the cells to the air.

The main drawback of this type of system is the limited space below the growth membrane that only allows a small volume of medium in each well to sustain cell growth during the air–liquid interface culture. This necessitates a short feeding cycle during the prolonged culture period required for cell differentiation and expansion. Performing medium changes with cell culture inserts can be a tedious task, as the inserts sit loose in the wells and must be worked around or removed during pipetting steps, increasing the chances of contaminating and damaging the 3D model or the porous membrane. The Nunc Carrier Plate System addresses these issues by suspending the cell culture inserts above the wells at the desired height. The carrier plate allows a greater volume of medium to be used in the wells during the air–liquid interface culture, potentially extending the time intervals between medium changes. If needed, the carrier plate can be removed from the wells to facilitate aseptic maneuvering, taking all of the installed inserts with it and allowing easy access for aspirating and pipetting the medium from the entire plate. The lid covering the carrier plate keeps the inserts and the cells protected from potential contaminants.

In this study, we established an effective system for culturing 3D skin epidermal tissue *in vitro* using the Nunc Cell Culture Inserts with Gibco™ EpiLife™ growth medium. We also used the adjustable-height capabilities of the carrier plate to simplify the experimental protocol, extending feeding intervals and saving time and labor.

Materials and methods

Materials	Cat. No.
Nunc Cell Culture Inserts in Carrier Plate Systems, 24-well, 0.4 µm pore size	141002
Human Epidermal Keratinocytes, adult (HEKa)	C-005-5C
EpiLife Medium, with 60 µM calcium	M-EPI-500-CA
Human Keratinocyte Growth Supplement (HKGS)	S-001-5
Antibiotic-Antimycotic (100X)	15240-062
Coating Matrix Kit Protein	R-011-K
FGF7 (KGF) Recombinant Human Protein	PHG0094
CyQUANT MTT Cell Proliferation Assay Kit	V13154
Ascorbic Acid	A4544-25G

Air–liquid interface culture on inserts

EpiLife growth medium was prepared by adding HKGS, 10 ng/mL KGF, 1X antibiotic-antimycotic solution, and 140 µM calcium chloride. Prior to using the medium, aliquots were supplemented with 50 µg/mL ascorbic acid. Cell culture inserts were precoated with a 1:100 dilution of the protein from the Gibco™ Coating Matrix Kit, according to the manufacturer's protocol.

For the initial cell attachment and expansion, all inserts were set in the lowest position of the carrier plate in their respective wells. Cells were seeded in precoated inserts at a density of 750,000 cells/cm^2. The culture area of the 24-well insert is 0.47 cm^2. Cells were seeded with 0.5 mL of growth medium in the lower compartment and 0.5 mL of cell suspension in the upper compartment. After 2 days of incubation at 37°C and 5% CO_2, the air–liquid interface was established by aspirating all of the medium from the wells and from inside of the cell culture insert, then adding the appropriate volume of growth medium to the lower compartment and repositioning the inserts at the desired hanging height in the 24-well plate (Table 1). The upper compartment, inside of the cell culture insert, was left empty. Subsequent medium changes were conducted by aspirating the medium from the lower compartment and replacing it with fresh medium supplemented with an additional 1.5 mM calcium chloride (1.7 mM total) at the desired interval (Table 1).

Table 1. Choose the insert hanging position and medium volume according to your desired interval for changing the medium.

Insert-hanging position	Volume of growth medium for lower compartment in a 24-well plate*	Interval for changing medium
Low	0.5 mL/well	2 days
Middle	1.0 mL/well	3 days
High	1.5 mL/well	4 days

* The volume for a 12-well carrier plate is twice that of the 24-well carrier plate.

Viability assay

Cell viability and metabolism were assessed after 23 days in culture using the Invitrogen™ CyQUANT™ MTT Cell Proliferation Assay Kit. The MTT reagent was added into the upper compartment of the inserts and incubated for 1 hour. The MTT solution was then aspirated, and the cells were washed. The formazan dye was extracted from the cell layer overnight using 100% isopropyl alcohol. The extracts were then transferred to individual wells in a clear 96-well plate and tested for absorbance using a Thermo Scientific™ Varioskan™ Flash Microplate Reader. Viability was assessed in 6 inserts.

Trans-epithelial electrical resistance (TEER) measurement

The TEER was measured at 2 time points during the growth of the skin tissue—at 11 and 23 days post-seeding. Measurements were taken using an EVOM2™ Epithelial Volt/Ohm (TEER) Meter and probe (World Precision Instruments). During the recording, the cell growth medium was aspirated and replaced with 0.5 mL phosphate-buffered saline (PBS) in both the upper and lower compartments. The probe was placed such that one electrode was submerged in the upper compartment and the other was submerged in the lower compartment. TEER values were recorded for 6 inserts at each time point.

Microscopic examination

Skin tissue in inserts was allowed to grow for 12 days post-seeding and then fixed using an overnight incubation in 4% formaldehyde at 4°C. Inserts were paraffin-embedded and sectioned, followed by processing for hematoxylin and eosin (H&E) staining. Tissue sections were photographed at 400x magnification to examine the stratification of cell layers.

Results

Initial experiments of cell attachment and expansion indicated that the Nunc Cell Culture Inserts were an excellent growth substrate for human epidermal keratinocytes. An MTT assay after 2 weeks of air–liquid interface culture showed good viability in all wells tested (Figure 1).

TEER was used to determine the strength of the barrier formed by the skin tissue established in the inserts. A mature layer of skin tissue should prevent the flow of ions across the porous growth membrane, as indicated by a high level of electrical resistance. Our measurements taken on culture days 11 and 23 showed high levels of resistance, indicating a strong barrier formed as early as day 11 and continuing to mature to day 23, 3 weeks after air exposure (Figure 2).

Following 12 days of air–liquid interface culture, examination of fixed and sectioned artificial skin tissue by microscope indicated good differentiation of the epidermal layers. All of the expected cell types were visible in the sectioned and stained tissues (Figure 3).

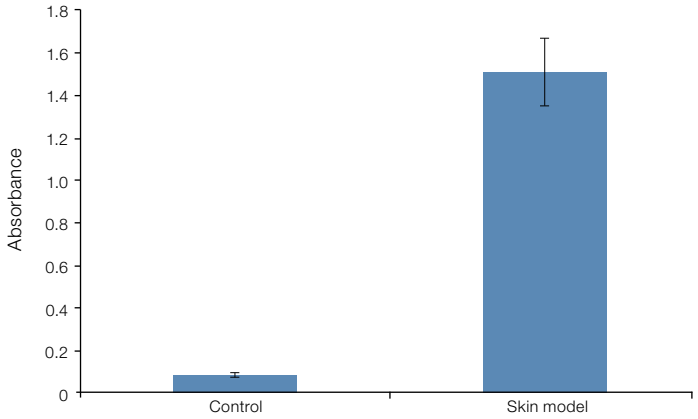

Figure 1. Assessment of cell viability by MTT assay. Mean absorbance of extracts from skin model samples compared to control inserts without cells. Error bars indicate standard deviation.

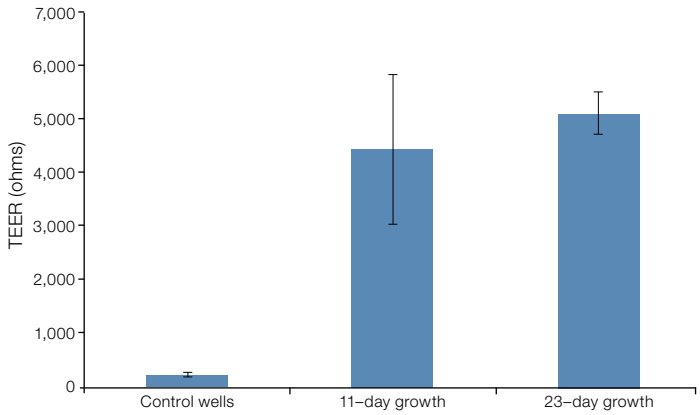

Figure 2. Assessment of skin model integrity using TEER measurement. TEER measurements were taken at 11 and 23 days after the initial seeding of the cells in the inserts. TEER values were compared to control inserts of the same size without cells. Error bars indicate standard deviation.

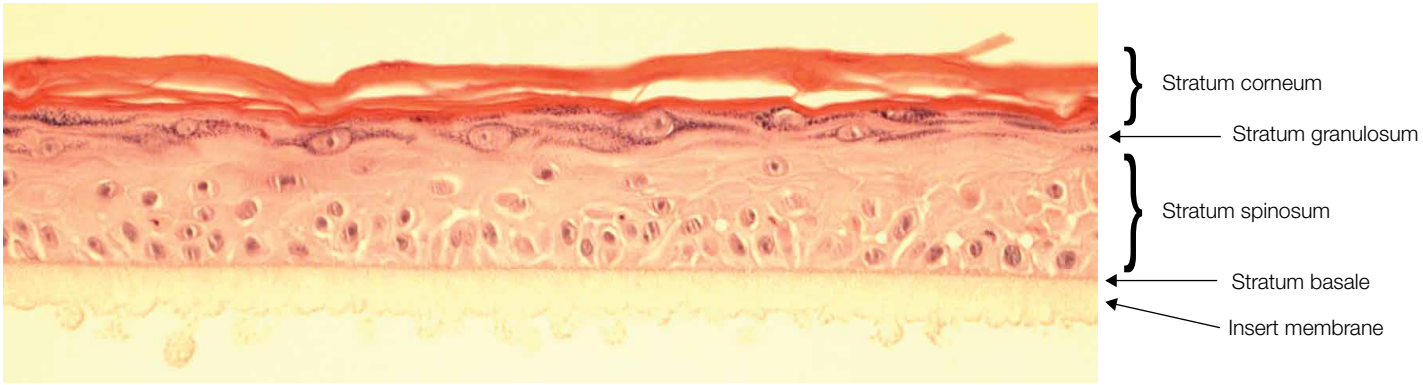

Figure 3. Stratification of the epidermal skin model on the insert membrane was shown by H&E staining.

Additional experiments were performed to determine whether feeding intervals had a significant impact on epidermal tissue formation in the cell culture inserts. We took advantage of the versatility of the carrier plates and tested different insert-hanging positions, and the corresponding increases in media volume for different media change intervals of 2, 3, or 4 days (Figure 4). For all intervals tested, the resulting skin tissue showed good differentiation of the cell layers after 12 days of air–liquid interface culture, indicating that the longer intervals worked as effectively as the shorter ones, and saved time and labor during establishment of skin tissue (Figure 5).

Figure 4. Cross-sectional view of the Nunc Carrier Plate with 3 hanging positions for the Nunc Cell Culture Inserts.

Conclusion

- The Nunc Cell Culture Inserts in Carrier Plate Systems provide an excellent and convenient method for culturing artificial models of human skin tissue.
- The multiple height settings of the carrier plate allow for increased volumes of growth medium during air–liquid interface culture, extending the medium change intervals for more convenient laboratory procedures.

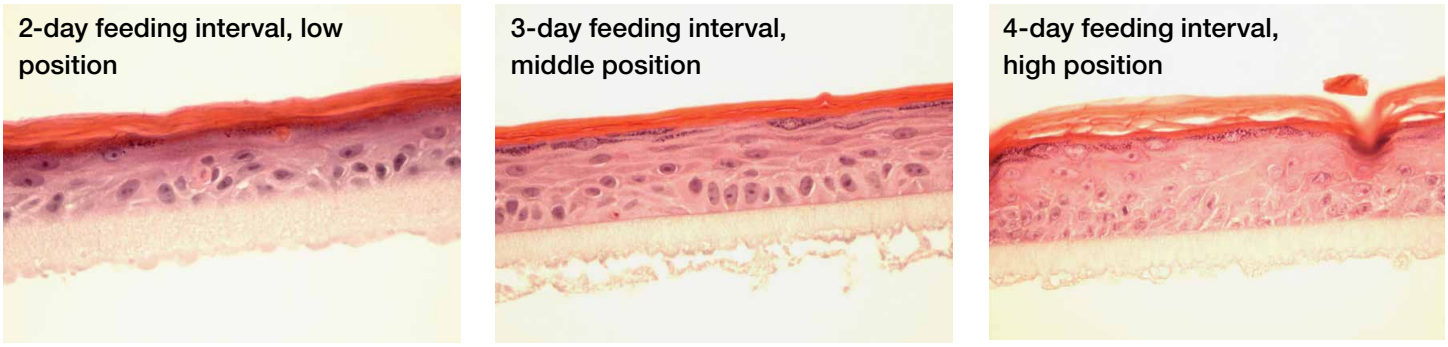

Figure 5. H&E staining of stratification of the epidermal skin model after 12 days of air–liquid interface culture with media changes at varying intervals. Different volumes of growth medium were used with different insert-hanging positions in the carrier plate to achieve the air–liquid interface culture. Epidermal tissue was cultured in 0.5 mL, 1.0 mL, or 1.5 mL medium per well and fed every 2, 3, or 4 days, respectively. Tissue sections were photographed at 400x magnification.

A.10

Generation of cancer spheroids—tips and tricks

Introduction

Tumor cells grown as spheroids offer an intermediate complexity between cancer cells grown in 2D monolayers and *in vivo* tumors. This potentiates their use as model systems to study tumor progression as well as to perform high-throughput screening of cytotoxic therapies, including chemotherapies and cell-based treatments.

Cancer spheroids are formed when cells are allowed to grow in suspension, as a result of which they aggregate, either on their own or with the aid of extracellular matrices. There are two factors critical in limiting variation in high-throughput assays with cancer spheroids. First, it is essential to have one spheroid per well in a multiwell plate, to reduce variability in readouts. Second, it is important that spheroids be of uniform shape and size—otherwise there can be variability between experiments. In our lab, we have tested spheroid generation conditions in nine human cell lines belonging to six cancer types. To summarize the results, we have compiled a general workflow and a few tips and tricks to help with the high-throughput generation of uniform and reproducible spheroids in Thermo Scientific™ Nunclon™ Sphera™ multiwell plates. The tips are specific to the cell type tested but can also be referred to for troubleshooting spheroid generation in other cell types.

General workflow

1. On the day of experiment, dissociate cells using **Gibco™ TrypLE™ Express Enzyme** and then neutralize the enzyme using 4 volumes of complete medium (medium will vary depending on cell line chosen).
2. Count cells using the **Invitrogen™ Countess™ II FL Automated Cell Counter**. Cell viability should be >90%.
3. Dilute the suspension at a ratio of 1:10–1:20 in complete medium or a medium containing required additives. Seed the required number of cells in respective wells of **Nunclon Sphera 96-well plates** using **Thermo Scientific™ Finnpipette™ F2 Multichannel Pipettes**.
4. Centrifuge plates at the required speed (250–450 x *g*) for 5–10 min at room temperature or 4°C, based on the use of additive (e.g., for **Gibco™ Geltrex™ matrix** addition, 4°C is necessary; and for collagen I, a temperature below 18°C is required).
5. Change the medium as necessary until spheroids are ready. Add the medium slowly along the side of the wells without touching the spheroids.

Considerations for growing cancer spheroids

Spheroid size

Depending on the cell line, spheroids differ in compactness. Figure 1 shows cancer spheroids generated from 5,000 cells of four different cell lines. As is evident, the seeding cell number does not correlate to spheroid size. Thus, to obtain spheroids of a specific diameter for use in a particular downstream assay, the seeding cell density for the respective cell line needs to be standardized. All brightfield images were captured using the Invitrogen™ EVOS™ M7000 Imaging System with a 4x objective unless stated otherwise.

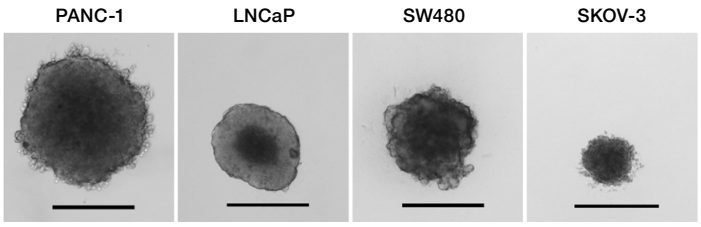

Figure 1. Spheroids generated from cancer cell lines on a Nunclon Sphera plate. PANC-1: pancreatic cancer; LNCaP: prostate cancer; SW480: colorectal cancer; SKOV-3: ovarian cancer. A total of 5,000 cells were seeded in each case. Scale bar: 500 µm.

Time

Cells have been shown to proliferate more slowly in 3D culture than in 2D culture [1]. Based on our observations, depending on the doubling time of the cells, some cancer spheroids are ready within 24 hr (for example, A549 and SKOV-3), while some might require 4–9 days (PC-3 and T47D). An ideal spheroid is translucent with a defined boundary and minimal dark core. However, certain cells, especially those that require an extracellular matrix for spheroid formation (see next section, "Extracellular matrices"), do not exhibit the ideal morphology. Figure 2 shows the morphological changes of T47D and SKOV-3 spheroids over time in culture. T47D spheroids grew in size and their cores became progressively darker over time; spheroids were ready by day 5. In contrast, SKOV-3 spheroids were ready on day 1; with increasing time in culture, the compactness increased (Figure 2B), and the cells seemed to be diverging from the spheroid.

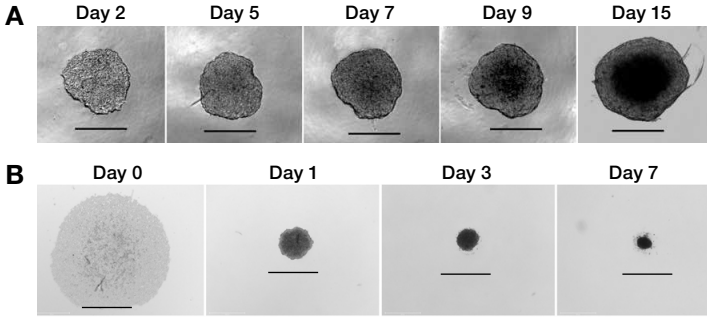

Figure 2. Morphological change in different spheroid types. **(A)** 4,000 T47D cells and **(B)** 10,000 SKOV-3 cells were seeded on Nunclon Sphera 96-well plates and observed on the indicated days. Scale bar: 500 µm.

Extracellular matrices

Some cell lines form spheroids on their own, while others form loose or tight cellular aggregates. Finicky cell lines require the assistance of various extracellular matrices (ECMs) to form spheroids. For example, PC-3 cells require Geltrex matrix (Figure 3). In order to optimize conditions for spheroid formation by MDA-MB-231 cells, various ECM components were tested in Nunclon Sphera 96-well plates with 1 x 10^4 cells seeded per well. The day after plating, complete medium containing various ECMs was added to the spent medium, and cells were observed on day 5. As depicted in Figure 4, we found that collagen I worked best in this case to form a spheroid with a defined boundary. In all other cases, the cells formed aggregates.

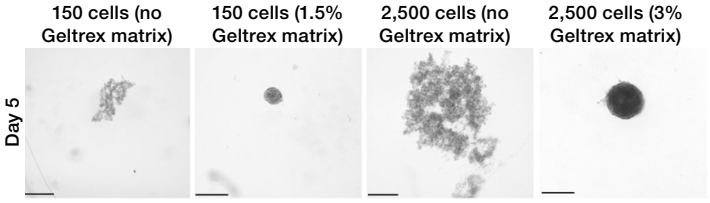

Figure 3. PC-3 cells seeded for spheroid formation with and without Geltrex matrix. Scale bar: 650 µm.

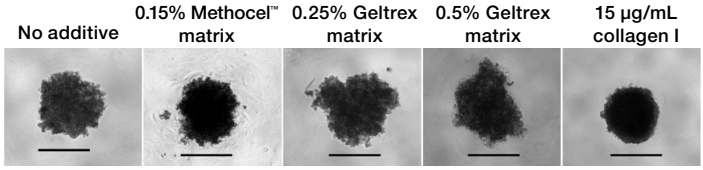

Figure 4. Effect of ECMs on spheroid growth. 10,000 MDA-MB-231 cells were seeded in medium supplemented with different ECMs. Scale bar: 500 µm.

We further standardized the collagen I concentration required for spheroid formation. Subsequent testing indicated that a final concentration of 3 µg/mL collagen I worked best, with higher concentrations leading to a disrupted spheroid morphology with cells diverging from the spheroid (Figure 5).

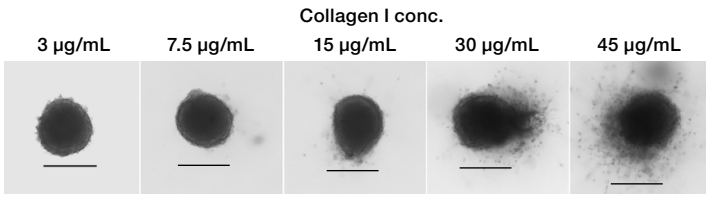

Figure 5. Standardizing collagen I concentration. 10,000 MDA-MB-231 cells were seeded in medium supplemented with different concentrations of collagen I. Scale bar: 500 µm.

To verify spheroid formation, we stained the cellular entities with Invitrogen™ DiI, a lipophilic membrane stain. All cells in the aggregate were easily accessible to the dye, whereas the compactness of the spheroid prevented the dye from entering the core (Figure 6).

While a single concentration of ECM worked for MDA-MB-231 cells, some cell lines such as SW480 required different ECM concentrations based on the seeding density. As seen in Figure 7, a concentration of 3 µg/mL of collagen I worked for 625–2,500 cells only. However, increasing the collagen I concentration for higher cell densities formed better spheroids than those formed using a single lower concentration of collagen I for those cell densities.

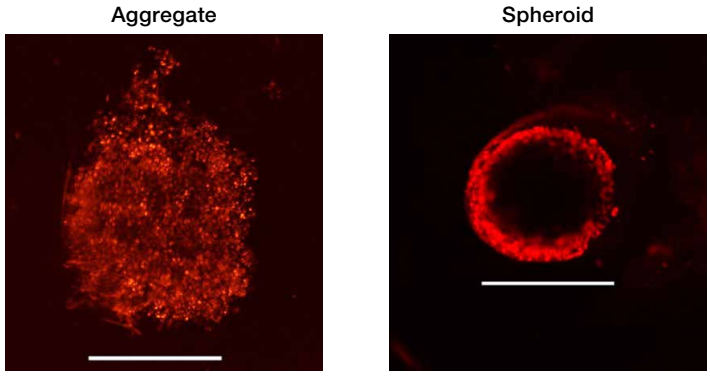

Figure 6. Verification of spheroid formation. 5,000 MDA-MB-231 cells in medium with or without collagen I were seeded onto Nunclon Sphera plates and stained with DiI 4 days later. Images were captured using the Thermo Scientific™ CellInsight™ CX7 High Content Analysis Platform with a 4x objective. Scale bar: 400 µm.

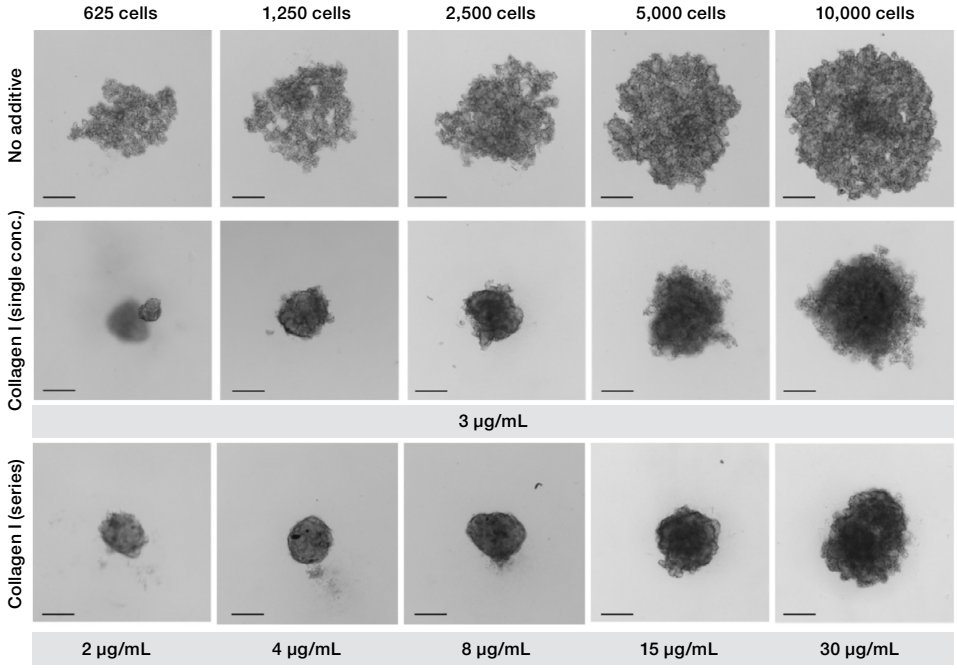

Figure 7. Higher seeding densities may require more concentrated ECM. SW480 cells were seeded (with increasing cell densities) in medium without additive or supplemented with either a single concentration or a concentration series of collagen I. Scale bar: 650 µm.

Plastic surface

The primary requirement for spheroid formation is a nonadherent surface. The Nunclon Sphera plates help to repel the cells from settling at the bottom and facilitate uniform spheroid formation upon centrifugation. We compared this surface to Corning™ ULA plates for spheroid formation. In our observations, out of nine cell lines tested, approximately 50% of cell lines formed satellite colonies around the spheroids on the Corning ULA surface. This was more evident at higher cell densities, as in the case of HepG2 (Figure 8A, lower panel). In contrast, Nunclon Sphera plates helped in consistent formation of a single spheroid per well for all cell lines tested.

Conclusion

By using the right plastic surface, medium, and extracellular matrix, and following the tips and tricks, uniform and reproducible cancer spheroids can be generated easily. In our observations, cells that have a circular morphology and cells that grow in clusters can form spheroids on their own. However, cells that don't grow in clusters require ECM support. Cells with elongated morphology vary in their requirement for ECM, so spheroid-generating conditions need to be optimized for each cell line. Our portfolio supports robust generation, characterization, and high-throughput applications and analyses of 3D cancer spheroids.

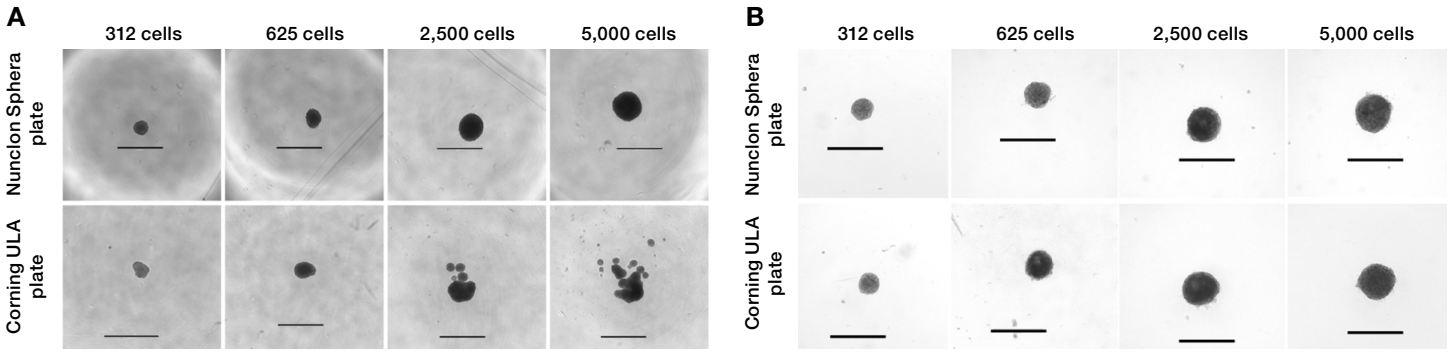

Figure 8. Effect of surface on spheroid formation in different cell lines. (A) HepG2 cells were seeded for spheroid formation on a Nunclon Sphera plate (top panel) and a Corning ULA plate (bottom panel). **(B)** PC-3 cells were seeded in medium supplemented with Geltrex matrix on a Nunclon Sphera plate (top panel) and a Corning ULA plate (bottom panel) for spheroid formation. Scale bar: 1,000 µm.

Reference

1. Anna C et al. (2013) Impact of the 3D microenvironment on phenotype, gene expression, and EGFR inhibition of colorectal cancer cell lines. *PLoS One* 8(3):e59689.

A.11

Harnessing new dimensions in your research: coming 'round to spheroid culture

Introduction

Cells cultured in 2D can differ in terms of both physiology and cellular responses compared with cells grown *in vivo*. These differences have led to a surge in the popularity of 3D culture techniques. Mounting evidence suggests that culturing cells in 3D is more representative of the *in vivo* environment, creating more physiological cell models, even to the extent that the gene expression profiles of cells from 3D cultures more accurately reflect clinical expression profiles than those observed in 2D cultures [1,2]. Spheroids, or sphere cultures, have become an especially exciting area of 3D *in vitro* culture due to their great potential for use in studies that investigate growth and function of both malignant and normal tissues. These sphere cultures have contributed considerably to our knowledge of cellular responses thanks to the accuracy with which they reflect the *in vivo* system. This is primarily because cells do not normally grow or interact in isolation, but instead form complex interactions with other cells and the surrounding microenvironment. Thus, the creation of a 3D environment that incorporates spheroids more closely mimics *in vivo* conditions, allowing researchers to incorporate cell–cell interactions, nutrient gradients, and diffusion kinetics in their *in vitro* models.

Spheroids offer particular benefits in cancer biology, where they contribute immense value in examining the growth and behavior of tumors since they share several key histomorphological and functional traits that include the formation of cell–cell contacts, decreased proliferation, increased survival rates, and a hypoxic core [3,4]. As more researchers recognize the benefits that spheroid cultures provide as a cell model, development efforts have increased to better aid spheroid generation, culture, and scale-up. Researchers are now moving toward advanced culture methods, employing hypoxic conditions, or co-culturing with different cell types to develop increasingly accurate *in vitro* models of disease and physiology.

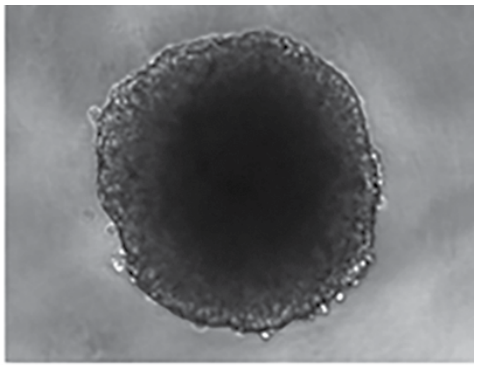

Brief history of spheroid development

Researchers have cultured cells in aggregates since the 1950s [5], but it wasn't until 1971 when the term "spheroid" was coined in work using Chinese hamster V79 lung cells as a model of nodular carcinomas, which happened to form perfect spheres [6]. Robert Sutherland's early research not only provided some of the first glimpses into the effects of nutrition and oxygenation on cell growth, but also allowed for the determination of the growth fraction following treatment with drugs or radiation.

By the 1980s, Mina Bissell and her team at Lawrence Berkeley National Laboratory began pioneering the use of 3D techniques for more accurate *in vivo* cell models. This shift away from traditional 2D culture systems was first published in a paper highlighting the importance of the extracellular matrix (ECM) along with the crucial role of the microenvironment [7]. These observations were critical for driving the uptake of spheroid culture as a widespread and biologically relevant system with obvious advantages over the widely used monolayer culture methods.

Since then, the field has expanded rapidly to investigate a number of topics from small-scale disease modeling to large-scale, high-throughput screening (HTS) platforms attempting to combat the rising attrition rates seen in existing drug discovery programs.

The ECM: an influential network

Industry has responded to these changes and supported spheroid culture in research through the development of specialized equipment and protocols for culture and maintenance, including plates, synthetic coatings, and cellular scaffolding. There are several common methods used in the generation of spheroids. These include the liquid overlay technique [8], spinner flask [9], gyratory [10], and hanging drop methods [11], or more recently, using suspension culture in individual wells for high-throughput analysis [12]. Following the initial generation of spheroids, the task of maintaining and culturing them can make use of a wide selection of techniques. Depending on the intended application, spheroid culture can involve extracellular matrices or scaffolds, modified surfaces, rotating bioreactors, microcarriers, magnetic levitation, hanging drop plates, or magnetic 3D bioprinting.

Successfully generating and culturing spheroids has a lot to do with the ECM. The ECM is generally composed of soluble proteins and insoluble collagen fibers. While collagen forms the rigid structures that allow tissues to tolerate mechanical stresses like stretching, the proteins within the ECM are involved in a variety of other processes. Proteoglycans, for example, can aid in signaling, binding growth factors, and binding hormones, while multiadhesive matrix proteins like laminin and fibronectin can bind both collagen and other ECM components.

The points at which the ECM makes contact with a cell's plasma membrane are known as focal adhesions. These vary between tissues but generally consist of integrin molecules that associate with both the intracellular and ECM components—making these ECM components functional units of intracellular signaling.

The ECM is also important when it comes to adhesion, not only between cells but also to the culture vessel. When culturing spheroids, the ECM proteins mediating adhesion will automatically adhere to the surface of a culture vessel. This can interfere with complete spheroid formation and may possibly result in the formation of multiple spheroids or satellite colonies. In an attempt to optimize spheroid formation, manufacturers have developed a number of synthetically modified culture vessel surfaces that specifically inhibit the adsorption of ECM proteins from initiating adhesion between the cell and the culture vessel, thereby prompting cell–cell aggregation and spheroid formation *in vitro*.

The Nunclon Sphera surface is superior for culturing cancer spheroids

The Thermo Scientific™ Nunclon™ Sphera™ hydrophilic polymer-coated surface has been shown to minimize surface variability. This polymer coating discourages ECM adsorption to the surface, thereby supporting the formation of consistent spheroids (Figure 1).

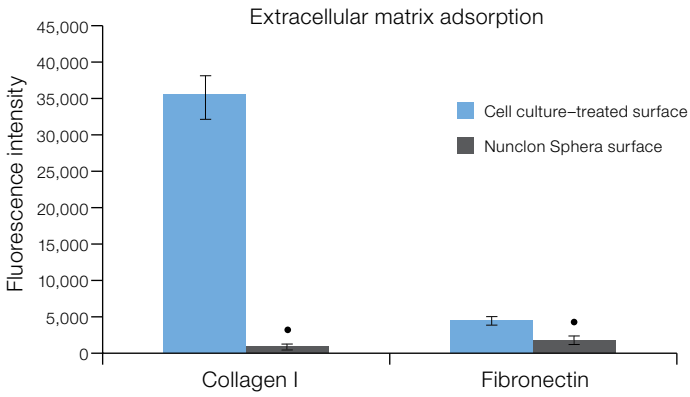

Figure 1. Extracellular matrix adsorption. The adsorption of collagen I and fibronectin to the Nunclon Sphera surface is extremely low compared to the standard cell culture–treated surface. Student's *t*-test, $P < 0.01$.

By combining a hydrophilic polymer coating with U-bottom–shaped wells, it is possible to culture spheroids without the production of satellite colonies. HCT 116 human colon carcinoma cells were seeded into Nunclon Sphera 96-well U-bottom plates in complete DMEM. Similarly, cells were seeded into 96-well U-bottom nontreated plates in complete DMEM containing 3% methylcellulose. Using different seeding densities of HCT 116 human colon carcinoma cells, it was shown that single spheroids with well-defined edges can be consistently generated in each individual well (Figure 2).

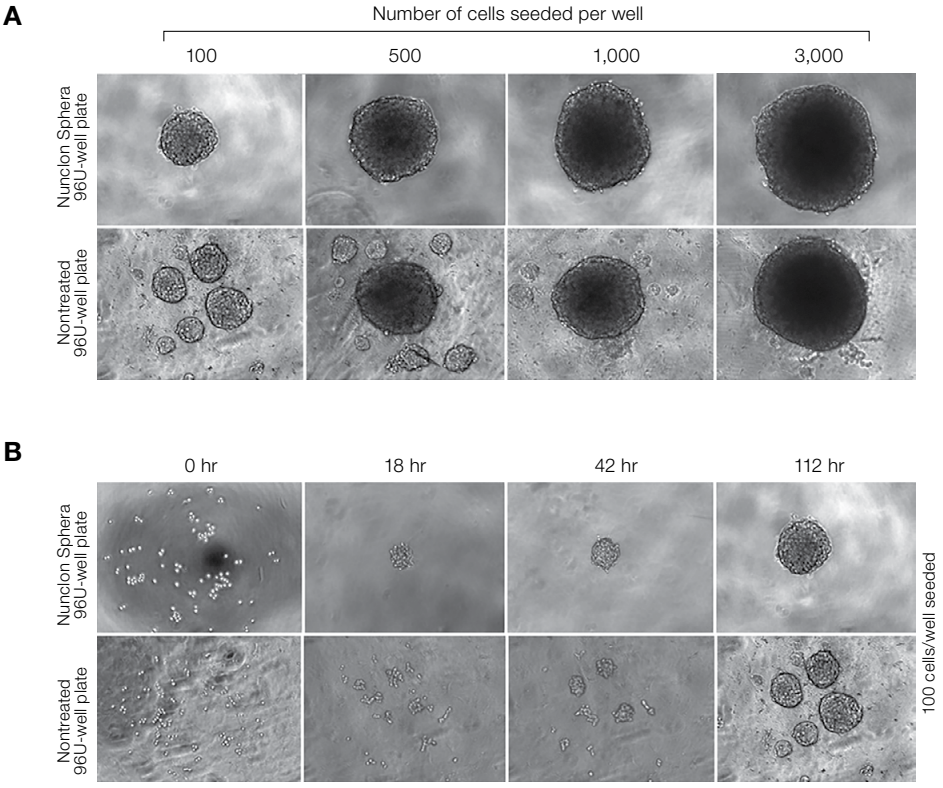

Figure 2. Advantages of Nunclon Sphera plates over nontreated plates and methylcellulose-containing medium. (A) High and consistent quality of cancer spheroids grown in the Nunclon Sphera plate. **(B)** Early formation of single cancer spheroids in the Nunclon Sphera 96-well U-bottom plate. (Courtesy of Professor Dolznig from the Institute of Medical Genetics at the Medical University of Vienna.)

To demonstrate spheroid growth, A549 human adenocarcinoma cells and HCT 116 human colon carcinoma cells were cultured at different densities in Nunclon Sphera plates for 2 weeks. Both cell types displayed adequate spheroid growth as demonstrated by size measurements (Figure 3A). Additionally, the cell health of A549 and HCT 116 spheroids were assessed by Invitrogen™ PrestoBlue™ cell viability assay (Figure 3B).

Data was normalized against spheroid size for better quantitative comparison—a higher ratio indicates healthier spheroids. Cell viability of cancer spheroids was further confirmed by Invitrogen™ LIVE/DEAD™ fluorescence staining assay (Figure 3C). All parameters indicated that cancer spheroids grown on Nunclon Sphera plates were healthy and robust, and that the Nunclon Sphera 96-well U-bottom plate is a reliable and convenient tool for both routine and high-throughput cancer spheroid applications.

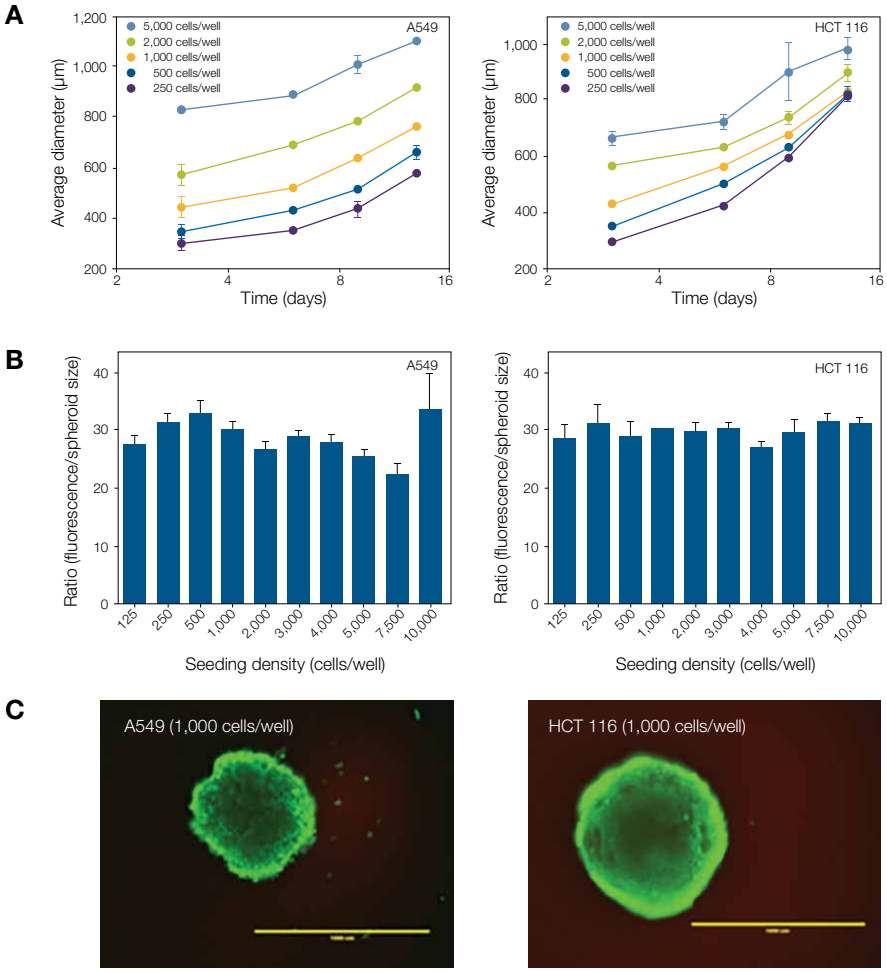

Figure 3. Assessments of spheroid growth, cell health, and viability on Nunclon Sphera plates. (A) Growth kinetics of A549 and HCT 116 cancer spheroids on Nunclon Sphera plates were evaluated over period of 13 days. Data represents the mean ± SD of 3 replicates for each cell number. **(B)** Spheroid cell health assessments on Nunclon Sphera plates were performed using the PrestoBlue cell viability assay with data normalized by spheroid size. **(C)** Spheroid cell viability was evaluated by LIVE/DEAD staining assay, where live cells are stained green and dead cells are stained red. Scale bar = 1,000 µm.

The hypoxic culture condition

In addition to specialized culture vessels, culturing spheroids requires precisely controlled abiotic conditions such as temperature, humidity, and pH. Gas condition is another vital requirement of cell culture, and typically this has meant mimicking atmospheric oxygen tension supplemented with 5–10% carbon dioxide. Yet, while atmospheric levels of oxygen are approximately 20%, the levels within the human body range from 12% to as low as 1%. In light of this, some researchers have taken to culturing their cells under hypoxic conditions.

The role of oxygen was seen as early as 1972 when Alan Richter and colleagues improved plating efficiency of mouse and rat embryonic tissues by cultivating in 1–3% oxygen [13]. The 21st century is seeing cell culture truly coming of age, taking positions in everything from routine cell culture to cell therapy and the development of personalized medicines. These applications have rekindled an interest in the levels of oxygen used in cell culture, and over the past decade or so, the hypoxic element came to the forefront of spheroid culture.

Cells cultured under hypoxic conditions grow faster, live longer, and show lower stress. A cell culture incubator that controls nitrogen gas, in addition to carbon dioxide, is the best way to achieve hypoxic conditions. So-called tri-gas incubators, such as the Thermo Scientific™ Heracell™ VIOS Incubator, optimize low-oxygen cultures to offer optimal growth and culture stability. However, the term "tri-gas" is a misnomer as only carbon dioxide and nitrogen are supplied, thereby reducing the internal oxygen levels to as low as 1%.

Detecting hypoxic conditions in real time is often carried out using a chemical that generates a fluorescent signal under specific conditions. A specialized hypoxia probe, in the form of a fluorogenic compound that is live-cell permeant and begins to fluoresce when oxygen levels fall below 5%, provides robust and reproducible measurements of hypoxia in cells (Figure 4). This reagent is preferable to using pimonidazole adducts that only respond to very low levels of oxygen (at a partial pressure of ≤10 mHg), below levels at which hypoxia may occur, potentially yielding false negative results. The Invitrogen™ Image-iT™ Hypoxia Reagent has a greater range of sensitivity and responds quickly to changing levels of oxygen, making it ideal for detecting hypoxic conditions in 3D cultures, spheroids, or neurons, for example [14,15].

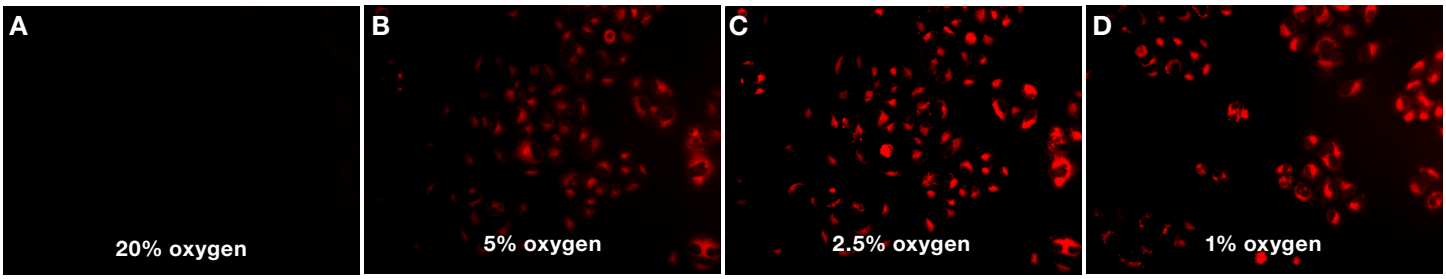

Figure 4. Detection of hypoxic conditions. A549 cells were grown on Thermo Scientific™ Nunc™ 35 mm glass-bottom dishes in complete medium at a density of 10^5 cells/dish. The cells were incubated in Gibco™ FluoroBrite™ DMEM with 5 µM Image-iT Hypoxia Reagent (red) at **(A)** 20%, **(B)** 5%, **(C)** 2.5%, and **(D)** 1% oxygen for 1 hr on an Invitrogen™ EVOS™ Onstage Incubator attached to an Invitrogen™ EVOS™ FL Auto Imaging System. The images were taken after 1 hr of incubation at each oxygen level. The hypoxia signal can be detected at oxygen levels as low as 5%, with increasing signal intensities at 2.5% and 1%.

Spheroids in cancer biology

Spheroid culture methods have made substantial contributions to the advances being made in our basic understanding of cell biology, as well as providing insights into cancer biology. The multicellular tumor spheroid (MCTS) model, using spheroids between 200–500 µm, has lent itself to cancer biology as it more accurately mimics the physiology of tumors, as mentioned earlier. Spheroids in this model develop chemical gradients of oxygen, nutrients, and catabolites just like a tumor *in vivo*, as well as possess similar histomorphological and functional features [16]. Internally, spheroids possess the same hypoxic core seen in solid tumors (Figure 5) where cells rapidly outgrow the blood supply, leaving the center of the tumor with an extremely low oxygen concentration. Chronically hypoxic regions of tumors are highly resistant to therapy as they are especially difficult to penetrate with chemotherapy [17].

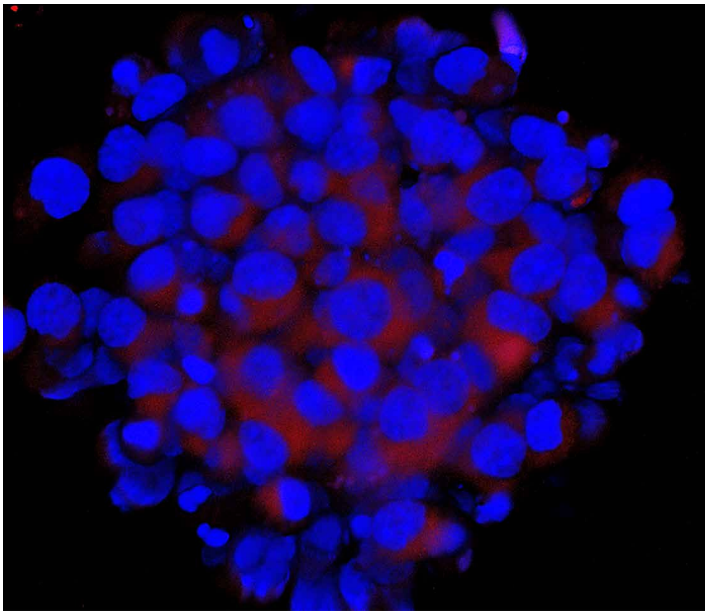

Figure 5. A single HeLa spheroid used in the assessment of hypoxic cores. HeLa cells were plated at a density of 1,000 cells/well. After two days of culture on Nunclon Sphera 96-well U-bottom plates, HeLa spheroids were stained with Image-iT Hypoxia Reagent (red) and Invitrogen™ NucBlue™ Live ReadyProbes™ Reagent (blue). Images were taken on a confocal microscope.

This gradient of oxygen in spheroids, progressing from normoxic cells at the periphery to hypoxic cells at the core, provides an excellent model for assessing novel pharmacological agents and drug delivery methods. MCTS models can be used to validate compounds that are activated under hypoxic conditions, thereby targeting the hypoxic core specifically, as well as evaluating drugs and signaling pathways [18,19].

While the ability of cancer spheroids to replicate key elements of tumors—such as hypoxia, necrosis, angiogenesis, and cell adhesion [20]—is intriguing, 3D cell cultures have also been used for studies of viability, clonogenicity, LD_{50}, and metastatic potential under a broad spectrum of conditions. The versatility afforded by the spheroid system has been a game-changer in how we understand and develop treatments for cancer.

Conclusions

The spheroid system of cell culture has major implications not only for our fundamental understanding of how the interplay between cells, tissues, and the ECM affects pathological states such as cancer, but also for the development of more robust drug screening programs and improved organotypic models.

- The Nunclon Sphera surface demonstrates extremely low ECM binding properties; it therefore effectively discourages cell attachment and promotes spheroid formation
- Nunclon Sphera 96-well U-bottom plates support consistent formation and growth of cancer spheroids across commonly used cancer cell lines
- The evidence for hypoxic cores in cancer spheroids indicates that 3D cancer spheroid culture on Nunclon Sphera plates presents an ideal *in vitro* system for modeling tumor growth

Methods: cancer spheroid culture

Cancer cell lines were maintained in Thermo Scientific™ Nunc™ Cell Culture Treated EasYFlasks™ before they were subjected to spheroid culture. To form cancer spheroids, cells were seeded in Nunclon Sphera 96-well U-bottom plates at densities of 100–5,000 cells/well in 200 µL/well of Gibco™ DMEM with GlutaMAX™ Supplement and 10% FBS, 1X MEM Non-Essential Amino Acids, 100 U/mL Penicillin-Streptomycin, and 25 mM HEPES. Nontreated plates were similarly seeded in the complete DMEM medium containing 3% methylcellulose. The plates were briefly centrifuged at 250 x *g* for 5 minutes. The cells were then incubated at 37°C and 5% CO_2, and re-fed every 72 hr by carefully removing 100 µL of medium from each well and replenishing with 100 µL of fresh growth medium using a multichannel pipette. The formation and growth of spheroids were examined using an Invitrogen™ EVOS™ imaging system.

References

1. Fennema E, Rivron N, Rouwkema J et al. (2013) Spheroid culture as a tool for creating 3D complex tissues. *Trends Biotechnol* 31(2):108–15.
2. Hirschhaeuser F, Menne H, Dittfeld C et al. (2010) Multicellular tumor spheroids: an underestimated tool is catching up again. *J Biotechnol* 148(1):3–15.
3. Heylman C, Sobrino A, Shirure VS et al. (2014) A strategy for integrating essential three-dimensional microphysiological systems of human organs for realistic anticancer drug screening. *Exp Biol Med* 239(9):1240–54.
4. Tanner K, Gottesman MM (2015) Beyond 3D culture models of cancer. *Sci Transl Med* 7(283):283ps9.
5. Moscona A (1957) The development *in vitro* of chimeric aggregates of dissociated embryonic chick and mouse cells. *Proc Natl Acad Sci U S A* 43(1):184–94.
6. Sutherland RM, McCredie JA, Inch WR (1971) Growth of multicell spheroids in tissue culture as a model of nodular carcinomas. *J Natl Cancer Inst* 46(1):113–20.
7. Bissell MJ, Hall HG, Parry G (1982) How does the extracellular matrix direct gene expression? *J Theor Biol* 99(1):31–68.
8. Carlsson J, Yuhas JM (1984) Liquid-overlay culture of cellular spheroids. *Recent Results Cancer Res* 95:1–23.
9. Sutherland RM, Durand RE (1984) Growth and cellular characteristics of multicell spheroids. *Recent Results Cancer Res* 95:24–49.
10. Moscona A (1961) Rotation-mediated histogenetic aggregation of dissociated cells: a quantifiable approach to cell interactions *in vitro. Exp Cell Res* 22:455–75.
11. Kelm JM, Timmins NE, Brown CJ et al. (2003) Method for generation of homogeneous multicellular tumor spheroids applicable to a wide variety of cell types. *Biotechnol Bioeng* 83(2):173–80.
12. Ivascu A, Kubbies M (2006) Rapid generation of single-tumor spheroids for high-throughput cell function and toxicity analysis. *J Biomol Screen* 11(8):922–32.
13. Richter A, Sanford KK, Evans VJ (1972) Influence of oxygen and culture media on plating efficiency of some mammalian tissue cells. *J Natl Cancer Inst* 49(6):1705–12.
14. Mandavilli BS, Chen A, Robinson V et al. (2015) Intracellular detection of hypoxia in live cells. Presentation at American Association for Cancer Research (AACR), Poster 3007.
15. Zhang S, Hosaka M, Yoshihara T et al. (2010) Phosphorescent light-emitting iridium complexes serve as a hypoxia-sensing probe for tumor imaging in living animals. *Cancer Res* 70(11):4490–8.
16. Thoma CR, Zimmerman M, Agarkova I et al. (2014) 3D cell culture systems modeling tumor growth determinants in cancer target discovery. *Adv Drug Del Rev* 69–70:29–41.
17. Das V, Bruzzese F, Konecny P et al. (2015) Pathophysiologically relevant *in vitro* tumor models for drug screening. *Drug Disc Today* 20(7):848–55.
18. Dufau I, Frongia C, Sicard F et al. (2012) Multicellular tumor spheroid model to evaluate spatio-temporal dynamics effect of chemotherapeutics: application to the gemcitabine/CHK1 inhibitor combination in pancreatic cancer. *BMC Cancer* 12:15.
19. Mead S, Foster R (2015) A multicellular tumor model: Applications for evaluating drugs and signaling pathways in a 3D system. Application note available from http://www.horizondiscovery.com/
20. Benien P, Swami A (2014) 3D tumor models: history, advances and future perspectives. *Future Oncol* 10(7):1311–27.

A.12

Analysis of cancer spheroids through high-throughput screening assays

Introduction

Cancer cells grown as spheroids resemble human tumors more closely than cells grown in monolayers, with respect to morphology, structural complexity, phenotype, and sensitivity to chemotherapeutics. Being more physiologically relevant model systems, they can be more predictive of drug profiling and cytotoxicity. So, early screens of drugs have become more dependent on 3D cell culture. In recent years, tumor-derived spheroids have been utilized to optimize cancer therapeutics for ovarian and hepatocellular carcinoma. However, there are some challenges to using spheroids for drug screening: primarily, the number of spheroids per well and the shape and size of spheroids need to be uniform in order to reduce variability between replicates. To address this challenge, we compiled tips for generating uniform, reproducible cancer spheroids for high-throughput screening (HTS) assays; see the application note "**Generation of cancer spheroids—tips and tricks**" in **Appendix A.10**. We have also outlined a workflow for robust 3D cancer spheroid generation in Figure 1.

Graphical workflow of 3D cancer spheroid generation

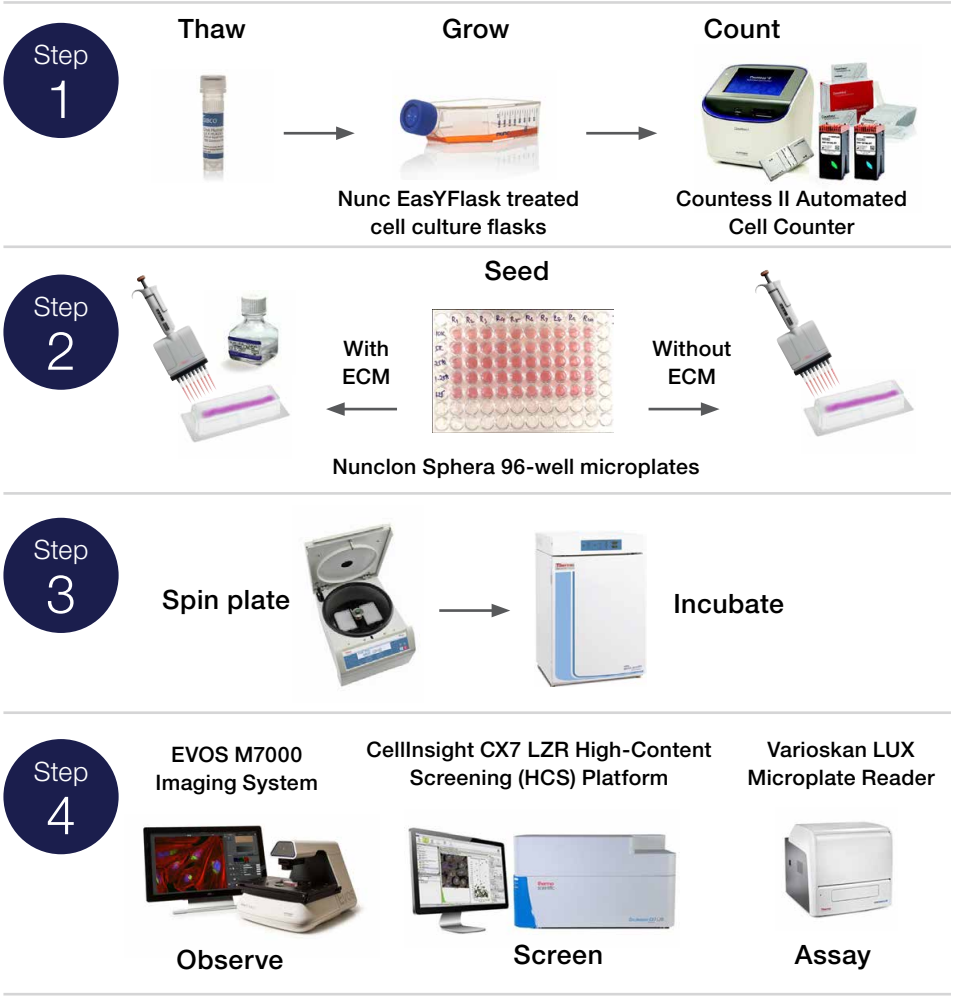

Figure 1. Schematic representation of the process of spheroid generation on Thermo Scientific™ Nunclon™ Sphera™ plates.

Another challenge in working with spheroids is determining penetration of drugs to optimize treatment times. Moreover, the use of spheroids can complicate experimental design and interpretation, but this can be overcome by using the right kinds of reagents, equipment, and protocols. Here we outline different kinds of HTS assays that can be performed on cancer spheroids to assess drug response. We also provide some useful guidelines for handling spheroids and acquiring data to get the most meaningful results. All spheroids were generated on Nunclon Sphera plates using the appropriate Gibco™ cell culture medium.

Assays with plate reader–based readouts

Cell viability and cytotoxicity assays using Invitrogen™ PrestoBlue™ HS Cell Viability Reagent

This straightforward assay utilizes resazurin as a cell health monitor. Upon entering healthy cells, resazurin is reduced in the mitochondria to resorufin, resulting in fluorescence (Ex/Em 560/590 nm). Using this assay, we compared the response of cells in 2D and 3D cultures to doxorubicin, a chemotherapeutic agent. Two different types of cancer cells (HepG2 and PANC-1) were considered. Spheroids and monolayers were treated with doxorubicin either 4 days (HepG2) or 7 days (PANC-1) after plating and allowed to incubate for 72 hours. PrestoBlue HS reagent was then added 1:10 (v/v) to the spent medium, and spheroids were incubated at 37°C for 6 hours.

Following this, high-throughput readouts were obtained using the Thermo Scientific™ Varioskan™ LUX Multimode Microplate Reader. We recommend taking a top read for homogeneity between experimental repeats. Nonlinear regression analysis was performed for variable slope of log (inhibitor) vs. response to calculate the IC_{50} using GraphPad Prism™ 5.01. As seen with PANC-1 (Figure 2A), doxorubicin treatment caused disintegration of spheroids with increasing dose, indicating cytotoxicity. For both cell lines, the IC_{50} of doxorubicin for 3D culture was at least twice that for the 2D culture (Figure 2B), suggesting increased sensitivity of 2D cultures towards the drug.

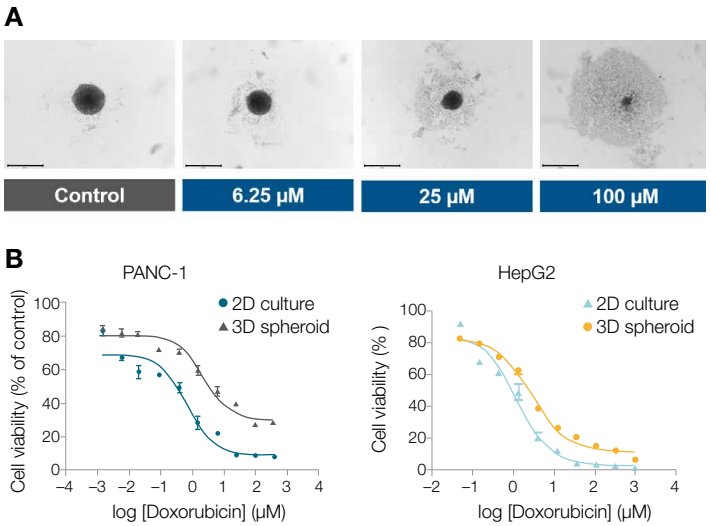

Figure 2. Morphology and effectiveness of doxorubicin treatment on spheroids in 2D and 3D cultures. (A) Morphology of control and doxorubicin-treated PANC-1 spheroids 72 hr posttreatment. Images were captured using the **Thermo Scientific™ EVOS™ M7000 Imaging System** under a 4x objective. Scale bar: 650 µm. **(B)** Dose response curves for doxorubicin-treated PANC-1 (left) and HepG2 (right) spheroids in 2D and 3D cultures.

Analyzing PSA levels using the Invitrogen™ PSA (Total)/KLK3 Human ELISA Kit

Prostate-specific antigen (PSA) in serum is a known biomarker for prostate cancer diagnosis. The PSA (Total)/KLK3 Human ELISA Kit has been successfully used to detect PSA in cell culture supernatant from 2D culture [4]. Using the manufacturer's instructions, we compared PSA secretion in 2D and 3D cell cultures. We chose the LNCaP cell line that expresses the *KLK3* gene (which in turn encodes PSA) endogenously. Medium from PC-3 cells, which do not produce PSA endogenously, was used as a negative control. LNCaP monolayers and spheroids were treated with 2 nM dihydrotestosterone (DHT, which enhances PSA expression) or 80 µM cisplatin (represses PSA expression) 4 days after plating, and incubated for 48 hours. Culture supernatant was collected, diluted 1:20 in diluent buffer, and assayed for secreted PSA using the PSA (Total)/KLK3 Human ELISA Kit and the Varioskan LUX Multimode Microplate Reader for colorimetric reading. The colorimetric readings were used to calculate relative PSA levels according to the kit instructions.

DHT treatment resulted in 17% and 21% increases in PSA secretion in 2D and 3D culture, respectively, while treatment with cisplatin reduced endogenous PSA secretion by 22–23% (Figure 3). However, 3D culture did not show any major difference in resting or induced PSA levels from 2D culture. This exemplifies how conditioned medium from spheroids can be used for high-throughput non–cell-based assays. In fact, using appropriate readouts, multiplexing of assays can also be performed.

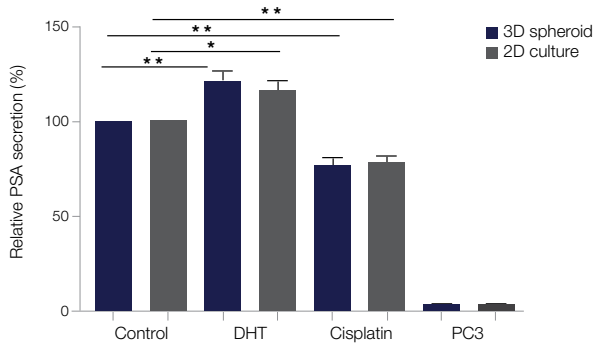

Figure 3. Quantification by ELISA of secretion of PSA following treatment with DHT and cisplatin. Error bars denote standard error of the mean. N = 2. *P < 0.01 and **P < 0.001 for difference from untreated control by one-way analysis of variance (ANOVA).

Assays with image-based readouts

Cell viability/cytotoxicity assay using Invitrogen™ LIVE/DEAD™ Kit

The LIVE/DEAD Kit is a two-color assay that measures cell viability based on plasma membrane integrity and esterase activity. It discriminates live cells from dead cells by staining live cells with Invitrogen™ calcein AM, which is converted to green-fluorescent calcein by intracellular esterase activity, and dead cells with red-fluorescent ethidium homodimer 1 (EthD-1), indicating loss of plasma membrane integrity. After 1 day in culture, SKOV-3 spheroids were treated with various concentrations of the chemotherapeutic drug paclitaxel for 72 hours, followed by incubation with 1 µM each of calcein AM and EthD-1 at 37°C for 3 hours. Following this, spheroids were washed by exchanging half of the medium with 1X PBS, then imaged. We found that exchanging the medium gently from the sides of the wells works better than centrifuging the plates and helps the spheroids stay at the center of the wells, thus aiding in image acquisition (Figure 4A). Spheroids were autofocused using the DAPI channel (they were incubated with **Invitrogen™ NucBlue™ Live ReadyProbes™ Reagent** along with calcein AM and EthD-1 staining), and the centered, maximum-intensity image projection was used to capture the z-stacks. Images were captured using the **Thermo Scientific™ CellInsight™ CX7 High-Content Screening Platform** and analyzed using the cell viability tool on Thermo Scientific™ HCS Studio Cell Analysis Software 4.0. Calcein fluorescence values in the treated samples were normalized to those of the control samples to calculate percentage of viable cells. Values were plotted against paclitaxel concentration using GraphPad Prism software. Increasing paclitaxel concentration led to concomitant reduction in cell viability (Figure 4B).

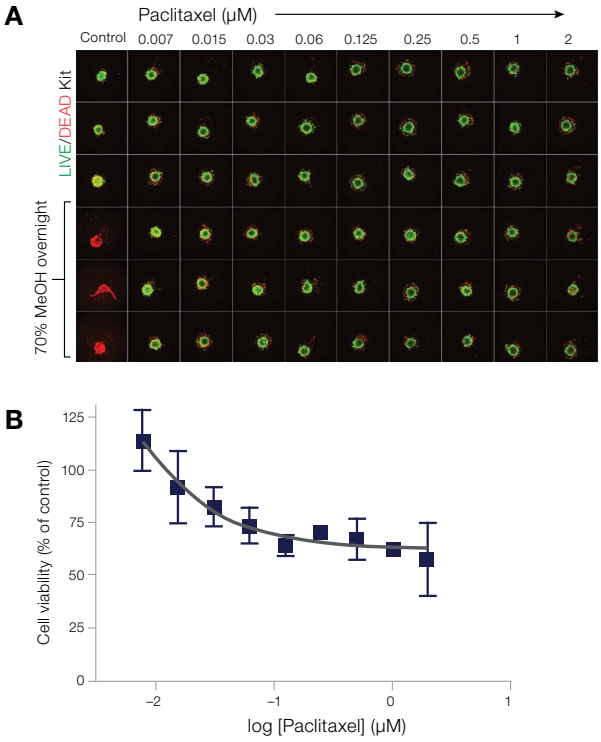

Figure 4. Cell viability assay analysis. (A) Image montage showing LIVE/DEAD staining of SKOV-3 spheroids following treatment with paclitaxel. Images were acquired using the CellInsight CX7 HCS Platform with a 4x objective and in confocal mode. Cells treated with 70% methanol (to kill cells) in the specified wells served as a negative control. **(B)** Plot of percent viability of cells with increasing paclitaxel concentrations. The values obtained using HCS Studio software were plotted with GraphPad Prism software and were fit to scale using nonlinear regression. N = 2.

Apoptosis assay using Invitrogen™ CellEvent™ Caspase-3/7 Green Detection Reagent

The reagent is a four–amino acid peptide (DEVD) conjugated to a nucleic acid–binding dye. The dye is nonfluorescent unless DEVD is cleaved by active caspase-3/7. Following DEVD cleavage, the dye is able to bind to DNA and give a fluorescence signal, providing a means to detect cells undergoing caspase-3/7–dependent apoptosis. MDA-MB-231 spheroids were formed using collagen I as previously **described**, and on day 4 treated with various concentrations of the caspase-dependent, apoptosis-inducing drug etoposide for 72 hours. Spheroids were then incubated with 2 µM of the CellEvent Caspase-3/7 Green Detection Reagent and 1 drop of Invitrogen™ NucBlue™ reagent per milliliter of PBS at 37°C for 2 hours. If PBS is used at this stage, spheroids do not require additional washing. Images were captured on the CellInsight CX7 High-Content Screening Platform under a 4x objective in confocal mode and analyzed using the spot measurement tool of HCS Studio software 4.1.

Compared to the control, there was an increase in caspase-3/7 signal with increasing etoposide concentration. However, beyond 6 µM etoposide, the caspase-3/7 signal decreased gradually, possibly owing to an increase in cell death (Figure 5A, B). Another point to note is that the extracellular matrix created background in staining, but using the background removal function for the green channel in HCS Studio software removed it (Figure 5C).

Cell proliferation assay using the Invitrogen™ Click-iT™ EdU Cell Proliferation Kit

This kit uses “click” chemistry to detect cells undergoing new DNA synthesis. T-47D cells were allowed to form spheroids for 24 hours, after which they were treated with 100 nM colchicine, an inhibitor of the mitotic phase of the cell cycle. After approximately 30 hours of treatment, 50% of the spent medium was exchanged with fresh medium containing 20 µM EdU and incubated overnight at 37^{0}C. Proliferating cells that had incorporated EdU

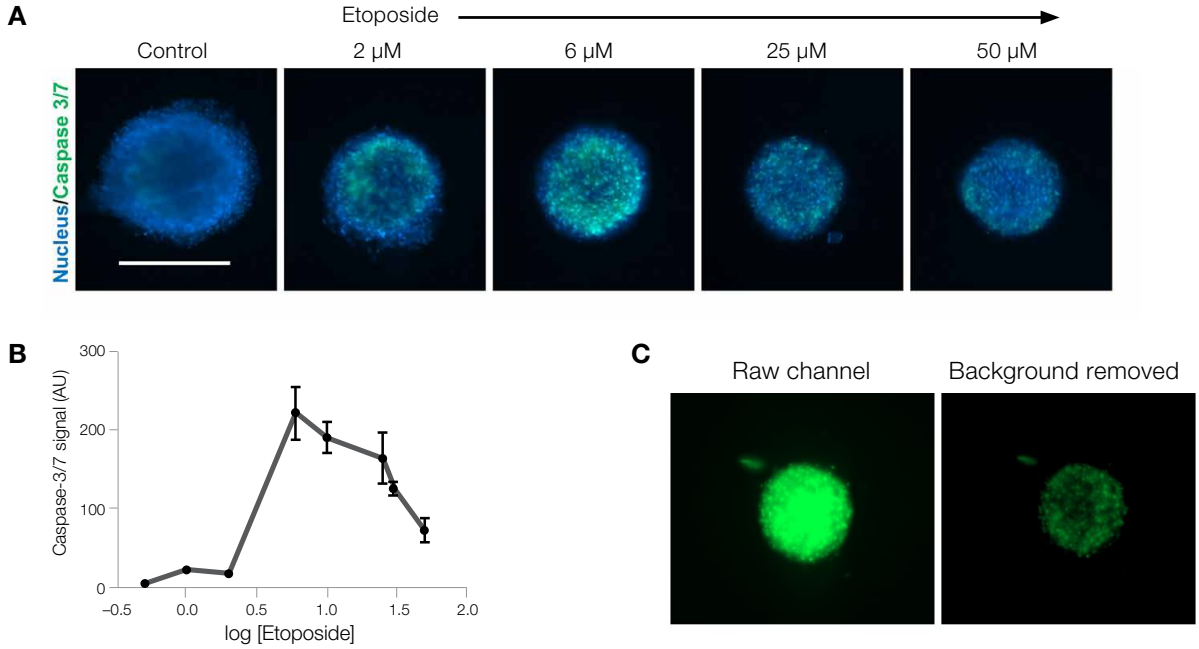

Figure 5. Apoptosis assay analysis. (A) Representative images of control and etoposide-treated MDA-MB-231 spheroids. Scale bar: 500 µm. **(B)** Plot of caspase-3/7 signal intensity against increasing concentrations of etoposide. Six spheroids were considered for every treatment concentration. The plot was generated using GraphPad Prism software from the data obtained from HCS Studio software. Error bars represent standard deviation; N = 2. **(C)** Representation of raw channel (left) and background-corrected channel image (right) for MDA-MB-231 spheroids.

were detected using the Click-iT EdU Cell Proliferation Kit with slight changes in the manufacturer's protocol. Briefly, cells were fixed in 3.7% Thermo Scientific™ Pierce™ Formaldehyde for 30 minutes and permeabilized with 0.25% Thermo Scientific™ Triton™ X-100 detergent for 1 hour, followed by incubation with Click-iT EdU dye detection cocktail overnight (as opposed to 30 minutes at room temperature as stated in the kit instructions). Due to multiple washes involved in the protocol, it is possible that spheroids get dislodged from the center of the well. As a result, they don't always fall completely in the path of light. This gives erroneous readings and variability between replicates. Thus, visualizing the spheroids followed by analysis gives more meaningful data.

An example is shown in Figure 6A. Here, both spheroids have been dislodged from the center of the well, but the spheroid in the right panel (shown with arrow) is only partially captured in the field of view. Hence it was excluded from the analysis. Also, small spheroids (200–400 µm) had to be used in the assay to capture most of the spheroids on the Thermo Scientific™ CellInsight CX7 and CX7 LZR HCS Platforms. However, this challenge has been resolved with a new software technology, Thermo Scientific™ EurekaScan™ Finder. EurekaScan Finder has a "seek and find" feature for the CellInsight CX7 LED and LZR HCS Platforms aimed at accelerating discovery by automating the identification and capture of irregularly seeded biological samples, including spheroids, at progressively higher magnifications. With the EurekaScan Finder feature applied, specimens are identified during low-magnification "seek" operations and, once "found", efficiently scanned at higher magnifications for optimal resolution. EurekaScan Finder allows scientists to first identify samples using low magnification across large surface areas, capture them at intermediate magnification, then evaluate them for rare events or improved resolution at higher magnifications.

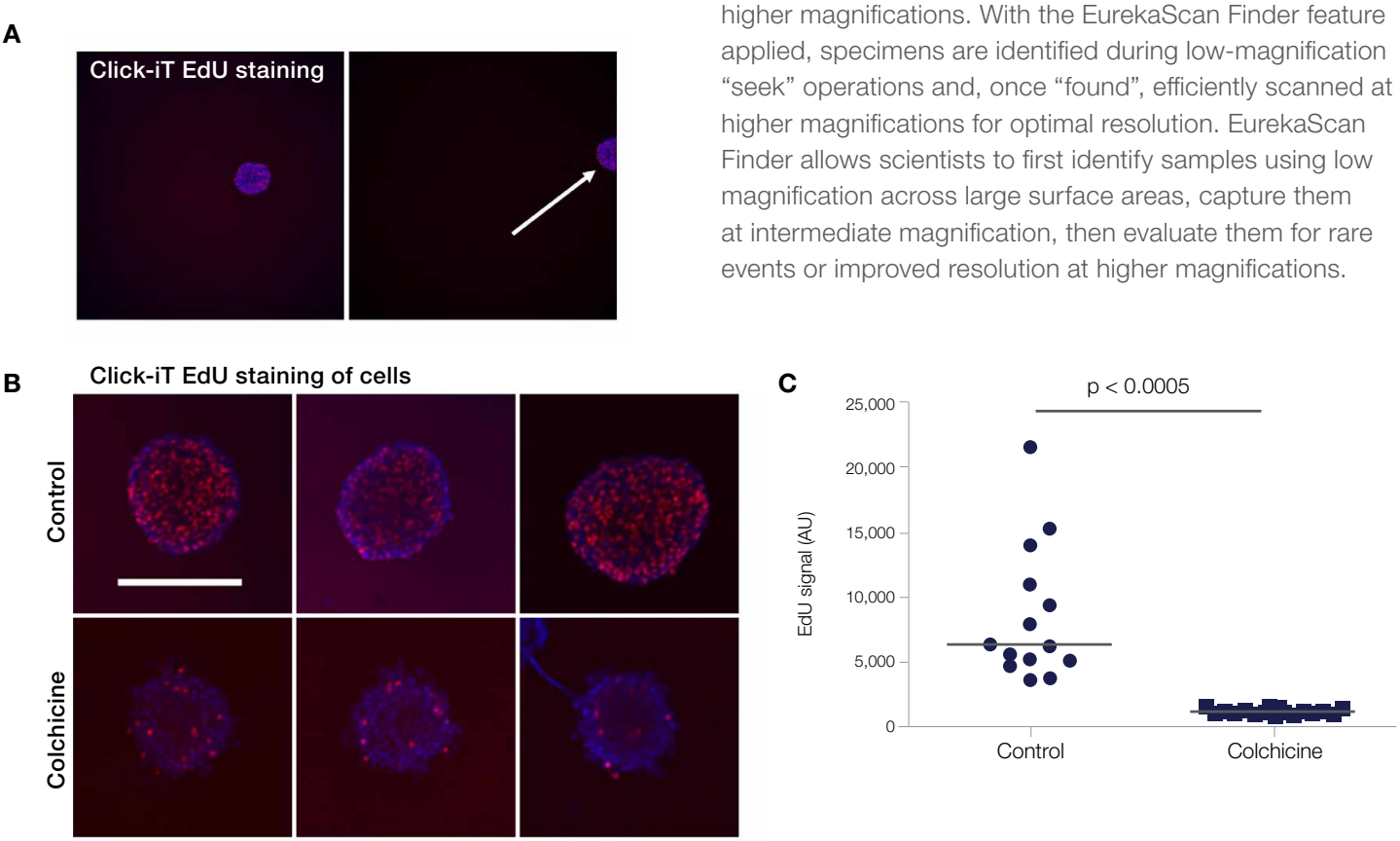

Figure 6. Cell proliferation assay analysis. (A) Field view of a fully captured (left) and a partially captured (right) spheroid as the latter got dislodged during washing. **(B)** Representative images showing Click-iT EdU staining (red) in T-47D spheroids without and with colchicine treatment. Images were acquired using the CellInsight CX7 HCS Platform under a 4x objective and in confocal mode. Scale bar: 200 µm. **(C)** Dot plot analysis of cellular proliferation in T-47D spheroids without and with colchicine treatment. The general intensity measurement tool in HCS Studio software 4.0 was used to analyze the Click-iT EdU signal (y-axis); N = 2. $P < 0.0005$ for difference from control by unpaired *t*-test.

Nevertheless, buffer exchanges should be performed carefully, as scratches in the wells give background signal during imaging, leading to noise in analysis.

For cell proliferation analysis, the spheroid was masked to negate background signal intensity. As depicted qualitatively in Figure 6B and quantitatively in Figure 6C, colchicine treatment led to a significant reduction in proliferating cells in spheroids, indicated by reduced EdU signals.

Conclusion

Though spheroids can be more complicated to analyze than cells cultured under standard 2D conditions, we have shown that a wide variety of cell-based as well as culture supernatant–based assays can be optimized to test drug responses in cancer cells grown in 3D. For the majority of cases, increasing the incubation time of drugs as well as detection reagent concentration for 3D cultures helps reagents better penetrate the spheroids and results in more meaningful data. We recommend keeping washes to a minimum and instead using media exchanges. Based on our observations, centrifuging spheroid-containing plates multiple times does not help to settle spheroids at the bottom, especially if the spheroids are fixed. So, exchanging buffer carefully and gently along the sides of wells is recommended. For comparative studies where analysis can be done on the medium rather than the cells, e.g., PrestoBlue HS Reagent or ELISA, a microplate-based readout is the preferred method. However, when the readout is cell based and involves multiple buffer exchange steps, such as the CellEvent Caspase-3/7 Green Detection Reagent for apoptosis studies or Click-iT EdU detection for cell proliferation studies, an image-based readout will yield more reliable and reproducible information about the cellular effect of drugs.

Notes

Find out more at **thermofisher.com/3dculture**

ThermoFisher SCIENTIFIC